TRACE METAL ANALYSIS BY SPECTROSCOPIC TECHNIQUES

ANTHONY CAMPBELL

A thesis submitted in partial fulfilment of the
requirements of the Council for National Academic Awards
for the degree of Master of Philosophy

JULY 1991

Nottingham Polytechnic in collaboration with
Rolls Royce plc

PS PHD 40

ABSTRACT

The prime responsibility of the Engine Support Services Laboratory (ESSL), within Rolls Royce, is to support the rig and engine projects in their development and production environment. Trace metal analysis forms an integral part of such activities as it is applied to the disciplines of fuel, lubricant, alloy and environmental evaluation.

As part of the laboratories endeavour to maintain adequate analytical capability an evaluation of Graphite Furnace Atomic Absorption Spectroscopy was undertaken.

However the nature of the laboratories analytical investigations invariably require some form of extraction prior to the analysis of the metal in question. 8-hydroxyquinoline was chosen because of its ability to chelate with a wide range of metals and for the purpose of this thesis would be applied to the likes of copper, lead, iron and aluminium.

The extraction of these metals were evaluated in the presence of two buffer systems, potassium hydrogen phthalate and sodium potassium tartrate. The results illustrating the the need for careful consideration of a given sample matrix when using extraction techniques.

The technique of Graphite Furnace Atomic Absorption Spectroscopy was new to the ESSL and its evaluation essential to maintaining our ability to meet future trace metal analysis demands placed upon it. The results have shown the technique to be excellent for trace metal analyses in aqueous matrices. The effect of hydrochloric, nitric, sulphuric and phosphoric acids has been evaluated in terms of their effect on the signal response of the elements under investigation.

Each element/matrix combination has shown the capability of the system to quantify to the 10ppb level, and to exhibit excellent linearity over the range 10-100ppb. The exception being iron in the presence of phosphoric acid which retained a high background contamination level of iron.

The evaluation of such elements in an organic matrix was restricted to the extraction of copper using 8-hydroxyquinoline in chloroform. The basic techniques of sample uptake, via a micropipette, and injection into the furnace came under close scrutiny, resulting in alternative micropipette tips being developed and assessed for improved consistancy of the results generated.

The results of such an evaluation have shown that significant practical limitations do exist when using chloroform based solutions. However these may be minimised by the use of alternative, less volatile, solvents. In addition some of the instrumental features offered by the Shimadzu AA-670, which at first glance appeared advantageous, were in fact compromised by the use of such solvents.

DECLARATION

During the course of this thesis, the author has attended symposia and conferences sponsored by the Royal Society of Chemistry, Rolls Royce plc and appropriate industrial concerns.

No portion of the work referred to in this thesis has been submitted in support of an application for another degree or qualification of this or any other Polytechnic, University or institute of learning.

ACKNOWLEDGEMENTS

The author wishes to express his sincere thanks and gratitude to the following :

Dr A Braithwaite, Department of Physical Sciences, Nottingham Polytechnic, Nottingham, for his guidance, help and advice throughout the course of this thesis.

T L Cotton, Engine Support Services Laboratory manager within Rolls Royce and Rolls Royce plc themselves for their continued support of this thesis.

Special thanks to Mr G Moorcroft, Industrial supervisor, Engine Support Services Laboratory, Rolls Royce plc. His help, guidance and encouragement has kept me going and allowed me to complete this thesis.

To my wife Dina, for her endless patience, support and encouragement, especially during the preparation of the final draft.

CONTENTS

SECTION 1.0

INTRODUCTION

SECTION 1.0 INTRODUCTION PAGE NO.

1.0 INTRODUCTION

1.1 Trace Analysis of Metals

The analysis of trace metals has long been an area of interest for analytical chemists and with increasing awareness of the biological and possible toxic properties of certain metals, this interest continues to increase. However toxicity, toxicological properties, medicinal properties and nutritional values are only a part of the reason for our interest in metal analysis. Industry has long felt the need to determine product purity and/or element composition because such factors directly affect the overall performance of various industrial alloys and the products to be derived from there.

This need for trace elemental analysis has seen the development and marketing of a large number of instruments to satisfy customer requirements in metal analysis. Over the years instrumental techniques have been developed such as flame atomic absorption (FAA), graphite furnace (or electrothermal) atomic absorption (GFAA), flame photometry, X-ray diffraction, X-ray photon spectroscopy, X-ray fluorescence, atomic fluorescence, flame emission and a number of other approaches [1-7]. All these instrumental techniques achieve total metal detection,that is, the basic instrumentation responds or produces a signal based upon the total amount (mass) of any given metal measured within the original sample. This is satisfactory if there is only a single form of the metal present, but even here the question remains of just what form it may be. Therefore, total metal content signifies nothing about speciation and form for any given metal within the original sample. There are many different forms or species that a metal may take in an

environmental, biological, industrial or consumer product sample. Metals may exist as the zero valent species (M°), these are non-ionic and bound, adsorbed or chelated to other substance(s). Many metals can also exist in one or more ionic forms and quite often the presence of more than one ionic form will be determined by, for example, the type of sample matrix, pH or salt concentrations that are present.

Some metals can exist in both cationic and anionic forms e.g. chromium (III), chromium (VI) and the chromate ion. A significant number of metals are present in the environment as stable oxyanions i.e. chromate or arsenate. Other metals exist as one or more cationic or anionic species. Various metals exist as stable, neutral organometallic compounds, covalently or ionically bound to organic moieties. Metals can also exist as organic chelates, generally ionic complexes that can have different equilibrium constants in aqueous media. In any event it is clear that metal speciation is an important analytical parameter, that is the identification and determination of which particular forms or species are present for any given metal in a given sample.

1.2 Metal Speciation by Gas Chromatography

Gas chromatography has shown a lot of promise in this field. The earliest studies of metal chelates were conducted by Lederer [8] who suggested that metal acetylacetonates might prove amenable to gas chromatography. However it was Biermann and Gesser [9] who described the first successful gas chromatographic elution of the acetylacetonates of beryllium, aluminium and chromium. This was followed by reports from Brandt and Heveran [10] on several metal diketonates, particularly chromium acetylacetonates. It is important for metal containing

compounds to have certain properties if they are to be analysed by gas chromatography. These can be summarised as follows,

(i) the compounds must be volatile.

(ii) they must be stable at temperatures required to maintain sufficient vapour pressures for the chromatographic elution.

(iii) they should be easily formed and isolated.

(iv) it is an advantage if special detection properties are present e.g. halogen in electron capture detectors.

The above factors influenced the use of B-diketones and particularly the fluorinated chelates derived from acetylacetone (ACAC), namely trifluoroacetylacetone (TFA) and hexafluoroacetylacetone (HFA), figure 1.1

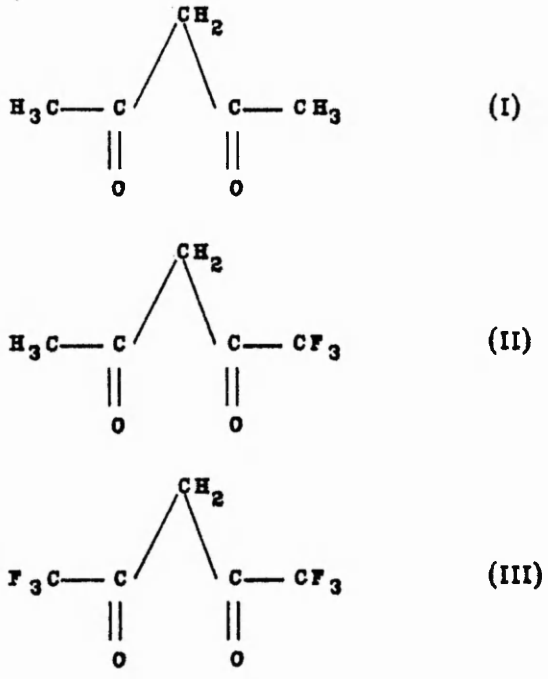

Figure 1.1 (I) Acetylacetone (ACAC), (II) Trifluoroacetylacetone (TFA), (III) Hexafluoroacetylacetone (HFA).

These compounds form stable, highly volatile chelates with aluminium (III), beryllium (II), chromium (III), rhodium and many other metal ions [12-19], figure 1.2

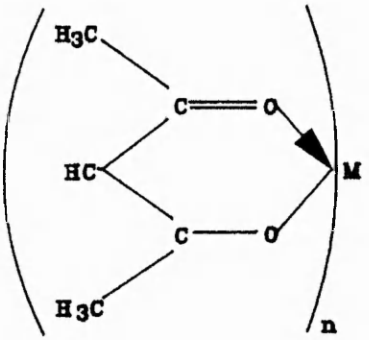

Figure 1.2 Acetylacetonate structure where n is the metal ion valency and M is the metal ion.

Chelates of hexafluoroacetylacetone were first examined by Moshier and Sievers [11] who found them to be more readily eluted than the acetylacetonates and trifluoroacetylacetonates at column temperatures only a little above room temperature. Aluminium, beryllium and chromium hexafluoroacetylacetonates are exceptionally volatile and elute before the solvent in many chromatograms. This is illustrated by the beryllium complex in figure 1.3,

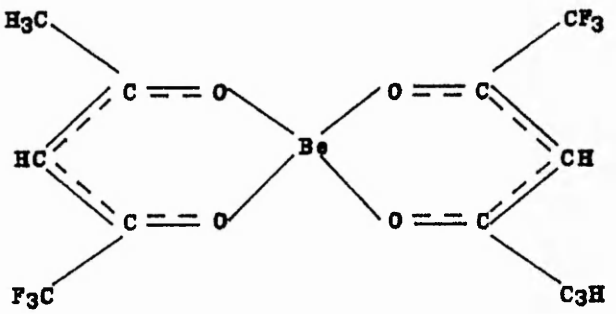

Figure 1.3 Beryllium acetylacetonate

Further developments in chelate gas chromatography have been discussed [20] including the use of a range of ligands, for example, diethyl and dialkyldithiocarbamates [21-24] for nickel, copper, lead, cadmium, zinc, palladium, arsenic, rhodium, selenium and platinum analysis. Dithiocarbamate complexes take the form shown in figure 1.4

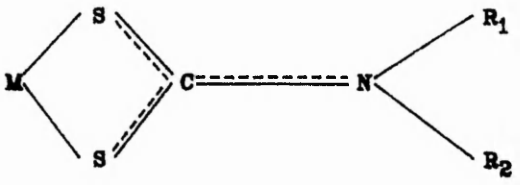

Figure 1.4 Dithiocarbamate complex where R_1 and R_2 are organic groups and M is a metal ion, charges have been omitted.

It is unfortunate that many limitations exist with the use of gas chromatography in trace metal analysis that ultimately inhibit its widespread use. Several metal HFA's are formed which incorporate co-ordinated water molecules making chromatography more difficult due to possible dehydration and polymerisation during chromatography. In addition HFA readily forms a tetrahydroxy compound [27] with water which is a much poorer co-ordinating moiety than the anhydrous B-diketonates. An example is shown in figure 1.5.

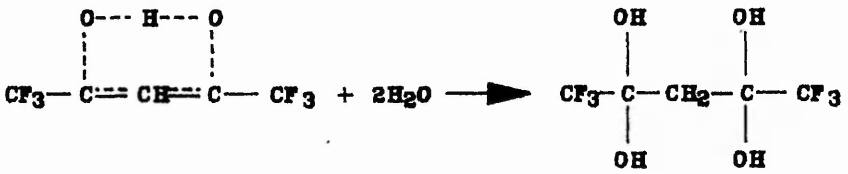

Figure 1.5 Formation of tetrahydroxy HFA complex.

This necessitates special sample introduction techniques such as enclosing the injection port in a dry box. Special precautions must also be taken to eliminate traces of moisture from the carrier gas. The resulting low yields of metal dithiocarbamates limit their use, even though fluorinated dithiocarbamates give a very high increase in volatility with unchanged thermal stability.

A number of metal halides are volatile and can be chromatographed in the gas phase. In the earlier work, Freiser [109] reported the separation of tin (IV) chloride and titanium (IV) chloride on a column containing n-hexadecane (Figure 1.6), and Juvet and Vachi [110] described the separation of antimony (III) chloride and titanium (IV) chloride with a fused salt stationary phase.

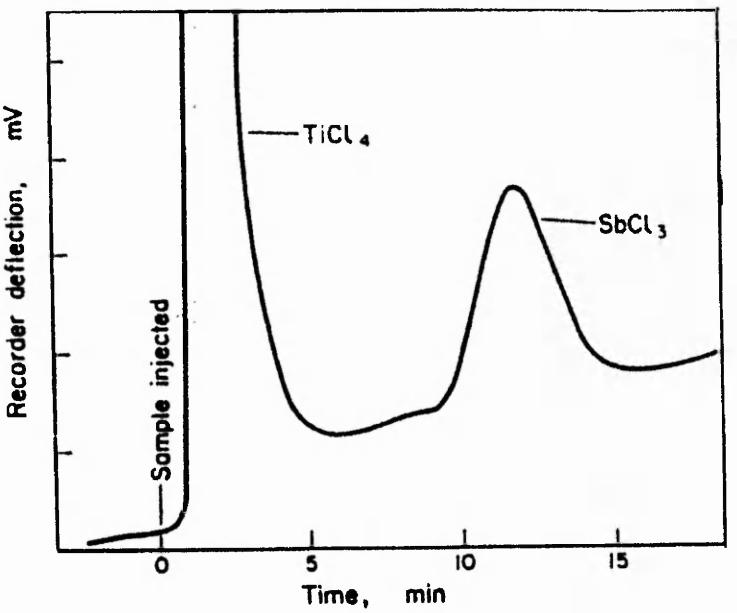

Figure 1.6 Separation of $TiCl_4$ and $SBCl_3$. Column: borosilicate glass, 12ft x 6 mm o.d., containing $BiCl_3$-$PbCl_2$ eutectic mixture on C-22 firebrick. Column temp.: 240°C.

Several metal chlorides have boiling points under 350°C (Table 1.1).

Metal	Boiling Point (°C)	Metal	Boiling Point (°C)
Boron (III)	12.5	Antimony (III)	222.3
Silicon (IV)	57.6	Niobium (V)	240.5
Germanium (IV)	83.1	Tantalum (V)	242.0
Tin (IV)	114.1	Gold (III)	265.0 (sub)
Arsenic (III)	130.2	Molybdenum (V)	275.6
Titanium (IV)	136.4	Tungsten (V)	300.0 (sub)
Antimony (V)	140.0	Zirconium (IV)	302.0
Vanadium (IV)	149.5	Mercury (II)	315.0
Aluminium (III)	177.8 (sub)	Iron (III)	315.0
Gallium (III)	201.2	Tungsten (VI)	346.7

Table 1.1 Boiling points of selected metal chlorides

The gas chromatographic behaviour of about half of the compounds listed has been studied and referenced earlier. However similar sample handling problems discussed in the previous paragraph are present and clearly limit the usefulness of such compounds in gas chromatography.

More recent investigations have included the use of capillary gas chromatography [25-26], which improves peak separation and overall sensitivity, but still suffers from on-column decomposition processes. Consequently, gas chromatography, although very useful for some metals forming volatile or semi-volatile chelates does appear to be somewhat lacking as a general method for metal speciation.

1.3 High Performance Liquid Chromatography (HPLC)

The application of High Performance Liquid Chromatography (HPLC) to the separation and determination of inorganics has lagged significantly behind the numerous advances reported in HPLC methodology for the

determination of organic compounds. Traditionally, cation exchange chromatography has been employed for the analysis of metal ions and has been extensively reviewed [28]. Trace metal analysis has also performed by thin layer chromatography and has been reviewed [29], however these methods yield results which are only semi-quantitative in nature.

1.3.1 Detection Methods in HPLC

True metal speciation is difficult to achieve without a detection system that is unique in its response for the particular metal of interest. Most conventional HPLC detectors today are general bulk property detectors which are non-selective and do not provide a great deal of specificity for a particular metal present in any given HPLC peak [30]. Thus, Ultra Violet (UV), Refractive Index (RI), Fluorescence Detection (FD), Conductivity Detection (CD), Electrochemical Detection (ECD) and Mass Spectrometry (MS) do not necessarily provide element specific detection as HPLC detectors. True metal speciation calls for good chromatographic separation, together with element specific or element selective type detectors, e.g. FAA, GFAA, DCP, ICP, and atomic fluorescence as defined in section 1.3.2.

1.3.2 HPLC-AA Techniques

The spectroscopic technique which has probably been used above all others for identifying is that of HPLC coupled to an atomic absorption spectrophotometer [31-34]. In general atomic absorption instrumentation falls into two discrete modes of sample introduction - atomisation, these being flame atomic absorption (FAA) and graphite furnace atomic absortpion (GFAA), both of which have been interfaced with HPLC. GFAA

offers significantly lower detection limits than FAA. However, GFAA operation requires a non-continuous, off-line sample introduction scheme. This is because the GFAA operation requires a discrete set of steps for final observation of the radiation absorbance phenomenon by the metal atom populations, formed from the sample solutions by a series of atomisation processes [2,6,35]. Although FAA permits on-line, continuous introduction of HPLC eluants directly into the flame, for certain mobile phases, it does not provide practical detection limits for most metals/elements.

Thus although HPLC-FAA would provide an on-line, continuous real time readout of HPLC eluants (which contain the elements of interest) it cannot as yet, provide suitable minimum detection limits for most industrial applications where sub part per million levels are of interest. A further limiting factor is the hollow cathode lamp, which at any one time can only be used to quantify one element. Therefore, most of the published HPLC-AA work has involved the offline, semi-continuous use of HPLC-GFAA, with an understanding that this is a less than ideal situation [31,36-40]. It is unfortunate that such a linked system cannot be investigated within the context of this project. This was due to the lack of availability of a suitable HPLC system. The project has therefore focused on the graphite furnace aspect of detection of trace metals, following their extraction from the relevant media, using a suitable chelating agent i.e. 8-hydroxyquinoline. The quantifying of the elemental content has focussed on the aqueous aliquot using the Shimadzu AA670 Atomic Absorption Spectrophotometer (section 2.4). Consequently having known the initial metal concentration, calculations can be carried out to calculate the extraction efficieny of the system being used.

1.4 Atomic Absorption

1.4.1 History

In 1859 and 1860 Kirchoff a physicist and Bunsen [41-42] a chemist, explained the origin of Fraunhofers lines and described the analytical utility of flame emission measurements and the conditions necessary for observing atomic absorption. An important part of their apparatus was the burner which Bunsen had invented a few years earlier. This burner enabled spectral observations to be made on a non-luminous, nearly transparent flame. Kirchoff [41,43] dealt with the general laws of emission and absorption which states that the ratio of the emission power (E) and absorption power (A) of a body depends only on the temperature of the body and not on its nature. The law is usually expressed as,

$$E/A = K(\lambda T) \qquad \text{.....(1)}$$

where $k(\lambda T)$ is a function of wavelength amd temperature.

Kirchoff also observed that bright lines, which could be seen in the flame spectrum when a metal salt was introduced, became dark lines if radiation of sufficient intensity was placed behind the flame. Such findings were used by Kirchoff to explain the composition of the sun's atmosphere, which ultimatlely led to experimentation with flames at different temperatures and with various alkali salts with known spectra and showed that the spectrum of a substance is entirely independant of the counter ions with which they are associated.

In spite of the potential of such a new technique it was many years before atomic absorption had been developed sufficiently for routine analysis. Emission spectrochemical analysis underwent extensive growth during the two decades from 1930-1950, based largely on electrical excitation. Flame sources were not used for this early work because only a few elements could be excited by the flame temperatures utilised. Early attempts at flame quantitative analysis were limited by insufficient sample introduction methods. The pneumatic nebuliser was subsequently developed by Gouy [44] as early as 1879, whilst he was investigating emission processes not quantitative analysis. The modern era of flame photometry began in about 1929 with the work of Lundegardh [49] a Swedish agronomist. He used a pre-mixed air acetylene flame, pneumatic nebuliser sample introduction and photographic detection. Eventually he developed a completely automated system that changed samples, controlled the photographic exposure, developed the exposed film, and produced a micro-photometer trace of the spectral line. Lundegardh tried direct photometry of the flame emission, also using photography [50], and also developed the spark-in-flame method [51-52] in which a condensed spark discharge was passed through the flame to enhance excitation of some elements. In 1934 Jansen et al [53-54] improved on direct photometry while Schwiknecht [55] observed sodium and potassium lines from the flame using filters. The filter photometers used selenium barrier layer photocells with galvanometers and led to the first commercial flame instruments produced by Evans Electro Selenium (EEL). This work has been reviewed by Koirtyohann [45]. The decade of the 1950's saw rapid expansion of the application of the flame methods. The advantages of using organic solvents, rather than water, and of chelate extraction techniques of the elements of

interest was developed by Dean et al [56,57]. Internal standardisation in filter instruments was developed by Hermann [46] in Germany, a multi-channel flame instrument for the determination of alkali and alkaline earth elements in the biological materials was described by Margoshes and Vallee [58]. The fuel rich flame which aided in the atomisation of oxide forming elements was developed by Fassel [64], and the use of high temperature flame burning cyanogen and oxygen was described by Vallee and Bartholomay [59].

Analytical atomic absorption was first described as a specific quantitative technique in 1955 by Walsh and Alkemade [47-48]. Kirchoff [42] somewhat belatedly described the conditions necessary for atomic absorption and Paschen had described the use of hollow cathode lamps in 1923.

The delay in the analytical use of atomic absorption can be attributed to the early flame work of Lundegardh [49], which was based on photographic detection methods. Atomic absorption can be carried out using photographic detectors, but it is much less convenient than recording the emission signal. Walsh [47] pointed out, when seriously examining the potential of atomic absorption as an analytical technique, that in order to measure the absorption coefficient of a given line in a white continuum, a spectrograph with a resolution of something like 500,000 lines per centimetre would be necessary. This is not practicable since the energy passed by the small spectral slit width would be too low to be measured by standard photoelectric methods. In any case the practical development of atomic absorption as an analytical method could hardly have preceded the introduction of electrical detection systems, since hollow cathode lamps are low energy sources. The use of photomultiplier detection and a-c amplification were

essential. Atomic absorption developed slowly in the next decade, but enjoyed rapid growth in the 1960's. The major flame atomisation technique at this time was the pre-mixed air acetylene flame, which could be used for the analysis of about thirty elements. Atomic absorption was extended to the refractory elements by the introduction of the nitrous oxide-acetylene flame. This flame showed the advantage of high temperature and strong reducing power but still had sufficiently low burning velocity to be used in burners of the Lundegardh type which was standard for atomic absorption at that time.

1.4.2 Principles of Atomic Absorption

Bohr postulated that various energy levels existed within an atom and that for an electron to be promoted between energy levels, an exact quantity of energy (i.e a photon) would be required to facilitate such a transition. An atom is said to be in its ground state when its electrons occupy their lowest energy level. When energy is transferred to a population of such atoms by means of thermal or electrical excitation, as in the various forms of emission spectroscopy, the transfer takes place by means of collision processes. The amount of energy transferred may vary considerably from atom to atom, resulting in a number of different excitation states throughout the population. However the proportion of excited to ground state atoms in a population, at a given temperature, can be considered with the aid of the Boltzmann relationship,

$$N_m/N_n = g_m/g_n \exp\{ -(E_m-E_n)/KT \} \quad \ldots\ldots\ldots\ldots(2)$$

where N is the number of atoms in a state n or m, g is the statistical weighting for a particular state and K is the Boltzmann constant. Examples of this relationship are given in table 1.2 where calculated Nm/Nn ratio's for caesium, sodium, calcium and zinc, covering a range of temperatures, are illustrated. In the cases quoted m refers to the first excited state and n is the ground state. The very low proportion of atoms in the first excited state, even at temperatures of 3000°K indicates that absorption of radiation, other than that originating from a transition involving the ground state, would be very small.

Element	Line(nm)	g_m/g_n	Nm/Nn			
			2000°K	3000°K	4000°K	5000°K
Cs	852.1	2	4.44×10^{-4}	7.24×10^{-3}	2.98×10^{-2}	6.82×10^{-2}
Na	589.1	2	9.86×10^{-6}	5.88×10^{-4}	4.44×10^{-3}	1.51×10^{-2}
Ca	422.7	3	1.21×10^{-7}	3.69×10^{-5}	6.03×10^{-4}	3.33×10^{-3}
Zn	213.9	3	7.29×10^{-15}	5.58×10^{-10}	1.48×10^{-7}	4.32×10^{-6}

Table 1.2 Atom populations

It is therefore obvious that the role of the flame temperature in producing a stable concentration of ground state atoms is paramount to the whole success of the atomic absorption process. Typical flame types and their temperatures are illustrated in table 1.3.

Oxidant - Fuel	Temperature (°C)
Air-Hydrogen	2000-2050
Air-Acetylene	2125-2400
Nitrous oxide-Acetylene	2600-2800

Table 1.3 Temperature of selected flames.

The longest practical and therefore most widely propagated method for the dissociation of a sample into atoms in atomic absorption spectroscopy is the spraying of a solution into a flame. Next to this, flameless atomisation procedures have gained considerable importance in recent years, and especially atomisation in a graphite tube heated by electrical resistance. Since the mechanisms of the procedures are completely different, atomisation in flame and flameless applications are treated separately in sections 1.4.3 and 1.4.4.

1.4.3 Flame Atomic Absorption

The basic flame atomic absorption spectrophotometer is shown in figure 1.7 The typical natural width of an atomic spectral line is of the order of 10^{-5}nm. Radiation from the source lamp, generating a sharp line spectrum characteristic of the desired element, passes through the flame into which the sample solution is sprayed as a fine mist. The region of the spectrum in the immediate neighbourhood of the resonance line to be measured is selected by the monochromator. The isolated line falls onto the detector, a photomultiplier, the output of which is amplified and recorded on a meter or chart recorder.

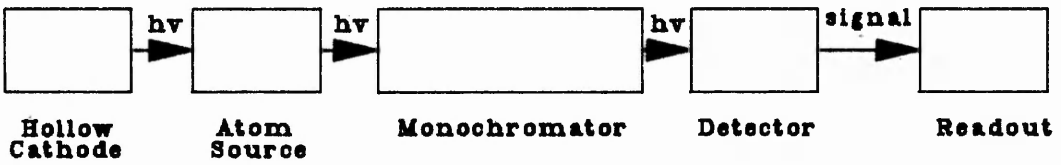

Figure 1.7 Functional parts of an Atomic Absorption Spectrophotometer

The intensity of the resonance line is measured with and without the sample passing into the flame. The ratio of these readings is a measure of the absorption and therefore of the amount of the element being determined, corrections for a sample matrix blank being made where appropriate. As an atom absorbs light at discrete wavelengths, it is necessary to use a spectral line source which emits wavelengths in the elemental line spectra of interest, if the absorption measurements are to be made with maximum selectivity and sensitivity. The wavelengths used for the elements relevant to this project which satisfy such requirements are summarised in table 1.4.

ELEMENT	RESONANT WAVELENGTH (nm)
Copper	324.8
Lead	217.0
Aluminium	309.3
Iron	248.3

Table 1.4 Elemental Line Spectra

The hollow cathode lamp is an excellent bright light source for most of the elements determined by atomic absorption. A hollow cathode lamp (figure 1.8) consists of a hollow cylindrical cathode (6-8mm diameter) of the metal whose spectrum is to be produced. The anode and cathode are sealed in a glass envelope filled with either neon or argon. A silica window transparent to the emitted radiation is fused to the end of the glass cylinder.

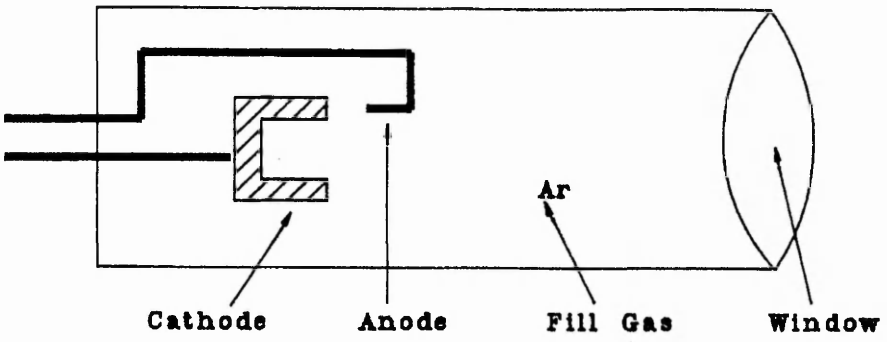

Figure 1.8 Hollow Cathode Lamp

When an electrical potential is applied between the anode and cathode, some of the filler gas atoms are ionised. These positively charged ions accelerate through the electrical field to collide with the negatively charged cathode and dislodge individual metal atoms in a process called "sputtering". Sputtered metal atoms are excited through collision with further filler gas ions. The excited atoms lose energy as emission lines characteristic of the element (figure 1.9).

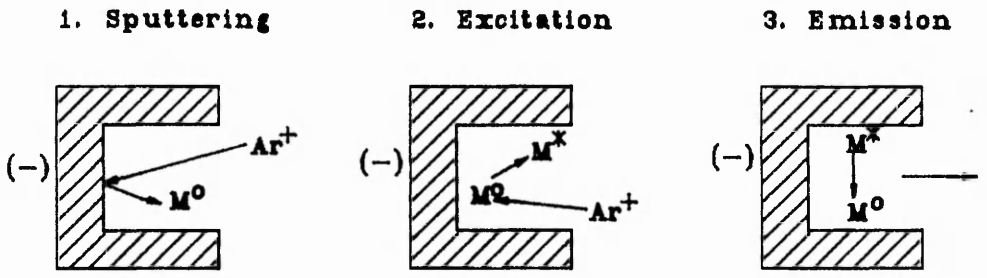

Figure 1.9 Hollow Cathode Lamp Process

The atomiser of an atomic absorption spectrophotometer must generate ground state atom populations in the optical path of the photometer. The most common technique used is the direct aspiration of the sample solution into a flame, usually via a pre-mix burner system (figure 1.10).

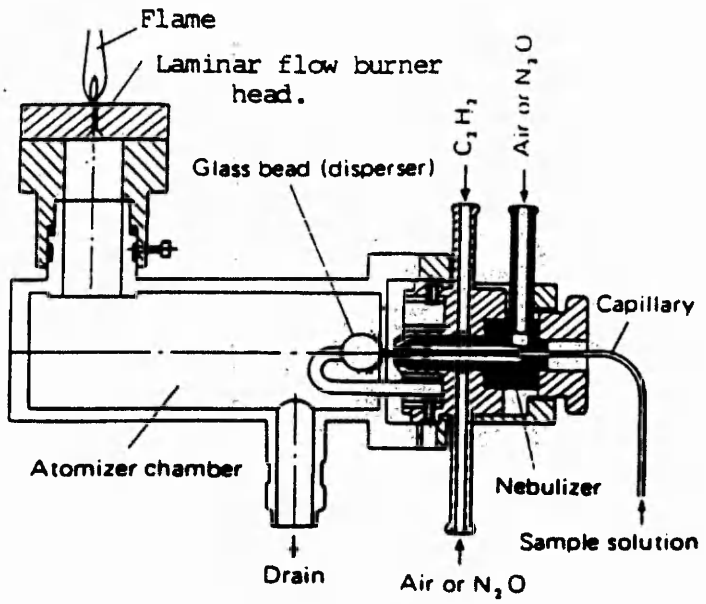

Figure 1.10 Pre-mix Type Laminar Flow Burner

In this system, typical of that used on the Shimadzu AA670, the analyte solution is aspirated through a nebuliser and sprayed as a fine aerosol into the mixing chamber. The sample aerosol is mixed with the fuel and oxidant gases and carried to the burner head. Pre-mixing of the sample and flame gases gives better atomisation, thus reducing chemical interferences. The nebuliser is a precision sprayer which sucks up sample solution through the capillary and feeds it into the atomiser chamber, an impact glass bead (disperser) is placed near the outlet of the nebuliser, such that the mist collides with it at great speed to be further dispersed into a fine mist. Larger droplets are removed through the drain, which accounts for approximately 85-90% of the sample. Because only the free mist and evaporated sample reach the flame, an even burning takes place, resulting in a quiet, stable background signal.

1.4.4 Background Absorbance and Correction

Background absorption or molecular scatter is an interference which causes absorbance of the resonance line by molecular species formed in the flame from the sample matrix. The net result is an increase in the absorption signal due to light scattering by solid particles passing across the light beam. The magnitude of this effect varies considerably with the wavelength at which measurements are being taken. For particles having a diameter of less than one tenth of the wavelength of the incident radiation, the amount of scatter according to Raleigh theory is proportional to X^{-4}, hence towards the lower wavelengths a very sharp increase in the effects of scatter are experienced. To compensate for this problem, the background absorption must be measured and subtracted from the total absorption measured to determine the atomic absorption signal. This can be carried out by utilising a nonatomic emission line very close (0.1nm) to the atomic line for measuring analyte atomic absorption, but far enough away so that atomic absorption is not observed. However nonatomic absorbing lines are not always available. An alternative is a continuum source, which has essentially zero atomic absorption sensitivity at the normal resolution for atomic absorption instruments, and can henced be used to measure only the background contribution to the absorption signal. However as both beams (hollow cathode and deuterium arc) are positioned so as to be combined and pass through the flame, there is a need to separate and measure both signals independantly. This can be achieved by having different frequencies for both light sources on a time sequence. Both result in correction moment after moment. With respect to the Shimadzu AA670 the frequency of the hollow cathode lamp is set at 500Hz and the deuterium arc at 1000Hz. The signal from both components is separated and then further processed by two synchronous rectifiers.

The flame processes involved in quantifying a respective element are as follows.

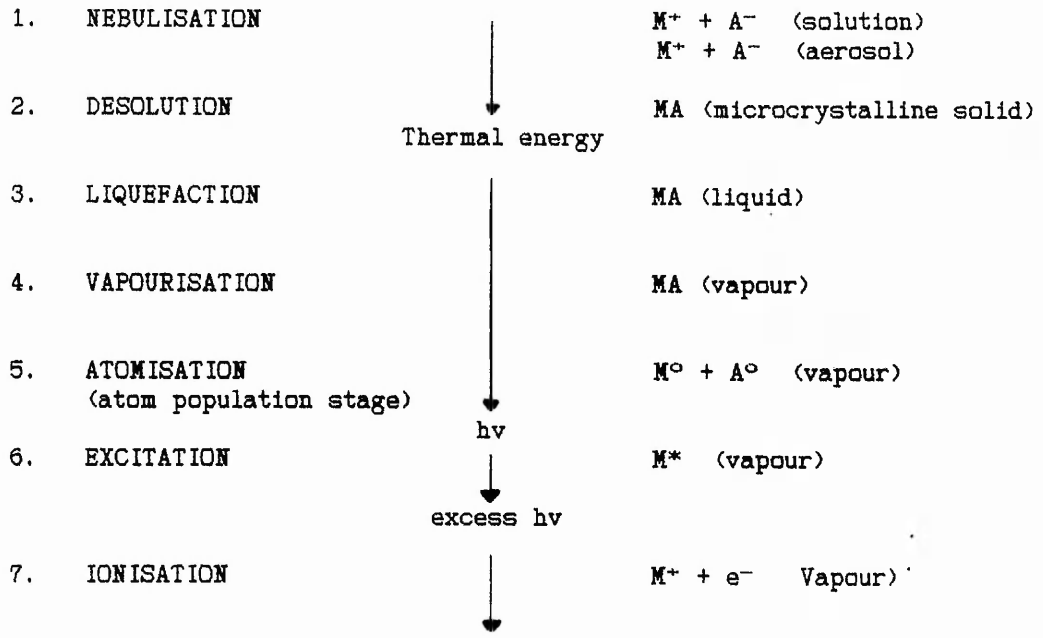

where M^+ is the analyte metal, A^- is the anion present and M° is the absorbing species.

Only stages 1-6 are of interest in atomic absorption, energy supplied in excess of that required for atomisation could produce ionisation, which would reduce the signal corresponding to the total element content.

The flame most frequently used in atomic absorption is the air-acetylene flame. For many elements it offers a suitable environment and a temperature sufficient for atomisation. Ionisation only occurs in a few cases, for example, gold, sodium, and potassium. However the air-acetylene flame temperature is still sufficient to dissociate a large number of refractory compounds or to prevent their formation in the flame. A great deal of work was carried out to overcome this problem in a hot oxygen-acetylene flame [61-66] frequently using organic solvents

[67-68] or even an oxygen cyanogen flame [69]. The addition of complexing agents was also investigated [70].

The most important development in flames was the introduction of the nitrous oxide-acetylene flame by Willis on 1965 [71]. As a result of its low combustion speed, this hot flame offers a favourable chemical, thermal and optical environment for virtually all metals that give difficulties in the air-acetylene flame. A large number of workers investigated the nitrous oxide flame soon after its introduction [72-79] and found it was largely free of interferences [80-82]. Marks and Welder [83] investigated the influence of the flame composition and instrumental settings on interferences in the nitrous oxide-acetylene flame. They established that the height of observation and the oxidant/fuel gas ratio had the strongest influences, and that with the correct selection of these parameters, interferences were reduced. The observation of the level of absorption is recorded when a steady signal is obtained on aspiration of the sample into the flame, either as direct reading or integration (to smooth signal, figure 1.11) over 5-10 seconds.

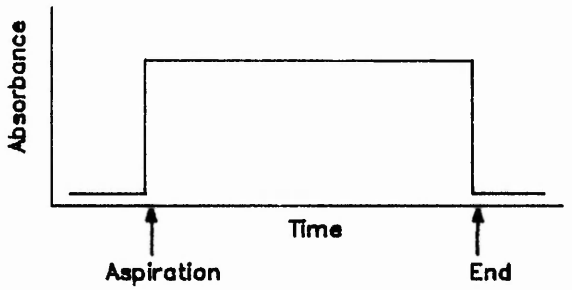

Figure 1.11 Steady State Signal

1.4.5 Alternative Atomisation Techniques

Conventional flame atomic absorption, with all its advantages over competing techniques, is limited in sensitivity by a relatively poor sampling efficiency and a lack of sensitivity for some elements,

particularly those producing refractory oxides or intermediates in the flame process. In the pre-mix burner design only a small fraction of the aspirated solution reaches the flame.

One of the first successful approaches to improving atomic absorption sensitivity for easily dissociated elements was the sampling boat, first described by Kahn et al [84]. The technique utilises a tantalum boat affixed to a mechanism which allows the operator to slide the boat into, and out of, the flame. The sample is first dried before entering the flame, so as to prevent losses from forced evaporation. Although the air-acetylene may be used, the boat itself may not attain the flame temperature, and the method is therefore limited to elements which are readily atomised such as arsenic, cadmium, indium, lead, mercury, selenium, silver and thallium. Detection limits depend on the type and volume of sample used. Typical detection limits for cadmium and silver, for a 1ml sample, are of the order of 0.0001ug ml^{-1}, some fifty times better than the conventional methods.

This method rapidly became very popular because elements of interest for toxicology and enviromental control could be determined with increased sensitivity, and biological samples such as urine and blood could be analysed directly [85]. The boat technique has also been applied to the analysis of water [86], milk [87] and other foodstuffs [88]. Later Delves [89] suggested a modification of the boat technique, which he had developed specially for the detection of lead in blood. The tantalum boat was replaced with a small round nickel cup, and to increase the sensitivity, an open tube was mounted over this. The beam path passed through the tube and the element of interest was atomised in the tube. This tube measured the residence time of the atoms in the beam path.

Other approaches to improving the sensitivity of atomic absorption is the use of the cold vapour mercury system [90], which is specific for low levels of mercury and the use of a hydride generation technique which is somewhat similar to the cold vapour mercury sampling system. In hydride generation the gaseous hydrides of certain metals are chemically produced by the addition of sodium borohydride up to 25ml of sample in a reaction flask. The flask is sealed off and the gaseous hydrides and hydrogen produced by the reaction are swept by an argon purge into an argon-hydrogen entrained air flame or alternatively into a heated quartz cell. When the sample vapour is atomised in the flame or heated cell, a peak signal is produced, the height of which is proportional to the amount of analyte in the sample.

1.5 Graphite Furnace Atomic Absorption

The search for techniques to improve the sensitivity of atomic absorption led ultimately to the graphite furnace. With this device many elements can be determined at concentrations a thousand times lower than can be detected by flame atomic absorption. The forerunner of all electrothermal atomisation devices as we know them today was the furnace of A.S.King [91] of the Mount Wilson Observatory. This was a graphite tube electrically heated to about 3000°C in an atmosphere of hydrogen. The neutral spectra of a number of elements were studied, sodium, calcium, iron, copper, magnesium and caesium at that time and progressing to tungsten and rhodium in 1932. However no use of the principle of electrothermal atomisation for quantitative analytical measurements was made until 1956. S.L.Mandelohtam [92] used an electrothermal vapourisation technique to separate and pre-concentrate trace elements onto a graphite electrode prior to emission spectrochemical analysis.

Three years later in 1959 L'vov [93] began to publish his classic work on the application of electrothermal furnace atomisers for quantitative atomic absorption analysis [94].

In the first L'vov furnace (Figure 1.12) the sample to be analysed was introduced into the horizontal graphite tube through a hole on the underside.

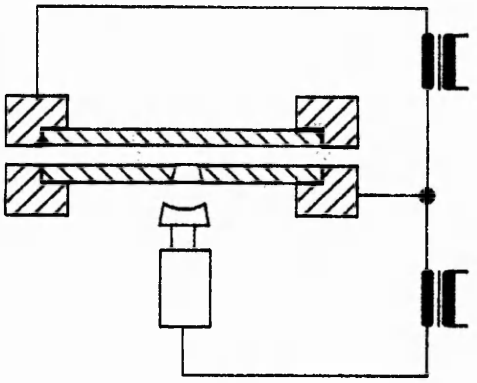

Figure 1.12 L'vov Furnace.

The furnace was 5-10cm in length and 3mm in diameter. Although the tube was heated, the atomisation temperature was obtained by striking an arc between the sample electrode and the graphite furnace tube. In later models the sample was atomised by passing a current through the narrowest section of the electrode to the furnace tube. This device was placed in a purged chamber and a batch of prepared sample electrodes placed on a turntable. However the use of this type of atomiser as a serious tool in analytical atomic absorption was not really considered until 1968 when both Woodriff [95] and Massmann [96] published work on enclosed graphite furnaces which were directly developed from L'vov's ideas. It is L'vov's ideas that have been utilised in the internal construction of the graphite furnace used in the Shimadzu AA670 Atomic Absorption Spectrophotometer as illustrated in figure 1.13.

As is evident from the diagram, the heating element graphite tube is surrounded by a pair of graphite holders. The furnace is further surrounded by a pair of symmetric metallic blocks (cooling blocks) which are connected with the power cables. Cooling water runs through these blocks so as to prevent damage due to high temperature.

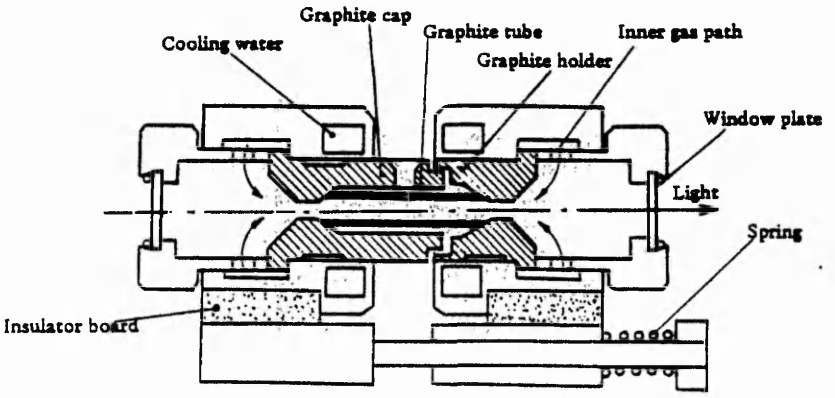

Figure 1.13 Construction of Graphite Tube and its Surroundings.

The graphite caps and holders on both sides are firmly pressed against the centre by threaded cylinders (window plate holders) from the outsides. A quartz window plate is mounted on the end plate each side. In order to prevent the heating element from being oxidised at the higher temperatures, inert gas (argon) is fed through both the inner and outer parts of the graphite tube. The inner gas flows from left and right hand side spaces into the tube interior as shown by arrows in figure 1.13 and upward from the sample injection hole of the tube. The outer gas is fed through two holes on the side of the graphite cap and holder into the space between the tube and the cap.

Electrical contact is ensured as the graphite tube is firmly held by the spring force between the graphite cap and holder. The graphite cap is provided with a hole of 2mm diameter at the middle of the graphite tube (not shown in figure 1.13). The temperature sensor monitors the emission from the graphite tube through this hole.

The graphite tube heating element is 30mm in length, 4.2mm internal diameter and 6.15mm external diameter. A sample injection hole of 2mm diameter is provided at the centre of the tube, and the sample is fed into the tube by using a micro-syringe through this hole. Two holes are perforated 7mm from the centre on both sides, for increasing the electrical resistance to augment heat production, so that the uniform temperature distribution is ensured within the tube in the axial direction.

1.5.1 Electrothermal Atomisers

The basic difference in atomisation techniques between the graphite furnace and the flame, results in a difference in the absorption response, which in turn alters some of the basic concepts of flame atomic absorption. The absorption signal for flame atomic absorption is steady state, that is, as long as the sample is being aspirated into the burner chamber the atom population in the flame is maintained and the absorbance is constant.

In graphite furnace absorption however, a sample aliquot of only a few microlitres is introduced into the furnace. The aliquot is totally consumed at atomisation, depending on the application, in a matter of only a few seconds or milliseconds. The resultant absorption signal is therefore transient in nature, reflecting the rapidly varying atom concentration within the furnace. However the question of which type of

measurement, peak height or peak area, is the better for calibration purposes still remains and has been the subject of previous investigations [59-60]. It is clearly advantageous for the analyst to be able to check the general shape of the absorbance peaks either on a fast recorder or by oscilloscope presentation, in order to be able to decide whether peak height or peak area measurement are likely to be the more satisfactory, in a given analysis. Simple definition of the two types of measurement are,

(i) peak height is equivalent to the concentration of analyte in the atomiser at any given time.

(ii) peak area is equivalent to the total amount of analyte introduced into the atomiser.

A number of factors contribute to preventing the recording or measurement of the true absorbance peak (figure 1.14a). In addition to instrumental electronic lag, include slow atomisation caused by too low an atomisation temperature and too high a dead volume in the furnace tube. Slow atomisation has the effect of lowering the peak absorbance and increasing the half width, as fewer than the maximum number of atoms contribute to the peak absorbance (see figure 1.14b)

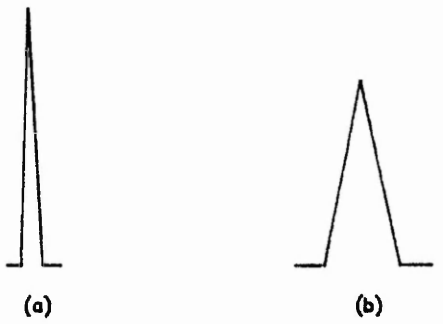

Figure 1.14 Representation of Absorbance Signal

In large tubes there may be a volume containing atoms capable of absorbing radiation but which is missed by the radiation beam. This

simply results in lower peaks. From a theoretical viewpoint, integration (peak area) is preferable for measurements at relatively low temperatures or low atomisation rates. However variation in matrix composition can cause differences in atomisation rate and subsequent differences in peak height. Peak area measurements can minimise this problem, but it is also avoided by close matching of samples and standards. The use of peak area measurement can give erroneous results where multiple peaks are observed (figure 1.15) during the atomisation stage (due to background signals).

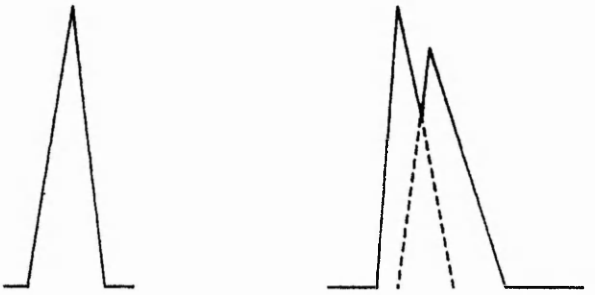

Figure 1.15 Depicts problems with peak area measurement.

The main problem being the difficulty in distinguishing between the various peaks. A possible advantage of peak area measurements is that the linear calibration range can be extended, provided it is not already limited by deviations from the absorption equation, by use of comparatively low atomisation temperatures in order to reduce analytical sensitivity.

$$A = Kcl \qquad \text{.....(3)}$$

where A is the recorded absorbance, K is the absorption coefficient, l is the sample optical path length and c the analyte concentration. The temperature programming involved in graphite furnace atomic absorption gives electrothermal atomisers the ability to separate the corresponding flame processes of desolvation, atomisation etc, therefore imparting a

degree of control to the technique which is unattainable with a flame. Different instrument manufacturers have developed their own variations, but all basically provide a system which, once the sample is injected onto the graphite tube, enables three separately controlled heating cycles to be applied to the sample.

(i) Drying

The importance of correct drying conditions cannot be over emphasised. During this phase the solvent is evaporated from the sample solution injected into the graphite tube. This step has to be achieved in a controlled manner such that there is a slow, even evaporation of the solvent from the matrix leaving behind the solid dried sample. The solvent must not be removed from the droplet by rapid boiling because the spitting and frothing actions which would then occur cause particles of the sample to be ejected. These particles can then be carried out of the graphite tube by the gas flow and 'lost'. The droplets behaviour was viewed throughout the drying stage to ensure that the correct drying time and temperature was being used.

(i) Ash

When trace metals are to be determined in varying amounts of matrix the ashing stage is the most significant. This stage heats the sample to the highest temperature possible in an attempt to remove the matrix, without any detectable loss of the element being determined. This requires the temperature and ashing duration to be optimised correctly, bearing in mind that the element of interest may be present in a form that is volatile at the temperature employed. In addition the element may be converted into a volatile form by the matrix or solvent system being used.

It is essential to study the chemistry of the analyte metal or the matrix in which it is present with the view of making the matrix more volatile than the element. The presence of high concentrations of alkali chlorides for example, not only causes high background absorbance problems, but also encourages formation of volatile forms of the analyte element. Such a matrix can be removed by the addition of an excess of ammonium nitrate to the sample solution (a matrix modifier). The following conversion then takes place during the ashing step,

$$NaCl + NH_4NO_3 \longrightarrow NaNO_3 + NH_4Cl \qquad .....(4)$$

Sodium Chloride boiling point, 1413°C

Ammonium Nitrate decomposes at 210°C

Sodium Nitrate decomposes at 380°C

Ammonium Chloride sublimes at 335°C

Thus all the resultant compounds are volatile below 500°C and can be successfully removed prior to atomisation of volatile elements. Other factors such as viscosity, surface tension, condensation effects and stable compounds formation will also contribute to the potential interferences that can be experienced. Consequently the optimisation of the instrument operating conditions and sample preparation are essential.

(iii) Atomisation

Such temperatures vary from element to element, but basically the analytical signal for each element is determined as a function of the atomisation temperature.

The three stages described, in addition to instrumental parameters and the chemical form of presenting the element of interest to the instrument, need to be optimised in order that interference effects can be reduced to a minimum. Upon completion of obtaining a satisfactory drying sequence, described in previous paragraphs, it is necessary to optimise the ash and atomisation temperatures by preparing the respective ash and atomisation curves. Utilising the drying sequence for each sample, the atomisation curve is defined in the absence of any ashing stage. An initial atomisation time and low temperature (such as 5 seconds at a setting of 1400°C) were set on the controller. The tube clean conditions were set at 3 seconds at nearly maximum power. A suitable volume, 10ul of an aqueous standard solution, was injected onto the graphite tube and the complete furnace program was carried out. The resulting peak height, if any, recorded during the atomisation step was plotted on a graph of peak height versus temperature. A total of three injections was carried out at each set of conditions and the atomisation temperature setting was increased before the next set of injections. As the power was increased the peak height also increased until the temperature is reached where the peak height does not increase (or the rate becomes much smaller). This gives the lowest temperature for complete atomisation. For the sample where a continually increasing peak height for increasing temperature is obtained, the point at which the rate of increase becomes smaller than the initial rate, is chosen. Then the selection of a lower temperature than maximum is normally advantageous because it results in increased tube lifetime, better precision of results, and in many cases reduced emission interferences. Such results are illustrated in 1.16a and 1.16b respectively.
When the best atomisation temperature is selected the correct time can be established by using a fast recorder speed at a known chart time, and

measuring the time taken for a peak to form and decay. The selected conditions for atomisation are left untouched on the controller.
To determine the correct ashing conditions a similar procedure is followed. The parameters are changed progressively whilst the drying, atomise and tube parameters remain constant. A time period of 20-30sec is usually chosen for this stage, this being a reasonable time to ash a typical matrix. The ash temperature settings are increased slowly from a lower power setting of about 150°C. Again triplicate peaks were obtained at each setting and a graph of peak height versus ash temperature was obtained.

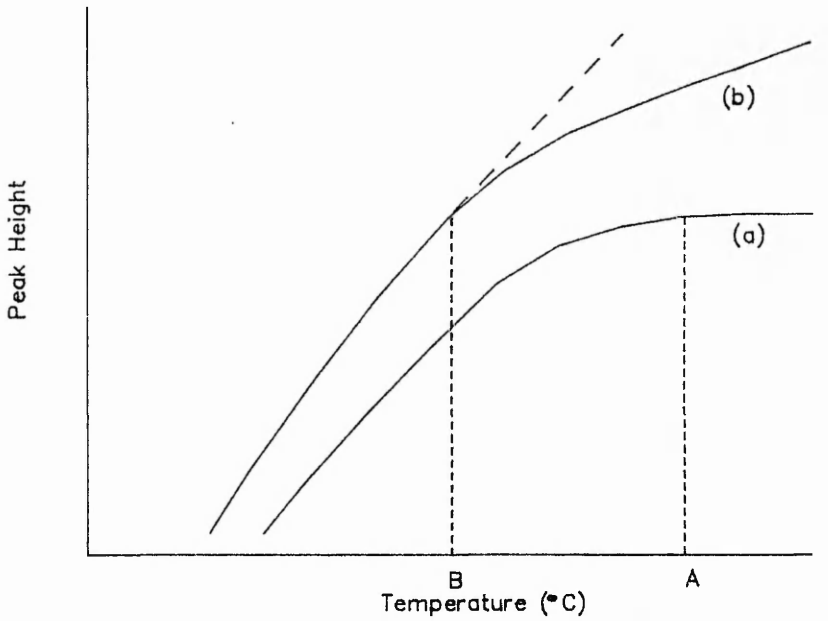

Figure 1.16 Selection of Atomisation Temperature.

This is typically a mirror image of the atomise graph because the measured peak height remains essentially constant until the point is reached where analyte begins to be lost. At this point the peak height diminishes rapidly with increased temperature setting. The safe ashing temperature is taken as the point 100°C approximately cooler than the turnover point, see figure 1.17.

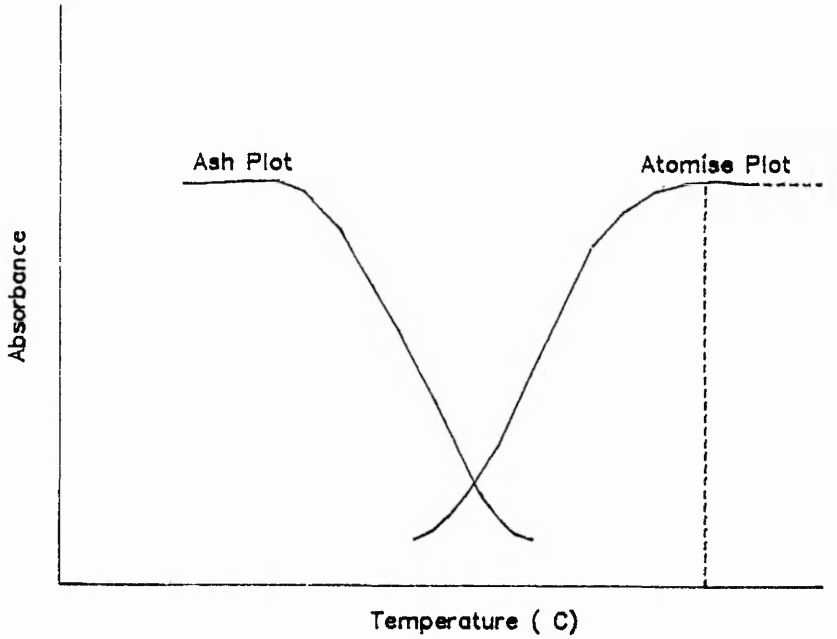

Figure 1.17 Ash/Atomisation Curve.

A successful ashing sequence should result in almost no visible vapour being produced during the atomisation phase, but this is not always possible. The smoke formed during atomisation has therefore to be compensated for by using background correction or by careful choice of atomisation conditions.

1.6 Solvent Extraction.

Despite the availability of the modern, more discriminatory methods of measurement, successful solutions to many analytical problems depend heavily on separation processes, and these have been utilised to good effect for many years. It was not until 1941 that Kolthoff and Sandell [97] gave the first quantitative description of the extraction process followed later by the likes of Stary [98] and Morrison and Freiser [99] who discussed the theoretical approach to the extraction of metal chelates.

Solvent extraction enjoys a favoured position among the separation techniques because of its ease, simplicity, speed and wide scope of application. Extraction procedures offer much to the analytical chemist, and are applicable to both macro and trace levels of metals. Simple apparatus for example, a separating funnel is required and the whole procedure takes only a few minutes to perform. Analysis of metals, is primarily concerned with samples in aqueous form. Liquid-liquid extraction thus involves an aqueous-organic solvent pair. Solubility in organic solvents is not a characteristic usually attributed to simple metal salts. As can be expected from their ionic nature, most metal salts are strong electrolytes whose relatively large solubility in aqueous media reflects the beneficial effect of the high dielectric constant of water on reducing the work required to separate the oppositely charged ions. An equally important factor is the tendancy of water to solvate the ions. In essentially all metal extraction systems some, or all, of the water molecules co-ordinated to the metal ions must be removed before it is possible to obtain a species that can be extracted into an organic solvent.

$$M^{n+} + n(HA)_{org} \longrightarrow (MA_n)_{org} + nH^{+} \qquad \text{.....(5)}$$

The formation of an uncharged species is a probable pre-requisite for extraction into organic solvents, which generally have a low dielectric constant. Such a species may be formed by metal containing ions through co-ordinates, involving chemical rather than physical bonds. In chelate extraction systems, compounds such as 8-hydroxyquinoline easily replace co-ordinated water from many metals to form neutral, essentially covalent chelate compounds many of which are soluble in organic solvents, such as hydrocarbons and chlorinated hydrocarbons.

1.6.1 8-Hydroxyquinoline (Oxine).

8-Hydroxyquinoline is a useful reagent for the extraction, separation and spectrophotometric detection of metal ions. It forms thermodynamically stable complexes and its extraction chemistry is well known [99]. The structure of oxine (figure 1.18) is such that the location of the hydroxyl group in relation to the nitrogen atom of the quinoline nucleus allow, upon reaction with the relevant metals, formation of five membered rings. The metal may be bound co-ordinately with either the nitrogen or oxygen atom.

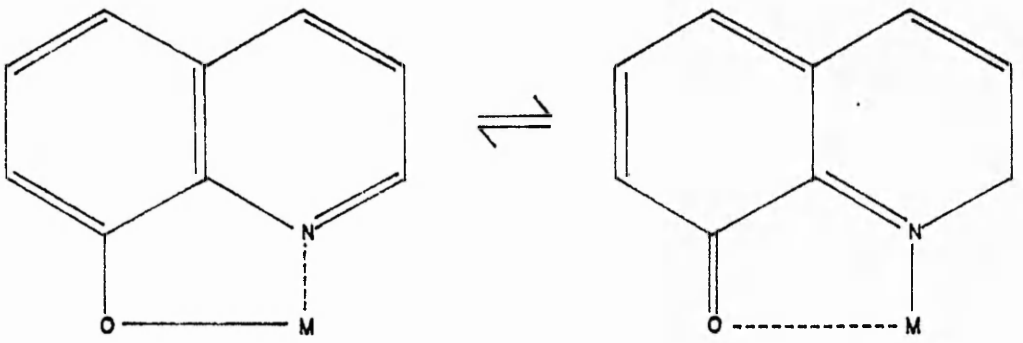

Figure 1.18 Structure of Oxine.

The versatility of oxine as a chelating agent has led to increased interest and this has gained momentum when considered in conjunction with the research into high performance liquid chromatographic (HPLC) techniques.

It would appear that oxine would be an ideal ligand to use for the separations of multielement mixtures by HPLC. This is due to its ability to complex with many metal ions to produce neutral chelates. Separations of metal-oxine chelates by column chromatography have been studied [100-103]. HPLC separations on hydrocarbon stationary phases

have also been reported [104]. In all modes the methodology has been limited by the decomposition of the complexes, mainly at trace level concentrations, on the stationary phase used.

The bulk of the chromatography to date has involved the use of silica gel as the stationary phase. This is mainly due to the fact that the complexes tend not to dissociate in organic solvents of low dielectric constant (e.g chloroform-methanol mixtures) which can be used as the chromatographic mobile phase. There are however problems with the use of silica gel in that the gel has to be exposed to solvents that are totally free of water. In addition the condition of the silica gel tends to change with time.

Other approaches, using 8-hydroxyquinoline, have been undertaken. These mainly involve the likes of cobalt and chromium [105] utilising reverse phase HPLC with pre-column derivatisation. Since several of these chelates possess native fluorescence, sensitivity could be improved considerably using this mode of detection. This is the case with respect to aluminium [106], whereby the oxinate was observed using fluorescence detection. In addition when considering some of the halogenated derivatives of oxines, which are used as fungicides or anti-infective agents. An additional HPLC method involving the separation of four 8-hydroxyquinolines (e.g oxine, 5-chloro-8-hydroxyquinoline, 5,7, dichloro-8-hydroxyquinoline and 5-chloro-7-iodo-8-hydroxyquinoline) and their fluorescence detection after post column derivatisation to the corresponding metal chelate has also been investigated [107]. The metals studied were magnesium (II), aluminium (III) and yttrium (III). Unfortunately precipitation, under alkaline conditions, of the aluminium and yttrium derivatives limited the success of the work to the magnesium chelates.

8-hydroxyquinoline is therefore a suitable chelating agent to study the extraction processes of selected metals. A study of the extraction steps and the overall efficiency of the process has therefore been carried out in this project.

1.7 Applications.

The role of the Engine Support Services Laboratory (ESSL) within Rolls Royce is one of wide and varied activities. Our prime responsibility is to support the rig and engine projects, both in the development and production environment and also to provide support to Rolls Royce customers.

The operation of the laboratory is divided into two mainstream activities, routine reactive work and method/technique development. The terminology, "routine reactive work", encompasses the prime responsibility to supporting our product through each stage of its development and ultimate production. This covers areas such as materials development, chemical processing, engine and rig health monitoring, environmental issues, fuel, lubricant and engine/rig emission quality and general investigative analytical analysis.

The area of method and technique development enables the laboratories to utilise and apply recent developments in analytical instrumentation and methodology, to maintain the company position at the forefront of technology.

Elemental analysis forms an integral part of laboratory activities as outlined below.

(a) **Fuels analysis** : severe demands are placed on aviation fuels as they pass through fuel delivery and combustion systems. The properties of fuel have a direct impact on engine

performance, reliability and service life of components in these systems. Two such properties of fuel that can be affected by the presence of trace elements are fuel thermal stability (108) and material compatability following combustion. Investigations into these areas is an ongoing activity and sensitive, accurate methods of analysis are obviously essential.

(b) **Lubricants** : A major concern with the analysis of lubricants is the identification and subsequent quantification of trace elements. The need for such analyses is related to engine health monitoring whereby the onset of component failure can be evaluated by monitoring certain elements indicative of component wear.

(c) **Environment** : The analysis of workplace atmospheres is a continuing exercise evaluating certain areas for a potential hazardous situation relating to the presence of particular elements of interest, e.g nickel, cobalt, chromium and cadmium.

(d) **Alloy analysis** : Analysis of alloys is an important area in the aero-engine. The need to be able to quantify a given element is essential, especially as the presence of certain trace elements can distort or enhance the physical and chemical properties of alloys. New alloys are continuously being developed and evaluated and require accurate analysis to fully characterise these materials.

(e) **Miscellaneous** : Investigational analysis and problem solving is a further important role of the laboratories. "what is it", "where is it from", and "how much is there", is an everyday request and requires the chemist to approach a given task, such as elemental analysis, in a variety of different ways.

that demand a high level of knowledge and experience. The need therefore to evaluate different techniques of sample preparation and analysis are essential if we are to maintain our ability to evaluate such problems. The techniques of extraction coupled with spectroscopy and chromatography were evaluated based on the equipment resident within the Engine Support Services Laboratory. Recommendations will be made as to their overall effectiveness and subsequent applicability within our environment.

SECTION 2.0

EXTRACTION STUDIES

SECTION 2.0 EXTRACTION STUDIES PAGE NO.

2.0 EXTRACTION STUDIES

The extraction of chelate compounds may be regarded as a heterogeneous chemical reaction. Although the extraction of such compounds involves a large number of equilibria, a quantitative description is possible in principle and is not too complex. Such calculations do however almost certainly involve basic assumptions, and omission of certain factors such as the production of certain intermediate complexes.

The theory of Stary [98], a simplified version of that of Morrison and Freiser [99], is based on the extraction equation,

$$M^{n+} + nHA_o \rightleftharpoons MAn_o + nH^+ \quad \text{.....(1)}$$

M^{n+} represents an aqueuos cation of charge n, MA and MA_n are the neutral (protonated) chelating ligand and neutral chelate and because of their hydrophobic nature both are considered to be largely concentrated in the organic phase. This two phase equilibrium is described quantitatively by the equilibrium constant (extraction constant).

$$K_{ex} = \frac{[MA_n]_o \ [H^+]^n}{[M^{n+}] \ [HA]_o^n} \quad \text{.....(2)}$$

If we restrict discussions to the pH range in which the formation of intermediate may be neglected, hydrolysis products and the products of reactions with extraneous complex forming substances in the aqueous phase, and if we further neglect the presence of the complex MA_n in the aqueous phase, the ratio $[MA_n]_o$ / $[M^{n+}]$ in equation 2 may be consideredequal to the distribution coefficient.

Equation 2 may then be represented as,

$$K_{ex} = \frac{D[H^+]^n}{[HA]_o^n} \qquad \text{.....(3)}$$

$$D = \frac{K_{ex}[HA]_o^n}{[H^+]^n} \qquad \text{.....(4)}$$

$$\text{or} \quad \log D = \log K_{ex} + npH + n \log [HA]_o \qquad \text{.....(5)}$$

Further, defining the percentage extraction, E, as

$$E = \frac{100(\text{moles of metal in organic phase})}{(\text{total moles of metal in organic and aqueous phase})} \qquad \text{.....(6)}$$

$$E = \frac{100([MA]_o V_o)}{[MA]_o V_o + [M] V_{aq}} \qquad \text{.....(7)}$$

V_o and V_{aq} are the volumes of organic and aqueous phases used respectively.

$$E = \frac{100 D}{D + \frac{V_{aq}}{V_o}} \qquad \text{.....(8)}$$

If $V_o = V_{aq}$ then,

$$E = \frac{100 D}{D + 1} \qquad \text{.....(9)}$$

$$\text{or} \quad D = \frac{E}{100 - E} \qquad \text{.....(10)}$$

It can then be seen from equation 5 that if the equilibrium concentration of the reagent is constant, the extraction will depend on the pH of the aqueous phase. The distribution coefficient of the metal is larger at higher pH values. The relationship between logD and pH should then be a straight line with a slope of n, the valency of the metal.

2.1 Reagents.

All reagents used were of analar grade and supplied by BDH Chemicals, Poole, Dorset unless otherwise stated.

8-Hydroxyquinoline

Potassium Hydrogen Phthalate

Sodium Potassium Tartrate

Potassium Chloride

1000ppm metal standards as their respective nitrates

Hydrochloric acid

Sodium Hydroxide

Chloroform - HPLC grade, supplied by Fisons Ltd, Loughborough, Leicestershire

Buffer solutions;

(i) pH 4.00 ± 0.02 at 20°C, this buffer solution was 0.05M potassium hydrogen phthalate, recommended in BSS1647 : 1961 as a primary standard.

(ii) pH 7.00 ± 0.02 at 20°C, this buffer solution is referred to 0.05M potassium hydrogen phthalate (pH 4.00 ± 0.02 at 20°C) BSS 1647:1961.

2.2 Extraction Technique

Aqueous samples containing the equivalent of 20ppm metal ions, were modified to the required pH by suitable additions of a known concentration of sodium hydroxide or hydrochloric acid. The pH was measured using a Pye Unicam model 292 Mk2 pH meter, which was calibrated using buffers of pH 4.0 and 7.0. The solution was then placed in a separating funnel and a suitable volume of 0.01M 8-hydroxyquinoline in chloroform was added. The mixture was shaken vigourously for a few minutes and left to stand to facilitate complete equilibrium and separation of the two phases. The organic layer was discarded and the aqueous layer retained for analysis using the Shimadzu AA-670 atomic absorption spectrophotometer. The results obtained were used to calculate the efficiency of extraction and hence generate the relevant extraction curves (figures 2.2-2.9). This procedure was used to obtain extraction curves for copper, lead, aluminium and iron in

(a) an essentially aqueous system,

(b) a system buffered with potassium hydrogen phthalate,

(c) a system buffered with sodium potassium tartrate.

2.3 Flame Atomic Absorption Studies

The atomic absorption instrument use throughout the duration of this project was a Shimadzu AA-670. The AA670 is composed of the spectrophotometer, the graphic printer PR-4, the gas control unit and is capable of performing quantitative analysis based on atomic absorption and flame emission spectrometry.

The AA-670 employs a microcomputer to control the operation of the instrument and is therefore different to conventional models in a number of ways,

(i) all the operational parameters, with the exception of burner position, can be stored in the control computer and used to automatically set the range of specified parameters for a given analysis,

(ii) the microprocesser controls the operation of lamp turret, beam combiner, needle valve, wavelength and slit width setting of the monochromator.

(iii) all the data including the operational parameters, absorption curves, working curves, and concentrations determined, are automatically recorded on a printout/chart paper,

(iv) a large variety of data processing functions are incorporated in the AA-670.

2.3.1 Spectrophotometer

The spectrophotometer main unit incorporates a hollow cathode lamp turret, a deuterium lamp, a burner, an optical system, a monochromator, a detector, an amplifier, and power sources for all electronics.

2.3.2 Hollow Cathode Lamp Turret and Deuterium Lamp

Eight hollow cathode lamps can be mounted in the turret of which two can be on simultaneously. If some elements are to be routinely measured, and the lamps for these elements are loaded in the turret, the turret position for each element can be stored in of the condition files together with other parameters for this element including lamp current, wavelength, slit width, fuel rate etc. Having stored the package of

conditions for each element, a key entry of the file number, automatically brings the lamp to the optical axis of the instrument. The deuterium arc lamp is used for the background correction in the wavelength range of 190-430nm.

2.3.3 Burner and Atomiser Chamber

The AA-670 uses a standard pre-mix type burner with a slot length of 100mm. This burner is capable of using air/acetylene or air(argon)-hydrogen flame. When using nitrous oxide-acetylene flame an optional high temperature burner head, with a 50mm slot length, is necessary.

2.3.4 Gas Control Unit

This gas control unit controls the pressure and flow rate of support gas and fuel gases supplied to the burner and incorporates the following safety mechanisms;

(i) automatic gas leakage checking;

(ii) air/acetylene flame priority ignition system;

(iii) automatic air/nitrous oxide changeover;

(iv) flashback prevention by pressure monitor

(v) automatic gas stop mechanism by flame monitor

(vi) flashback protection at power failure by support gas changeover system.

2.3.5 Optical System

The optical system consists of a dual beam spectrophotometric design, the reference beam and sample beam being irradiated from the hollow cathode lamp and the deuterium lamp and are directed onto the same optical axis by the beam combiner, figure 2.1. The combined beam passes through the flame and is absorbed by atoms or co-existing substances.

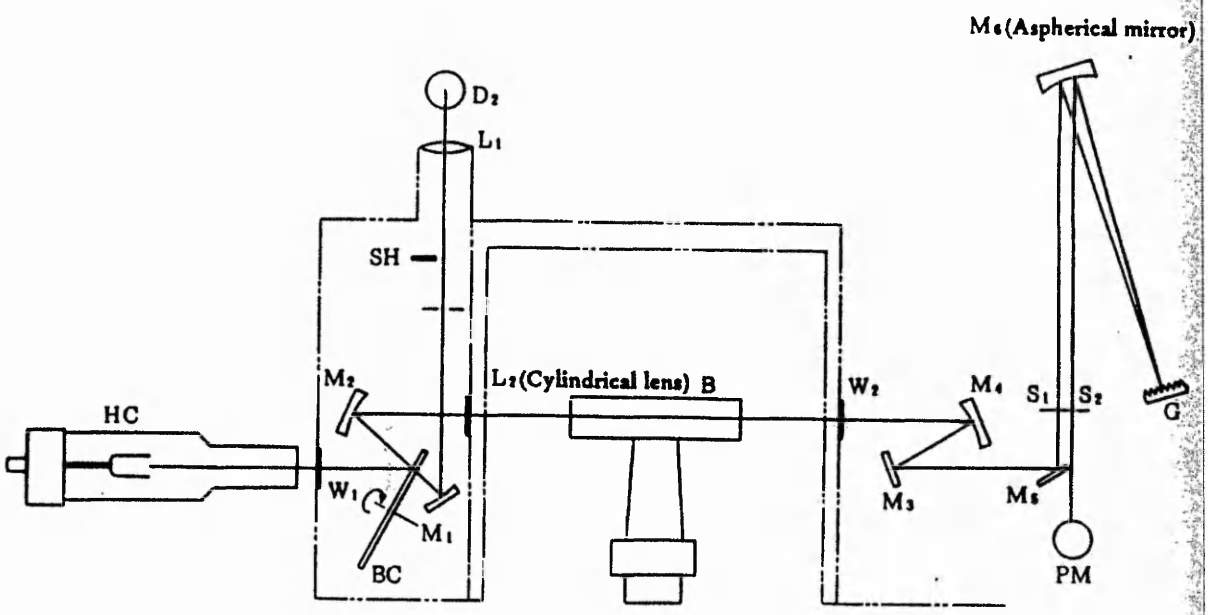

HC	:	Hollow cathode lamp	SH	:	Shutter
D_2	:	Deuterium lamp	B	:	Burner
$M_1 \sim M_6$	:	Mirror	S_1, S_2	:	Slits
BC	:	Beam combiner	G	:	Diffraction grating
L_1, L_2	:	Lenses	PM	:	Photomultiplier
W_1, W_2	:	Windows			

Figure 2.1 Optical System.

The emerging beam is collimated and passes through the monochromator and onto the photomultiplier.

The beam combiner is made of a quartz plate which has four segments of different reflectance/transmittance ratios. The optimum segment is automatically selected in the optical path in accordance with the measurement mode. Also the shutter, mounted in the deuterium lamp

optical path, automatically selects its position in accordance with the mode selected (refer to table 2.1)

MEASUREMENT MODE	BEAM COMBINER	SHUTTER
Emission/ Hollow cathode	The segment of the maximum reflectance (90%) is set on the optical path.	closed
BGC	The beam is automatically set at such a segment that should minimize the diference of the lamp intensities on the combined light path.	opened
D_2	The segment of the maximum transmittance (60%) is set on the optical path.	opened

Table 2.1 Functioning of Beam Combiner and Shutter.

In background only mode, the hollow cathode lamp is automatically removed from the optical path. All the optical elements are sealed from the external atmosphere by the window plates W1 and W2 and the lenses L1 and L2, to protect them from the dust, dirt or corrosive gases.

The monochromator of a high resolution Littrow type employs a non-spherical main mirror to correct aberration. The slit width can be varied continuously between 0.02nm and 3.00nm.

2.4 RESULTS

The results relating to the extraction studies undertaken in this programme of work are detailed as follows,

(i) The extraction data applicable to the elements, Copper, Lead, Iron and Aluminium in both buffered and unbuffered systems is referenced below,

Copper	Tables 2.2-2.4
Lead	Tables 2.5-2.7
Iron	Tables 2.8-2.10
Aluminium	Tables 2.11

(ii) The extraction curves and logD vs pH relationships are illustrated as follows,

Copper	Figures 2.2-2.3
Lead	Figures 2.4-2.5
Iron	Figures 2.6-2.7
Aluminium	Figures 2.8-2.9

pH	pH Modifier		Corrected Initial Concentration (ppm)	Aqueous Layer Concentration (ppm)	Element in Aqueous Layer (%)	Overall Extraction Efficiency (%)	Distribution Coefficient (D)	Log D
	HCl(cm^3)	NaOH (cm^3)						
0.55	10.00	–	6.66	6.60	0.90	99.10	0.03	−1.56
0.95	1.50	–	15.38	15.35	0.20	99.80	0.00	−2.58
1.11	0.80	–	17.24	15.86	8.00	92.00	0.10	−1.00
1.21	0.60	–	17.86	8.30	53.53	46.47	1.29	0.11
1.31	0.50	–	18.18	2.02	88.89	11.11	8.80	0.94
1.38	0.40	–	18.52	0.48	97.41	2.59	40.62	1.61
1.54	0.20	–	19.23	0.39	97.97	2.03	50.19	1.70
1.71	0.10	–	19.60	0.28	98.57	1.43	70.31	1.85
1.97	–	–	20.00	0.11	99.45	0.55	180.82	2.26
2.35	–	0.50	18.18	0.16	99.12	0.88	123.90	2.09
2.57	–	0.70	17.54	0.06	99.66	0.34	334.15	2.52

Buffer : None
8–Hydroxyquinoline : 1% by weight
Copper : 20ppm
Hydrochloric Acid : 1.0 M
Sodium Hydroxide : 0.1M

LogD vs pH, gradient = 9.6
$pH_{\frac{1}{2}}$ = 1.2

Table 2.2 – Extraction of Copper (No Buffer).

pH	pH Modifier		Corrected Initial Concentration (ppm)	Aqueous Layer Concentration (ppm)	Element in Aqueous Layer (%)	Overall Extraction Efficiency (%)	Distribution Coefficient (D)	Log D
	HCl(cm^3)	NaOH (cm^3)						
2.50	0.00	–	20.0	0.13	99.35	0.65	152.85	2.18
1.80	0.50	–	18.2	0.77	95.77	4.23	24.90	1.40
1.50	1.00	–	16.7	0.51	96.95	3.05	38.14	1.58
1.37	1.50	–	15.4	1.54	90.00	10.00	11.70	1.07
1.33	1.75	–	14.8	2.68	81.89	18.11	6.10	0.79
1.28	2.00	–	14.3	5.91	58.67	41.33	1.99	0.30
1.25	2.25	–	13.8	8.73	36.74	63.26	0.84	−0.07
1.21	2.50	–	13.3	11.21	15.72	84.28	0.28	−0.55
1.18	3.00	–	12.5	10.19	18.48	81.52	0.36	−0.44
1.15	3.50	–	11.8	11.00	6.78	93.22	0.12	−0.91
1.11	4.00	–	11.1	10.01	9.82	90.18	0.20	−0.71
1.09	5.00	–	10.0	9.02	9.80	90.20	0.22	−0.66
1.05	6.00	–	9.1	8.35	8.24	91.76	0.20	−0.70
1.02	7.00	–	8.3	7.56	8.92	91.08	0.24	−0.63

Buffer : Potassium Hydrogen Phthalate
8–Hydroxyquinoline : 1% by weight
Copper : 20ppm
Hydrochloric Acid : 0.4M
Sodium Hydroxide : N/A

LogD vs pH, gradient = 2.0
pH = 1.2

Table 2.3 – Extraction of Copper (Potassium Hydrogen Phthalate)

pH	pH Modifier		Corrected Initial Concentration (ppm)	Aqueous Layer Concentration (ppm)	Element in Aqueous Layer (%)	Overall Extraction Efficiency (%)	Distribution Coefficient (D)	Log D
	HCl(cm^3)	NaOH (cm^3)						
0.45	10.00	–	6.66	6.10	91.60	8.40	0.28	−0.55
0.56	5.00	–	10.00	8.59	85.90	14.10	0.33	−0.48
0.80	2.00	–	14.28	12.11	84.80	15.20	0.25	−0.60
1.04	1.00	–	16.67	12.89	77.32	12.68	0.19	−0.70
1.11	0.80	–	17.24	9.94	57.65	42.35	0.85	−0.07
1.20	0.70	–	17.54	4.43	25.26	74.74	3.37	0.53
1.27	0.65	–	17.70	0.97	5.48	94.52	19.49	1.29
1.28	0.60	–	17.86	0.88	4.92	95.08	21.64	1.33
1.38	0.50	–	18.18	0.33	1.81	98.19	59.67	1.77
1.50	0.40	–	18.52	0.15	0.81	99.19	132.25	2.12
1.60	0.35	–	18.69	0.18	0.96	99.04	110.38	2.04
1.84	0.20	–	19.23	0.13	0.67	99.33	154.18	2.20
3.80	–	0.20	19.23	0.18	0.94	99.06	109.59	2.04

Buffer : Sodium Potassium Tartrate
8–Hydroxyquinoline : 1% by weight
Copper : 20ppm
Hydrochloric Acid : 1.0M
Sodium Hydroxide : 0.1M

LogD vs pH, gradient = 6.4
$pH_{\frac{1}{2}}$ = 1.2

Table 2.4 – Extraction of Copper (Sodium Potassium Tartrate).

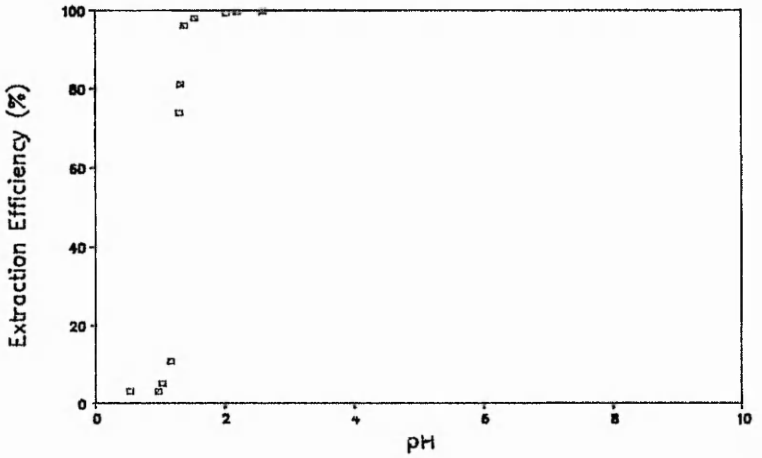

No buffer (a)

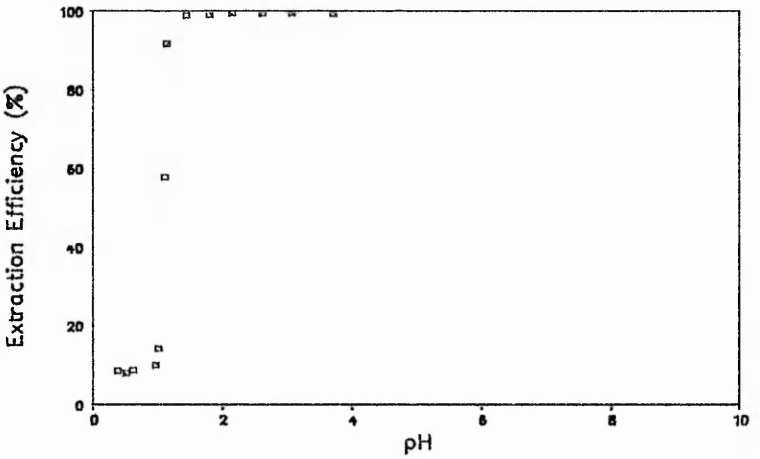

Sodium Potassium Tartrate (b)

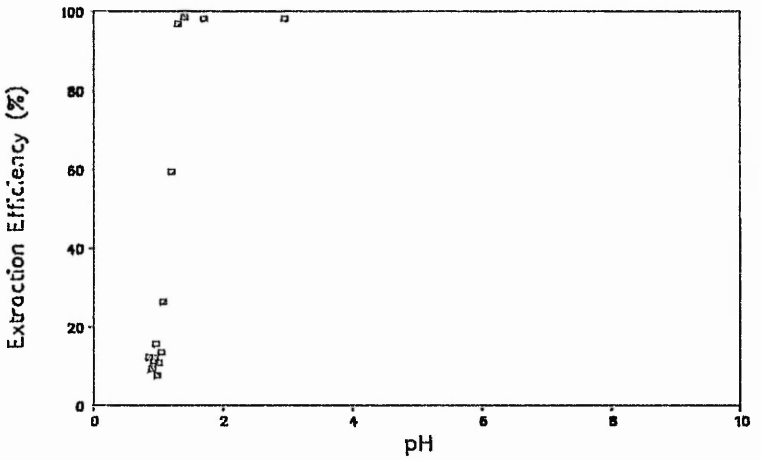

Potassium Hydrogen Phthalate (c)

Figure 2.2 — Extraction Curves for Copper

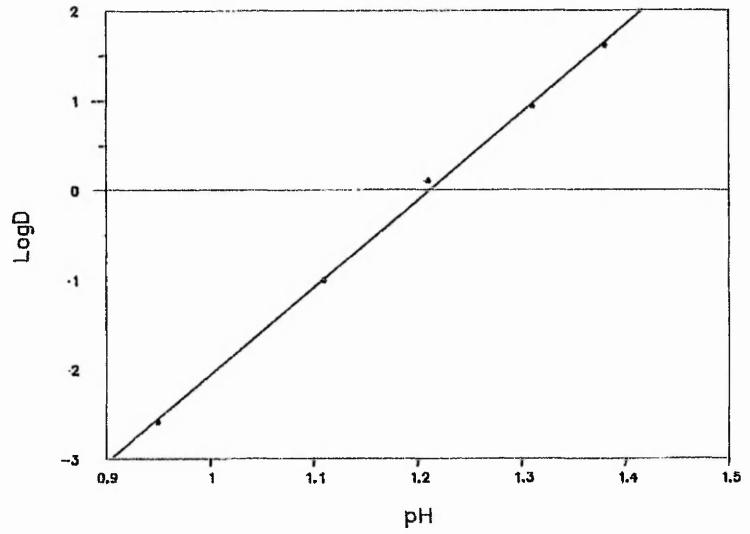

No Buffer (a)

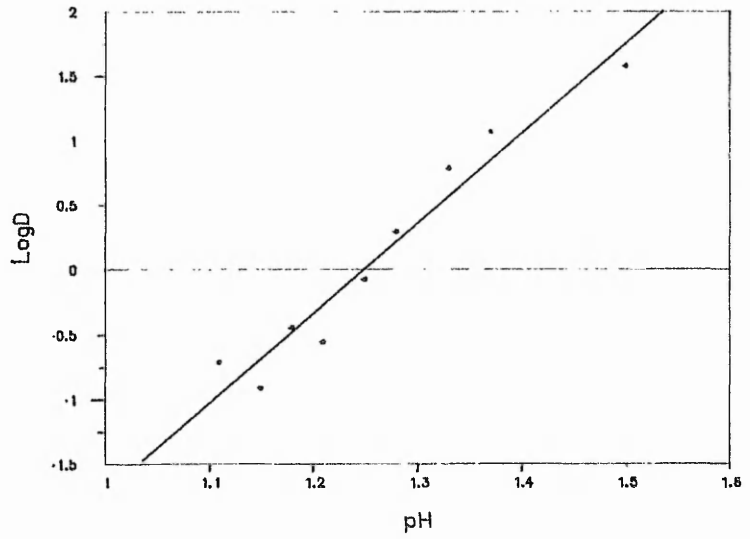

Potassium Hydrogen Phthalate (b)

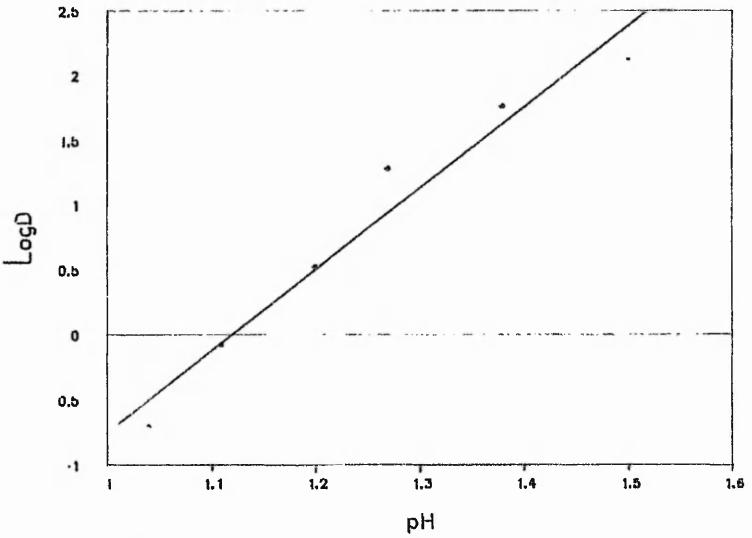

Sodium Potassium Tartrate (c)

Figure 2.3 – LogD vs pH for Copper Extraction Systems

pH	pH Modifier		Corrected Initial Concentration (ppm)	Aqueous Layer Concentration (ppm)	Element in Aqueous Layer (%)	Overall Extraction Efficiency (%)	Distribution Coefficient (D)	Log D
	HCl(cm^3)	NaOH (cm^3)						
2.95	–	1.0	1.66	1.60	96.4	3.6	0.04	−1.34
3.00	–	0.0	2.00	0.66	32.8	67.2	2.05	0.31
3.07	–	2.0	1.43	1.42	99.3	0.7	0.01	−2.00
3.30	–	4.0	1.11	0.80	72.3	27.7	0.69	−0.16
3.50	–	6.0	0.91	0.43	47.7	52.3	2.41	0.38
3.65	–	7.0	0.83	0.32	38.3	61.7	3.87	0.59
3.85	–	8.0	0.77	0.13	16.7	83.3	12.97	1.11
4.10	–	9.0	0.71	0.18	25.3	74.7	8.27	0.91
4.60	–	9.5	0.69	0.01	1.50	98.5	–	–
4.80	–	10.0	0.67	0.01	1.50	98.5	–	–
5.50	–	11.0	0.63	0.00	100	0.0	–	–

Buffer : No Buffer
8–Hydroxyquinoline : 1% by weight
Iron : 2.0ppm
Hydrochloric Acid : N/A
Sodium Hydroxide : 0.001M

LogD vs pH, gradient = 2.5
$pH_{\frac{1}{2}}$ = 3.5

Table 2.5 – Extraction of Lead (No Buffer).

pH	pH Modifier		Corrected Initial Concentration (ppm)	Aqueous Layer Concentration (ppm)	Element in Aqueous Layer (%)	Overall Extraction Efficiency (%)	Distribution Coefficient (D)	Log D
	HCl(cm^3)	NaOH (cm^3)						
3.10	–	2.0	1.43	1.51	100.0	0.0	–	–
3.20	–	1.0	1.66	1.35	81.3	18.7	0.27	−0.56
3.25	–	3.0	1.25	0.91	72.6	27.4	0.60	−0.22
3.31	–	5.0	1.00	0.73	72.9	27.1	0.74	−0.13
3.32	–	4.0	1.11	0.72	64.6	35.4	0.98	−0.01
3.58	–	6.0	0.91	0.32	35.6	64.4	3.98	0.60
3.70	–	7.0	0.83	0.07	9.0	91.0	24.30	1.38
3.90	–	8.0	0.77	0.00	0.0	100.0	–	–
4.08	–	9.0	0.71	0.00	0.0	100.0	–	–

Buffer : Potassium Hydrogen Phthalate
8–Hydroxyquinoline : 1% by weight
Lead : 2.0ppm
Hydrochloric Acid : N/A
Sodium Hydroxide : 0.001M

LogD vs pH, gradient = 3.5
$pH_{\frac{1}{2}}$ = 3.5

Table 2.6 – Extraction of Lead (Potassium Hydrogen Phthalate).

pH	pH Modifier		Corrected Initial Concentration (ppm)	Aqueous Layer Concentration (ppm)	Element in Aqueous Layer (%)	Overall Extraction Efficiency (%)	Distribution Coefficient (D)	Log D
	HCl(cm^3)	NaOH (cm^3)						
4.25	–	–	8.00	7.87	98.4	1.6	0.02	−1.79
4.75	–	4.0	4.44	3.79	85.4	14.6	0.31	−0.51
4.85	–	5.0	4.00	3.51	87.7	12.3	0.28	−0.55
5.10	–	6.0	3.64	2.73	75.0	25.0	0.73	−0.13
5.23	–	6.5	3.48	2.46	70.7	29.3	0.95	−0.02
5.50	–	7.0	3.33	1.66	49.8	50.2	2.42	0.38
5.65	–	7.2	3.28	1.23	37.5	62.5	4.07	0.61
5.85	–	7.4	3.22	0.87	27.0	73.0	6.71	0.83
6.25	–	7.6	3.17	0.37	11.7	88.3	19.02	1.28
6.95	–	8.0	3.08	0.10	3.2	96.8	74.65	1.90
9.36	–	8.2	3.03	0.06	2.0	98.0	129.36	2.11
10.00	–	8.4	2.98	0.01	0.3	99.7	890.65	2.95

Buffer : Sodium Potassium Tartrate
8–Hydroxyquinoline : 1% by weight
Lead : 8.0ppm
Hydrochloric Acid : N/A
Sodium Hydroxide : 0.005M

LogD vs pH, gradient = 1.2
$pH_{\frac{1}{2}}$ = 5.5

Table 2.7 – Extraction of Lead (Sodium Potassium Tartrate).

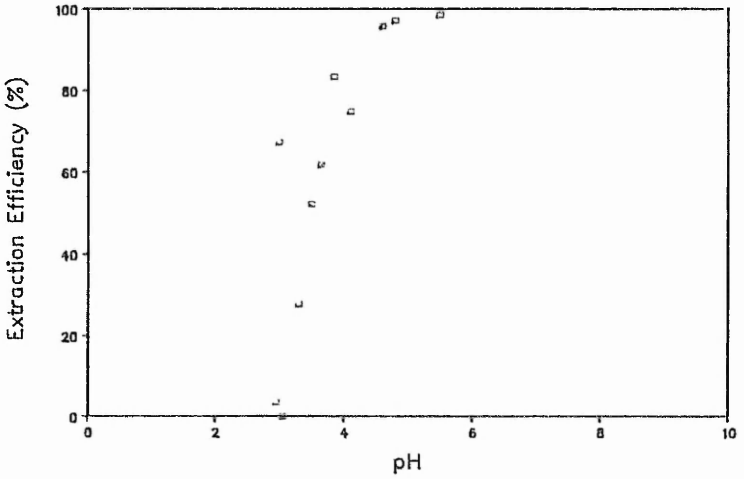

No buffer (a)

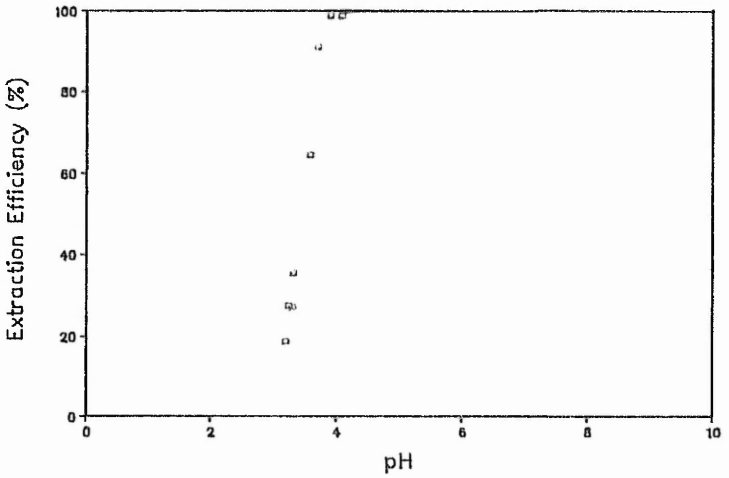

Potassium Hydrogen Phthalate (b)

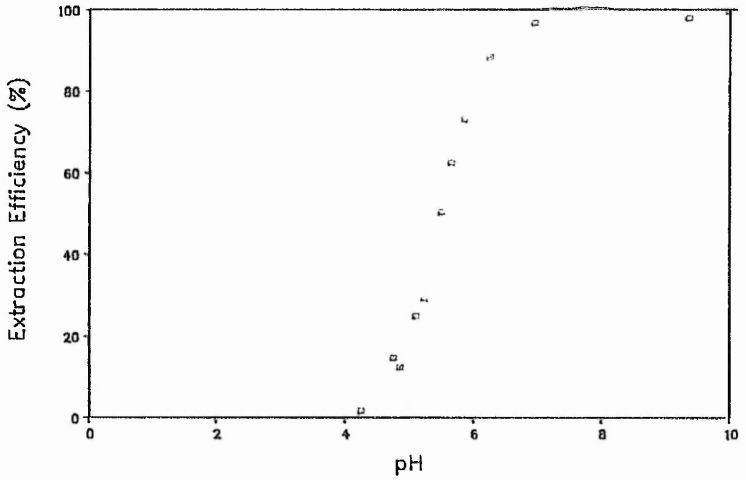

Sodium Potassium Tartrate (c)

Figure 2.4 – Extraction Curves for Lead

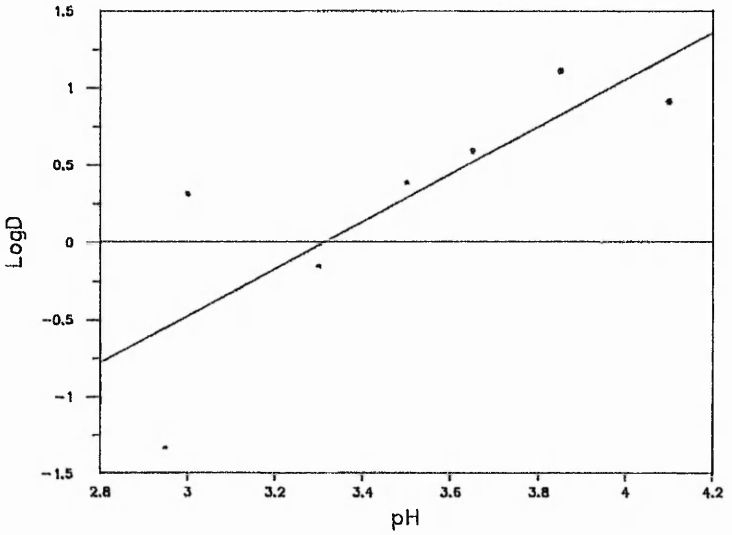

No Buffer (a)

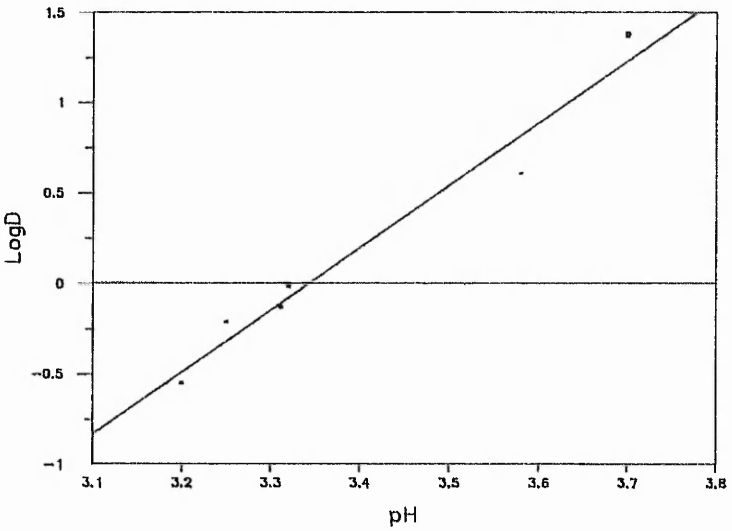

Potassium Hydrogen Phthalate (b)

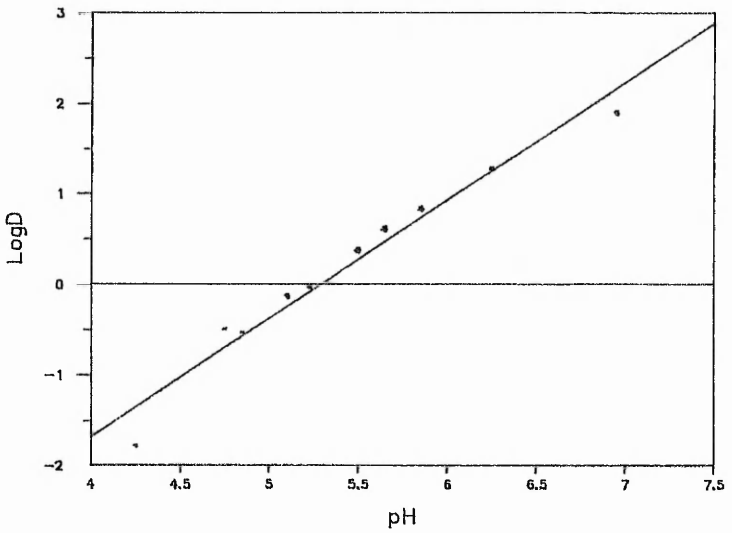

Sodium Potassium Tartrate (c)

Figure 2.5 – LogD vs pH for Lead Extraction Systems

pH	pH Modifier		Corrected Initial Concentration (ppm)	Aqueous Layer Concentration (ppm)	Element in Aqueous Layer (%)	Overall Extraction Efficiency (%)	Distribution Coefficient (D)	Log D
	HCl(cm^3)	NaOH (cm^3)						
0.58	10.00	–	6.66	6.57	98.60	1.40	0.04	−1.37
0.70	5.00	–	10.00	9.30	93.00	7.00	0.15	−0.82
0.72	4.00	–	11.10	10.00	90.10	9.90	0.20	−0.70
0.76	3.00	–	12.50	10.90	87.20	12.80	0.23	−0.63
0.79	2.75	–	12.90	11.20	86.80	13.20	0.24	−0.63
0.82	2.50	–	13.33	11.00	82.50	17.50	0.32	−0.50
0.85	2.00	–	14.28	10.50	73.50	26.50	0.50	−0.30
0.91	1.75	–	14.81	7.00	47.30	52.70	1.50	0.18
0.93	1.50	–	15.38	5.00	32.50	67.50	2.70	0.43
1.05	1.00	–	16.66	0.70	4.20	95.80	27.37	1.44
1.28	0.50	–	18.18	0.40	2.20	97.80	48.90	1.69
1.70	–	–	20.00	0.40	2.00	98.00	49.00	1.69
2.10	–	3.0	12.50	0.20	1.60	98.40	98.40	1.69

Buffer : No Buffer
8–Hydroxyquinoline : 1% by weight
Iron : 8.0ppm
Hydrochloric Acid : 0.5M
Sodium Hydroxide : 0.1M

LogD vs pH, gradient = 5.0
$pH_{\frac{1}{2}}$ = 1.0

Table 2.8 – Extraction of Iron (No Buffer).

pH	pH Modifier		Corrected Initial Concentration (ppm)	Aqueous Layer Concentration (ppm)	Element in Aqueous Layer (%)	Overall Extraction Efficiency (%)	Distribution Coefficient (D)	Log D
	HCl(cm^3)	NaOH (cm^3)						
1.16	6.00	–	3.64	3.23	88.74	11.26	0.28	–0.55
1.26	4.00	–	4.44	3.20	72.10	27.90	0.69	–0.15
1.41	2.00	–	5.71	2.92	51.14	48.86	1.34	0.13
1.51	1.50	–	6.15	3.00	48.78	51.22	1.36	0.13
1.65	1.00	–	6.66	3.21	48.20	51.80	1.29	0.11
1.79	0.75	–	6.96	2.90	41.67	58.33	1.61	0.21
1.95	0.50	–	7.27	2.74	37.70	62.30	1.82	0.26
2.25	0.25	–	7.62	2.89	37.92	62.08	1.72	0.23
2.82	–	–	8.00	2.30	28.75	71.25	2.48	0.39
3.05	–	0.10	7.83	1.52	19.41	80.59	4.20	0.63
3.15	–	0.20	7.69	0.82	10.66	89.34	8.70	0.94
3.58	–	0.30	7.55	0.37	4.90	95.10	20.60	1.30
3.70	–	0.40	7.41	0.49	6.60	93.40	15.30	1.18
4.75	–	0.50	7.27	0.11	1.5	98.50	72.20	1.86

Buffer : Potassium Hydrogen Phthalate
8–Hydroxyquinoline : 1% by weight
Iron : 8.0ppm
Hydrochloric Acid : 1.0M
Sodium Hydroxide : 0.1M

LogD vs pH, gradient = 3.0
$pH_{\frac{1}{2}}$ = 1.5

Table 2.9 – Extraction of Iron (Potassium Hydrogen Phthalate).

pH	pH Modifier		Corrected Initial Concentration (ppm)	Aqueous Layer Concentration (ppm)	Element in Aqueous Layer (%)	Overall Extraction Efficiency (%)	Distribution Coefficient (D)	Log D
	HCl(cm^3)	NaOH (cm^3)						
0.68	10.00	–	6.66	6.12	93.10	6.90	0.22	−0.65
0.81	5.00	–	10.00	10.00	100.00	–	–	–
0.85	4.00	–	11.11	10.50	94.60	5.40	0.10	−0.99
0.93	3.00	–	12.50	11.10	88.80	11.20	0.20	−0.69
1.00	2.50	–	13.30	11.10	83.30	16.70	0.30	−0.52
1.05	2.00	–	14.28	8.31	58.20	41.80	1.00	0.00
1.09	1.75	–	14.81	6.91	46.60	53.40	1.55	0.19
1.15	1.50	–	15.38	4.38	28.50	71.50	3.26	0.51
1.30	1.00	–	16.66	3.87	23.20	76.80	3.97	0.60
3.39	–	–	20.00	0.20	1.00	99.00	99.00	1.99

Buffer : Sodium Potassium Tartrate
8–Hydroxyquinoline : 1% by weight
Iron : 8.0ppm
Hydrochloric Acid : 1.0M
Sodium Hydroxide : 0.1M

LogD vs pH, gradient = 0.56
$pH_{\frac{1}{2}}$ = 1.2

Table 2.10 – Extraction of Iron (Sodium Potassium Tartrate).

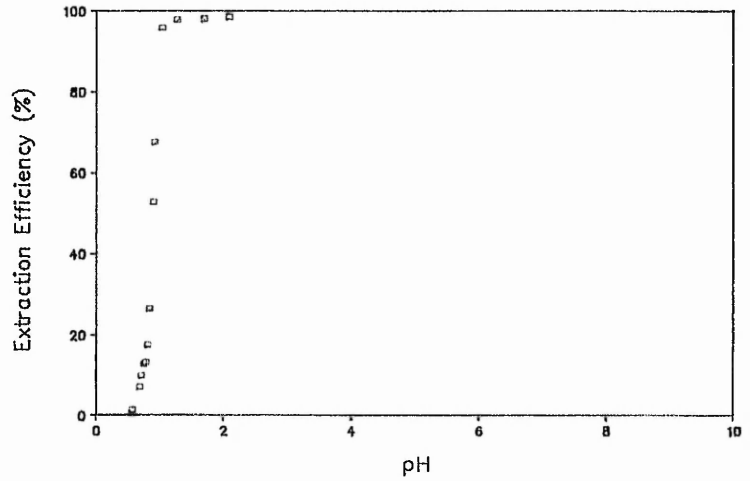

No buffer (a)

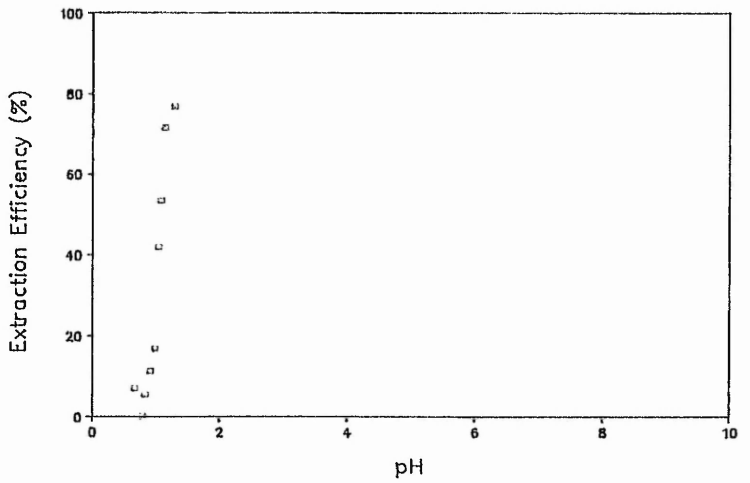

Sodium Potassium Tartrate (b)

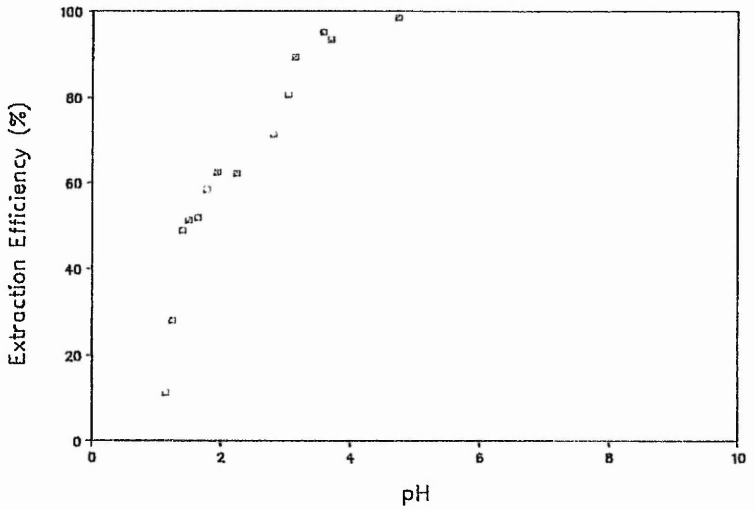

Potassium Hydrogen Phthalate (c)

Figure 2.6 — Extraction Curves for Iron

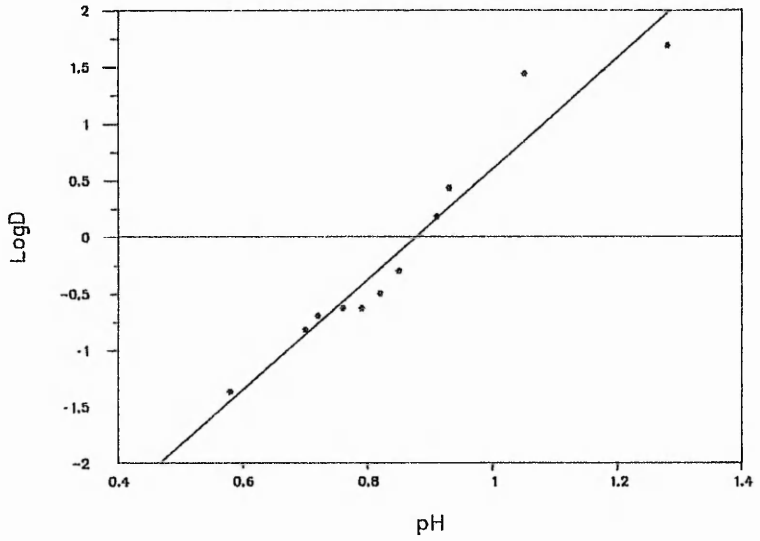

No Buffer (a)

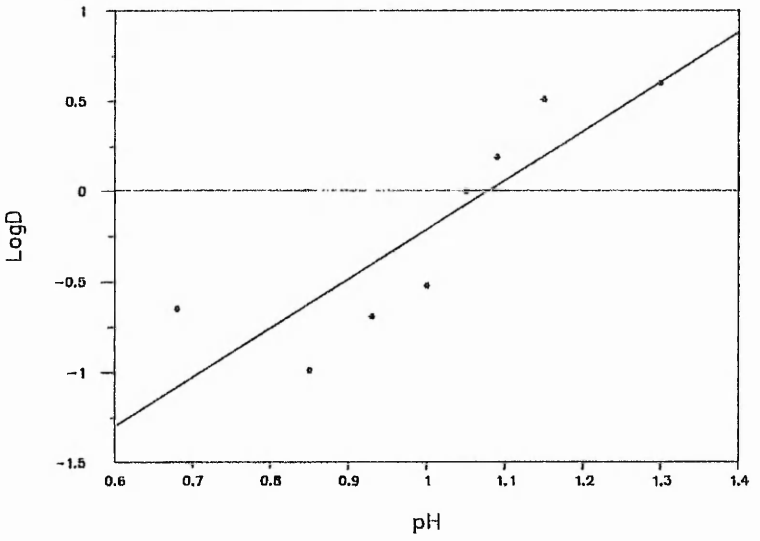

Potassium Hydrogen Phthalate (b)

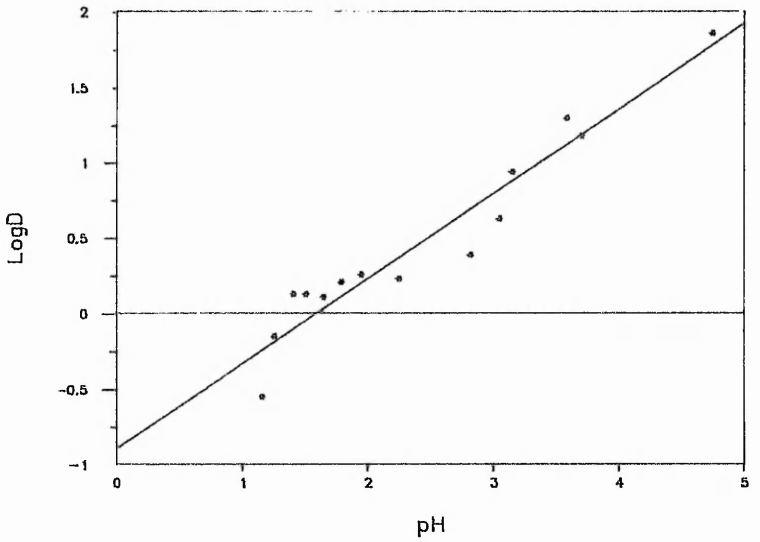

Sodium Potassium Tartrate (c)

Figure 2.7 – LogD vs pH for Iron Extraction Systems

pH	pH Modifier		Corrected Initial Concentration (ppm)	Aqueous Layer Concentration (ppm)	Element in Aqueous Layer (%)	Overall Extraction Efficiency (%)	Distribution Coefficient (D)	Log D
	HCl(cm^3)	NaOH (cm^3)						
1.73	0.1	–	19.6	18.7	95.4	5.60	0.11	−0.97
1.80	0.2	–	19.2	17.4	90.6	9.40	0.06	−1.22
1.90	–	–	20.0	16.6	83.0	17.0	0.02	−0.70
1.95	–	0.5	18.2	9.50	52.2	47.8	1.00	0.00
2.02	–	1.0	16.7	9.30	55.7	44.3	0.95	−0.02
2.12	–	2.0	14.3	8.80	61.5	38.5	0.87	−0.06
2.20	–	3.0	12.5	7.90	63.2	36.8	0.93	−0.03
2.35	–	4.0	11.1	6.20	55.8	44.2	1.42	0.15
2.64	–	5.0	10.0	2.90	29.0	71.0	4.90	0.70
2.68	–	6.0	9.10	3.30	36.3	63.7	3.86	0.60
2.85	–	7.0	8.30	1.50	18.1	81.9	10.85	1.03
3.30	–	8.0	7.70	1.10	14.3	85.7	15.60	1.20

Buffer : No Buffer
8–Hydroxyquinoline : 1% by weight
Aluminium : 20ppm
Hydrochloric Acid : 0.4M
Sodium Hydroxide : 0.01M

LogD vs pH, gradient = 1.5
$pH_{\frac{1}{2}}$ = 2.0–3.0

Table 2.11 – Extraction of Aluminium (No Buffer)

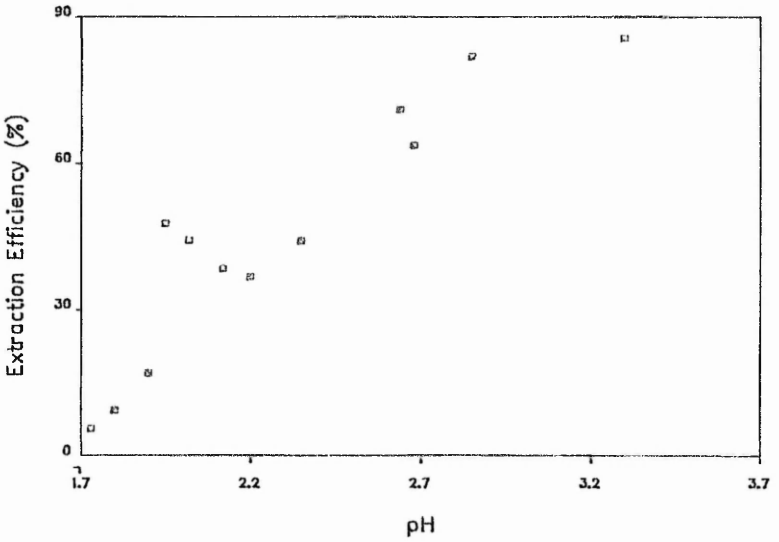

No Buffer (a)

Figure 2.8 – Extraction Curve for Aluminium

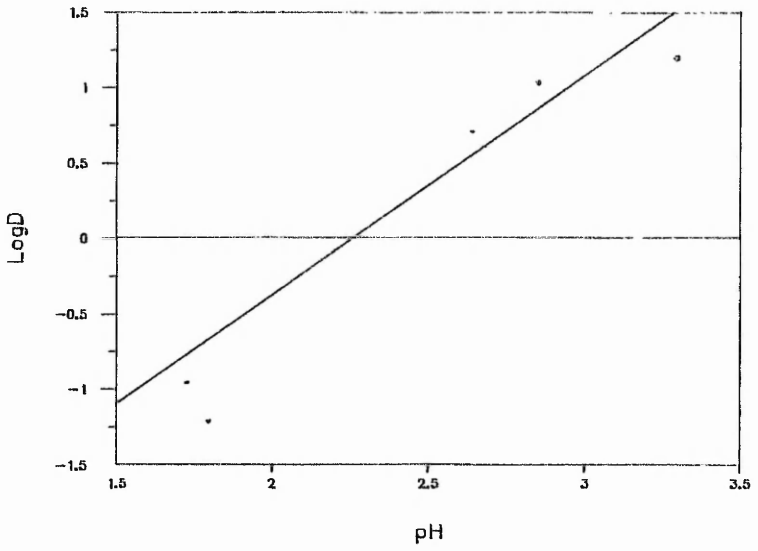

No Buffer (a)

Figure 2.9 – LogD vs pH for Aluminium Extraction System

2.5 Discussion

The major objective of these investigations was to assess various approaches to trace elemental analysis utilising equipment available, or expected to be available within the Engine Support Services Laboratory, Rolls Royce, Derby. The elements of interest were copper, lead, iron and aluminium which are frequently associated with problems of engine lifetime and performance when present even at trace levels in for example alloys, fuels and lubricating oils. The areas investigated were as follows,

(i) extraction utilising, a suitable chelating agent capable of being applied to all four elements with subsequent elemental analysis using Flame Atomic Absorption Spectroscopy or chromatographic techniques;

(ii) graphite furnace atomic absorption spectroscopy, utilising either the method of extraction and/or direct injection analysis of aqueous or organic samples.

This section summarises the work undertaken with respect to the extraction studies and section 3.0 and 4.0 discuss the work relating to graphite furnace applications.

2.5.1 Extraction Studies

The extraction of traces of metallic elements into organic solvents as metal-chelate complexes, followed by their determination using atomic absorption spectroscopy, has become an established method in many laboratories (90). These methods have the important advantage of lower limits of detection and excellent selectivity compared with earlier methods which depended on solution spectrophotometry (111). However extraction techniques are not so well suited to multi-elemental analysis.

for example analysis of polluted water samples where chemical pre-treatments, different analyte concentrations and the need to change hollow cathode lamps and monochromator settings can be disadvantageous for routine analysis.

It is for this reason that this investigation concentrated on defining the extraction technique with a view to applying the extracted sample to HPLC, which would provide complete separation of the metal chelates prior to the use of a non-selective method of detection, namely ultraviolet. Similar investigations have been undertaken using dithizone (112) and diethyldithiocarbamate (98) which utilised their high molar absorptivities and their ability to form strong complexes with metals such as lead.

However the lack of available facilities with regards HPLC equipment, redirected the investigation towards using atomic absorption spectrophotometric analyses.

8-Hydroxyquinoline (oxine) was chosen as the chelating agent because of its ability to chelate with a wide range of elements including the elements of interest copper, lead, iron and aluminium, and its relative ease of use and robustness of the method. A number of investigations concerning the solvent extraction of metal oxinates have been reported (113-118), but few theoretical studies were undertaken. The work completed by Stary (119) was a rare example of a complete, systematic study of 32 metals chelated with oxine in chloroform and confirms the ability of oxine to chelate with a wide range of metals.

Oxine is amphoteric in nature, equilibrium under normal conditions is best depicted in figure 2.10. It is acidic by virtue of its phenolic grouping and basic due to its pyridine component.

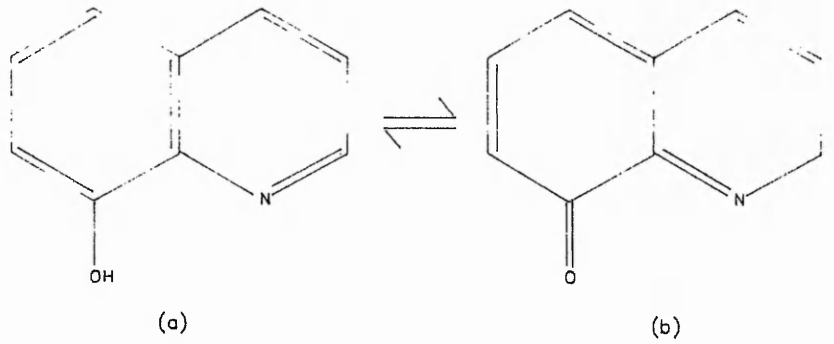

Figure 2.10 Equilibrium of Oxine under normal conditions.

The salts formed with mineral acids are water soluble. Its salt forming ability arises from its phenolic nature and the proximity of the hydroxyl group to the nitrogen atom in the ring. Complexes with metals are generally insoluble in water but are extremely soluble in organic solvents, which suggests that the complexes are members of the class of inner complex salts. The structure in figure 2.11a is usually assigned to these complexes and corresponds to the phenolic tautomer, figure 2.10a. However the resonant structure, figure 2.11b has also been suggested and corresponds to the formulation of oxine as a quinone, figure 2.10b.

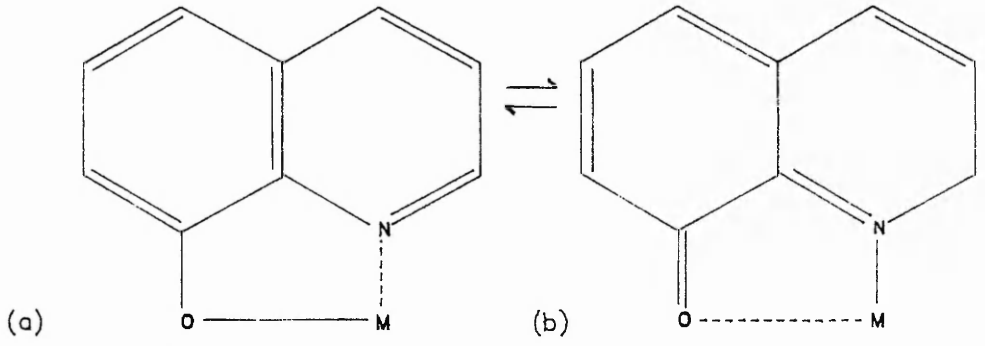

Figure 2.11 Resonant structures of Oxine.

When considering the extraction of a chelate compound the following expression represents the equation of the equilibrium.

$$M^{n+} + nHA_{(o)} \rightleftharpoons MAn_{(o)} + nH^{+}$$

where M^{n+} represents an aqueous cation of charge n, $HA_{(o)}$ and $MAn_{(o)}$ are the neutral (protonated) chelating ligand and the neutral chelate.

The mathematics of the equilibrium have been discussed in section 2.0 (extraction studies), and as such the equation,

$$\log D = \log K_{ex} + npH + \log[HA]_o$$

where K_{ex} is the equilibrium constant, can be used to verify the proposed extraction model. That is if the equilibrium concentration of the reagent is constant, the extraction will depend on the pH of the aqueous phase. Within the valid range of the expression, the distribution coefficient of the metal is larger the higher the pH. The relationship between logD and pH should then be a straight line with a slope of n, the valency of the metal under investigation (see figure 2.2 for examples).

A slope larger than n is obtained if the reagent undergoes basic dissociation in the range studied and the resulting cationic form passes into the aqueous phase. Such behaviour is typical of 8-hydroxyquinoline.

The approach to the extraction studies was by investigating three extraction systems. The first being the basic, unbuffered aqueous system, the others utilising sodium potassium tartrate and potassium hydrogen phthalate buffered systems. The use of the buffers was to impart a degree of control and stability over the pH variations and assess the extraction efficiency of oxine in such systems. The results

with respect to each element will be discussed individually.

(a) Copper

The extraction of copper was consistant with respect to to all three systems in that complete extraction could be attained above a pH value of 2.0 with little change being observed in the $pH_{\frac{1}{2}}$ value which was approximately 1.2.

The results corresponding to the extraction data for each system are illustrated in tables 2.2-2.4 and graphically represented in figures 2.2. The verification of the extraction model, utilising the logD verses pH relationship has highlighted the problems occurring with oxine at pH values below pH 4.0. Two of the three systems evaluated using this relationship exhibited gradients in excess of the valency of copper (figure 2.3), the exception being potassium hydrogen phthalate which exhibited a gradient of 2.

The results in terms of the overall sigmoidal shape of the curve and range (pH 2-12) for complete extraction of copper agree well with literature values (119). Closer examination of the curves produced, does indicate a greater control of the extraction system by using the potassium hydrogen phthalate system. This is more evident when considering the steep part of the extraction curve, whereby a greater control, and consequently a greater number of data points could be generated. Consequently the extraction of copper from an aqueous system, buffered with potassium hydrogen phthalate, would on this evidence, be the preferred system. However, reservations as to the extent of its use should be made as the complete pH range was not investigated.

Stary (119) has clearly identified that using other systems can induce significant deviations of the extraction curve from that of a simple sigmoid curve. Figure 2.12 illustrates this point very clearly, whereby the presence of oxalic acid and ethylenediaminetetraacetic acid can cause such deviations.

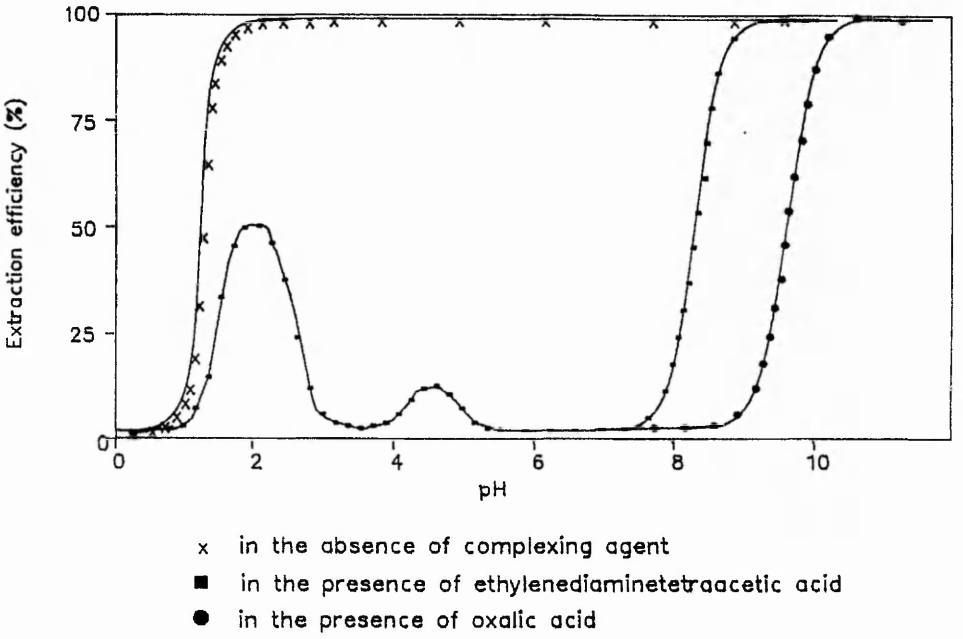

Figure 2.12 The Effect of Complexing Agents on Extraction Efficiency

However, the use of such chelating agents can influence the approach to selective extraction and is discussed in more detail later. Figure 2.13 illustrates the effect of pH on the equilibrium concentration of a variety of organic reagents, $[HA]_o$, in differing solvent systems.

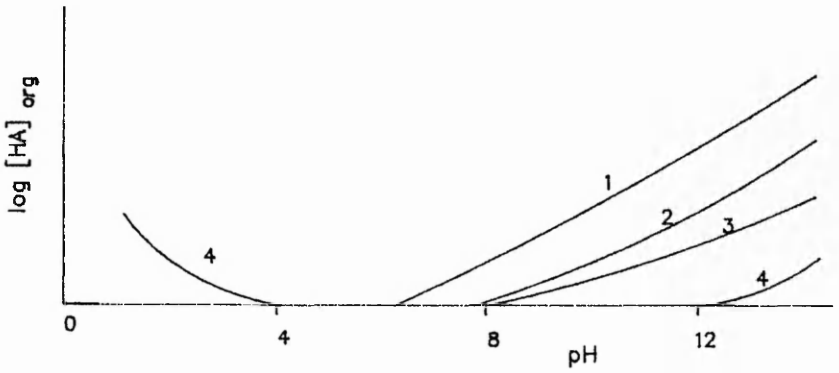

(1) cupferron – chloroform system
(2) diethyldithiocarbamate – carbon tetrachloride system
(3) dithizone – carbon tetrachloride system
(4) 8–hydroxyquinoline – chloroform system

Figure 2.13 The Effect of pH on the Equilibrium Concentration of Organic Reagents.

With particular reference to oxine the pH range of 4-11 is the area of consistant concentration in the organic phase. It is unfortunate that the problems of basic dissociation below pH 4.0 will dominate the extraction studies undertaken in this work.

However if the experimental slope of the ascending branches of the extraction is found to be less than n, then this could be attributed to hydrolysis of the metal ion, complex formation with extraneous substances or intermediate complex formation with the reagent. These aspects will be considered as and where appropriate at a later stage in the discussion.

(b) Lead

The extraction of lead from an aqueous system using oxine in chloroform was significantly affected by the use of the two buffer systems described earlier. The results of which are tabulated in tables 2.5-2.7 and graphically represented in figure 2.4. The absence of any buffer resulted in a trend which demonstrated complete extraction above pH 6.0 (figure 2.4a). Unfortunately the extraction curve was not smooth and illustrated significant inconsistancy for any given data point.

The logD verses pH curve (figure 2.5a) generated a gradient of 2.5 (via best straight line fit), the valency of the element. The standard deviation indicates the uncertainty of the result and highlights further the problems of dissociation of oxine below pH 4.0.

The use of potassium hydrogen phthalate did little to improve the situation. Although the sigmoid curve was significantly improved in smoothness (figure 2.4b). The $pH_{\frac{1}{2}}$ value was 3.5, the same as the unbuffered system and the gradient from the logD verses pH relationship (figure 2.5b) had worsened to 3.5, indicating that the dissociation of

oxine was more prominant.

The use of sodium potassium tartrate resulted in a dramatic shift in pH for the extraction curve with a significant improvement in the control of the pH (figure 2.4c). Small additions of sodium hydroxide resulting in small changes to the pH, with a smoother sigmoid curve. The $pH_{\frac{1}{2}}$ value was now 5.5 and the resultant gradient 1.2 (figure 2.5c).

The advantages of using this system is that it avoids the pH range which causes oxine to dissociate, but in addition provides a means of either selectively extracting or not extracting lead from certain mixtures. The fact that copper is not totally biased to any particular buffer system also provides no complication in preparation as both copper and iron can be used within the tartrate system.

(c) Iron

The extraction of iron in an unbuffered system can be considered a 100% above a pH of 2.0 (figure 2.6a). The sigmoid curve produced was both smooth and repeatable with a $pH_{\frac{1}{2}}$ value equal to 1.0. This is in good agreement with the work completed by Stary (119). The gradient from the logD verses pH relationship was equal to 5.0 (figure 2.7a), however the valency of iron in this instance should be 3.0. The Fe(II) state being oxidised to Fe(III) below pH 4.0. A lower value for the gradient usually indicates the presence of competing reactions which appear in this case to override the dissociation of oxine.

The use of the two buffer systems has a significant effect on the extraction curves produced. The sodium potassium tartrate system, although maintaining the relative smoothness of the sigmoid curve, was more difficult to control. Complete extraction was still obtained above a pH value of 2.0 (figure 2.6b), although due to the lack of data points

the accuracy of the data should be interpreted with caution. A slight shift in the $pH_{\frac{1}{2}}$ value was also incurred, 1.2, and the gradient recorded for the logD verses pH relationship was 0.56 (figure 2.7b). Obviously the use of sodium potassium tartrate provides a source of competing reagent, resulting in the dissociation of oxine dominating the extraction system.

The use of potassium hydrogen phthalate resulted in the distortion of the sigmoid shape in the pH region 1-4 (figure 2.6c). The general shape is indicative of competing reactions occurring. The gradient obtained from the logD verses pH relationship was 3.0 (figure 2.7c) and resulted in the $pH_{\frac{1}{2}}$ value shifting to 1.5 and complete extraction occurring at a pH value greater than 5.0. The lack of repeatability of this system would make it difficult to operate in a practical situation and as such the use of the unbuffered system is recommended.

(d) Aluminium

The extraction of aluminium was extremely difficult to carry out and produce any measure of repeatability. Significant effort was taken in trying to produce a smooth sigmoidal curve for an unbuffered system with little success. The curve illustrated in figure 2.8 represents the best curve produced from many attempts. The repetative nature of the curve minima indicates the presence of a significant contribution from the competing reactions and, coupled with the dissociation of oxine, results in the curve variation described. It is difficult to assess at what point a 100% extraction is attained or even the value of $pH_{\frac{1}{2}}$.

Although it would appear to lie in the region of pH 2-3 which agrees with the work carried out by Stary (119). The gradient obtained from the plot of logD verses pH was 1.5 (figure 2.9). Clearly supporting the theory of extraneous reactions occurring.

However closer examination of the graphs shows two distinct phases of extraction. The first stage between pH 1.5-2.0 produces a gradient equal to 3.0, the valency of aluminium. However upon passing through a curve minima the gradient between pH 2-4 was nearer 1.0. Clearly showing different phases being undertaken in the reaction sequence. Unfortunately because of time restraints this work was not completed and consequently the evaluation was incomplete.

The extraction studies have shown the great potential of the technique in either extracting all elements of interest or one in particular. By the correct choice of additional complexing agents and the control of pH the selective extraction of an element can be achieved. However it should be noted that the many instances of competing reactions and the subsequent deleterious effects on the extraction systems have to be carefully considered and evaluated before implementing an extraction system on a routine basis within the laboratory.

SECTION 3.0

GRAPHITE FURNACE STUDIES

3.0 GRAPHITE FURNACE STUDIES

3.1 System Optimisation

The graphite furnace is readily installed into the Shimadzu AA-670 Atomic Absorption system by replacing the burner unit in the combustion chamber situated in the main spectrophotometer unit. Prior to the operation of the system a sequence of optimisation stages need to be implemented.

(i) Alignment of graphite furnace,

(ii) Alignment of micropipettes for sample injection,

(iii) Setting of instrumental parameters,

(iv) Temperature calibration of graphite furnace

(v) Preparation of temperature programme.

Each stage of optimisation will be discussed in more detail in the forthcoming sections.

3.1.1 Alignment of graphite furnace

Once the graphite furnace has been installed, as described in section 1.5, it was aligned and set to the optimised position such that the beam emitted from the hollow cathode lamp passes through the graphite tube. The vertical and horizontal positions with respect to the optical axis were adjusted to obtain the required optimum working conditions.

3.1.2 Alignment of Micropipette for Sample Injection

The Shimadzu AA-670 system has the facility for automatic sample injection. To ensure the sample aliquot was injected onto the graphite tube in the correct manner, the initial alignment was carried out manually.

This was implemented by utilising the horizontal (x-axis) and vertical (y-axis) controls for the manipulation of the injection tip into the correct injection position within the graphite tube. The depth of the micropipette into the tube was controlled by manipulation of the z-axis control. The resultant micropipette position ensures the injection phase was operated in a repeatable manner.

3.1.3 Instrumental Settings

The instrument was set up to obtain the best noise free conditions compatable with good sensitivity. The Shimadzu AA-670 employs a microcomputer to control the operational parameters, with the exception of furnace height, and was used to automatically set the range of specified parameters for a given analysis. Figure 3.1 illustrates the parameters set and the temperature programme used for a particular analysis.

3.1.4 Temperature Calibration of Graphite Furnace

Before the system can be used for any quantitative analyses the graphite furnace was required to be temperature calibrated.
The heating of the graphite tube is controlled via two systems;

(i) heating under current control, used when the set temperature is between room temperature and 1099°C;

(ii) heating under temperature control, used when the set temperature is between 1100°C and 3000°C;

A block diagram of the heating control system is shown in figure 3.2,

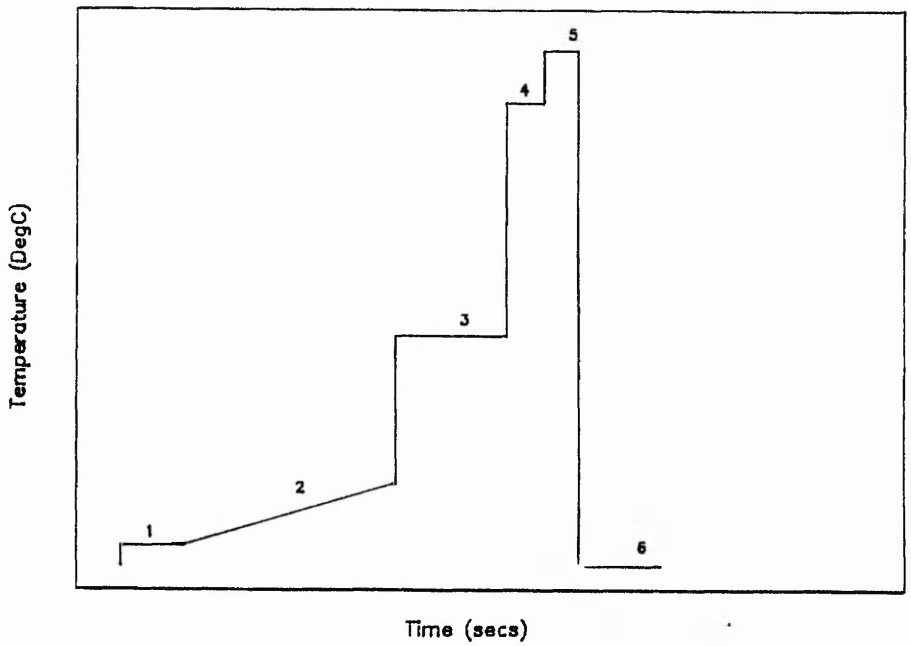

Stage	Temperature (DegC)	Time (secs)	Ramp	Step
1	15	20	–	Y
2	25	15	Y	–
3	600	20	–	Y
4	2300	3	–	Y
5	2800	3	–	Y
6	0	20	–	Y

General program for all elements

The exceptions to this program were,

Copper (using sulphuric acid) – stage 2, time = 30secs

Lead – stage 3 = 250°C, stage 4 = 1300°C for all acids except with sulphuric acid, stage 3 = 350°C

Iron – stage 3 = 200°C for all acids except phosphoric acid = 1000°C

Aluminium – stage 3 = 800°C, stage 4 = 2600°C

Figure 3.1 – Temperature Heating Program

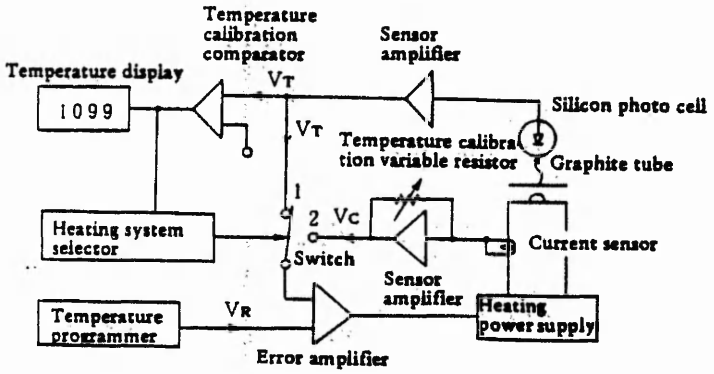

Figure 3.2 Heating Control System

3.1.5 Heating Under Current Control System

The relationship of the current sensor output to the tube temperature (room temperature to 1099°C) and that of the light sensor (silicon photocell) output to the tube temperature, for the standard tubes, have been factory determined, and the conversion curves are stored in the temperature program control unit. When heating starts, the output signal of the current sensor Vc is compared by the error amplifier with the reference signal Vr corresponding to the set temperature, and the current fed into the tube is automatically controlled so as to equalise the two signals. In this system the tube temperature rises after a delay when the current is supplied in stepwise increments as shown in figure 3.3.

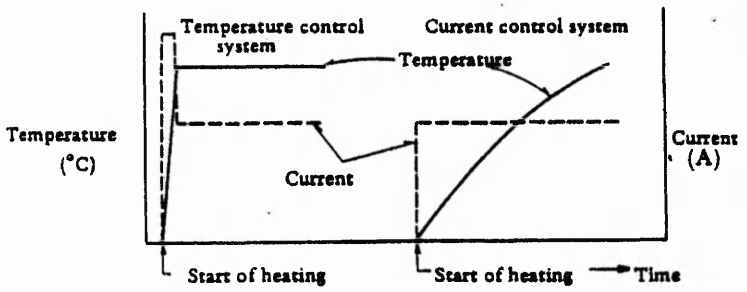

Figure 3.3 Changes in Current and Temperature Under the Temperature Current Control Systems

Normally, the tube temperature attains at least 97% of the set temperature in 20-25 seconds after start of the heating cycle. Since constant current is supplied for a certain set temperature the temperature may vary despite the same setting. This is due to a change in tube resistance by wear or fluctuations in ohmic properties of different tubes.

3.1.6 Heating under Temperature Control System

The light emitted from the tube passes to the temperature sensor unit through the light detect hole on the graphite cap, and the infrared rays selected by the built in narrow band pass optical filter, fall onto the silicon photocell. The photocell output signal is related to tube temperature, the relationship being previously determined and stored in the temperature programmer. When heating starts, the silicon photocell output signal Vt is compared with the reference signal Vr corresponding

to the set temperature at the error amplifier. The current applied to the tube is automatically controlled so as to equalise the two signals. Since in this system an excess current flows at the initial stage of heating, the temperature rises very rapidly. As the tube temperature is measured directly, the current is not affected by changes in the tube resistance and the tube is thus heated to the set temperature.

3.1.7 Temperature Calibration Function in Current Control System

The current control system has the advantage that the temperature fluctuates upon changes in the tube resistance. In order to improve this defect the graphite control system includes the temperature calibration function, figure 3.2. When the calibration variable resistor is adjusted, the gain of the current sensor amplifier varies and consequently the relationship between the set temperature and the tube current changes. However, the silicon photocell output signal is processed by the temperature calibration comparator. When the tube temperature rises to 1100°C or higher, the comparator is actuated, to flash the temperature display. Signifying that the preset temperature of 1100°C is attained.

3.1.8 Preparation of Temperature Programme

The furnace controller enables the basic stages, drying, ash, atomisation, and tube clean up, to be carried out in a sequential form, each stage governed by the particular phase of the controller programme. Each of these stages has to be carefully optimised to obtain the best results for any particular analysis and have been considered in sequence in section 1.5.1.

3.2 Reagents

All reagents were of premium analytical grade and supplied by British Drug House Chemicals, Poole, Dorset unless otherwise stated.

1000ppm metal standards as their respective nitrates.

Hydrochloric, sulphuric, nitric and phosphoric acid

The respective trace inpurity content of the acids used (quoted as part per million) is illustrated as follows

	Nitric Acid (Aristar)	*Nitric Acid (Primar)
Copper	0.005	0.005
Lead	0.002	0.002
Iron	0.100	0.200
Aluminium	0.050	-

	Sulphuric Acid	Phosphoric Acid
Copper	0.02	-
Lead	0.05	-
Iron	1.00	100
Aluminium	0.10	-

	Hydrochloric Acid (GPR)	*Hydrochloric Acid (Primar)
Copper	-	0.002
Lead	5.00	0.001
Iron	1.00	0.200
Aluminium	-	-

* FSA Laboratory Supplies, Loughborough, Leics.

3.3 Sample Preparation

The main objectives of the following programme of work was,

(i) to determine the effects, if any, that different acid matrices would have on the responses of copper, iron, lead and aluminium.

(ii) to develope an analytical method capable of quantifying these elements in a varying matrix to the required degree of confidence in the overall preparation and analytical procedures.

The following solutions were prepared for each element of interest by utilising suitable dilutions of the 1000ppm stock solution in the various acid media outlined below.

(i) Two single solutions 40 and 80ppb, of the relevant element, in a 1% acid matrix were prepared separately. A 1ml sample was taken twelve times from each solution and analysed using graphite furnace atomic absorption. Consequently assuming the different sample vials were of equal cleanliness, and that the sample injection was consistant this approach was used to assess the precision of the technique.

(ii) Twelve separately prepared 80ppb solutions of the relevant element enabled the overall repeatability of the technique to be assessed. This was repeated for each acid matrix.

(iii) To assess the calibration capability a set of standards covering the range 0-100ppb, in 10ppb increments, were prepared. These solutions were prepared for the various elements in the different acid matrices.

The sample solutions were prepared for each element in a 1% nitric acid mixture and were repeated for the sulphuric, hydrochloric and phosphoric acids.

3.4 Statistical Approach

The direct application of classical statistics to a small number of replicate measurements (2 to 20) often leads to false conclusions regarding the probable magnitude of indeterminate error. Fortunately modification of the relationship have been developed such that the random error associated with just two or three values can be calculated. The equation used throughout this investigation for the determination of the standard deviation of a set of data was,

$$s = \sqrt{\frac{\sum (x_i - \bar{x})^2}{N - 1}}$$

where N is the number of individual measurements within a sample set and N-1 equates to the number of degrees of freedom. X_i is the individual measurement, X is the arithmetic mean of the sample set and s is the standard deviation.

The coefficient of variation is a measure of the standard deviation as a percentage of the arithmetic mean and was used as an additional indication of the measurement variation.

For analysis purposes all samples were placed in 1ml sample vials and analysed in triplicate. The results obtained were considered acceptable if the triplicate analyses were to within a coefficient of variance (CV) of 4%. The control program used was such that if this was exceeded an

additional analysis was carried out and a statistical assessment, using the best three analyses, was used to quote an acceptable mean.

The single solutions of 40ppb and 80ppb, were each placed in twelve separate vials and triplicate analyses of each was obtained. The results of each analysis were grouped, using the sample mean, and a simple statistical approach adopted. That is, the group would be considered acceptable at a 95% confidence limit if all results were within two standard deviations of the mean value. Such results can be viewed in section 3.5.

A similar approach was adopted for the assessment of twelve separate solutions of 80ppb, (tabulated in table 3.8) and the calibration curve over the range 0-100ppb (refer to table 3.5 and figure 3.5).

3.5 Results.

The results relating to the analysis of copper, lead, iron and aluminium, in the four acid matrices, using graphite furnace atomic absorption spectroscopy, are summarised in the following paragraphs,

The ash/atomisation data relating to the analysis of the above named elements are tabulated as follows,

Copper	Tables	3.1-3.4
Lead	Tables	3.9-3.12
Iron	Tables	3.17-3.20
Aluminium	Tables	3.25-3.28

The results are graphically represented in figures 3.4, 3.6, 3.8, and 3.10 respectively.

The heating programme used throughout these analyses is outlined in figure 3.1.

The calibration data relating to the four elements is tabulated in tables 3.5, 3.13, 3.21, and 3.29, respectively. The results are graphically presented in figures 3.5, 3.7, 3.9,and 3.11 respectively.

The results relating to the repeatability exercise, using the single solution of 80ppb of the element of interest, are summarised in tables 3.6, 3.14, 3.22, and 3.30 respectively.

The reults relating to the repeatability exercise, using the single solution of 40ppb of the element of interest, are summarised in tables 3.7, 3.15, 3.23, and 3.31 respectively.

The results relating to the repeatability exercise using twelve individually prepared solutions of 80ppb of the elements of interest are summarised in tables 3.8, 3.16, 3.24, and 3.32 respectively.

Ash		Atomisation	
Temperature (°C)	Absorbance	Temperature (°C)	Absorbance
500	0.262	–	–
600	0.265	–	–
700	0.264	–	–
800	0.263	–	–
900	0.257	–	–
1000	0.256	–	–
1100	0.186	–	–
1200	0.138	–	–
1300	0.088	–	–
–	–	1500	0.105
–	–	1600	0.157
–	–	1700	0.202
–	–	1800	0.235
–	–	1900	0.260
–	–	2000	0.274
–	–	2100	0.270
–	–	2200	0.271
–	–	2300	0.262

Table 3.1 – Ash/Atomisation Curve for Copper in 1% Hydrochloric Acid

Ash		Atomisation	
Temperature (°C)	Absorbance	Temperature (°C)	Absorbance
400	0.374	-	-
600	0.380	-	-
700	0.374	-	-
800	0.382	-	-
900	0.372	-	-
950	0.362	-	-
1000	0.311	-	-
1050	0.350	-	-
1100	0.277	-	-
1150	0.253	-	-
1200	0.236	-	-
1250	0.220	-	-
1300	0.179	-	-
1350	0.150	-	-
1400	0.095	-	-
-	-	1600	0.171
-	-	1700	0.279
-	-	1800	0.321
-	-	1900	0.351
-	-	2000	0.368
-	-	2100	0.385
-	-	2200	0.375
-	-	2300	0.370

Table 3.2 – Ash/Atomisation Curve for Copper in 1% Nitric Acid

Ash		Atomisation	
Temperature (°C)	Absorbance	Temperature (°C)	Absorbance
500	0.331	–	–
600	0.346	–	–
700	0.348	–	–
800	0.339	–	–
900	0.334	–	–
1000	0.330	–	–
1050	0.290	–	–
1100	0.175	–	–
1200	0.139	–	–
1300	0.064	–	–
–	–	1400	0.112
–	–	1500	0.133
–	–	1600	0.209
–	–	1700	0.261
–	–	1800	0.284
–	–	1900	0.299
–	–	2000	0.297
–	–	2100	0.299
–	–	2200	0.312
–	–	2300	0.304

Table 3.3 – Ash/Atomisation Curve for Copper in 1% Phosphoric Acid

Ash		Atomisation	
Temperature (°C)	Absorbance	Temperature (°C)	Absorbance
500	0.304	–	–
600	0.305	–	–
700	0.311	–	–
800	0.307	–	–
900	0.298	–	–
1000	0.291	–	–
1100	0.225	–	–
1200	0.192	–	–
1300	0.135	–	–
1400	0.064	–	–
–	–	1400	0.059
–	–	1500	0.093
–	–	1600	0.142
–	–	1700	0.188
–	–	1800	0.234
–	–	1900	0.260
–	–	2000	0.276
–	–	2100	0.279
–	–	2200	0.281
–	–	2300	0.278
–	–	2400	0.286

Table 3.4 – Ash/Atomisation Curve for Copper in 1% Sulphuric Acid

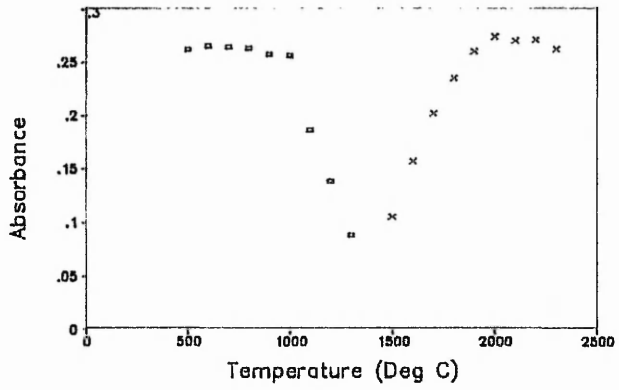

▪ Ash
x Atomisation

1% Hydrochloric Acid (a)

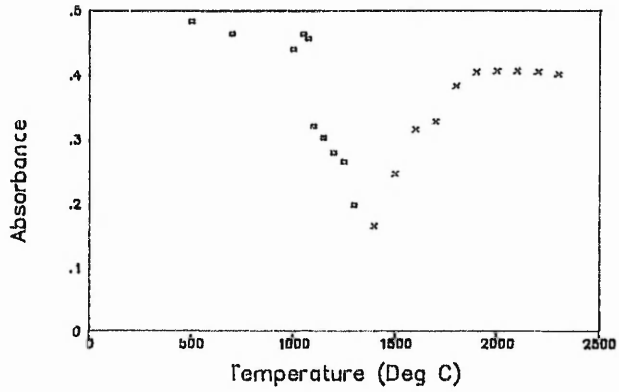

1% Nitric Acid (b)

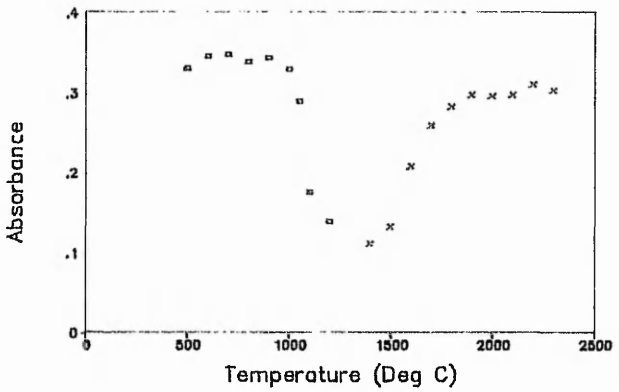

1% Phosphoric Acid (c)

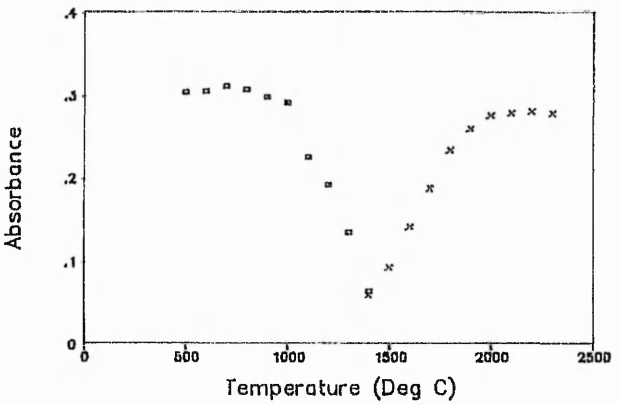

1% Sulphuric Acid (d)

Figure 3.4 – Ash/Atomisation Curves for Copper

Concentration (ppb)	Hydrochloric Acid		Sulphuric Acid		Nitric Acid		Phosphoric Acid	
	Absorbance	CV	Absorbance	CV	Absorbance	CV	Absorbance	CV
0	0.025	8.397	0.013	7.687	0.020	3.800	0.042	0.882
10	0.057	2.379	0.059	1.709	0.066	0.950	0.080	3.225
20	0.092	2.338	0.094	1.577	0.101	0.703	0.121	2.066
30	0.147	1.166	0.126	1.533	0.140	2.025	0.160	0.592
40	0.160	0.629	0.176	1.825	0.194	1.200	0.190	0.090
50	0.176	0.488	0.203	2.668	0.209	3.570	0.223	1.101
60	0.228	2.099	0.243	1.237	0.259	1.670	0.259	0.936
70	0.264	1.093	0.272	1.399	0.288	1.532	0.294	2.302
80	0.262	2.210	0.314	2.467	0.332	0.284	0.336	2.654
90	0.301	0.542	0.359	1.038	0.365	0.995	0.367	0.537
100	0.378	3.370	0.388	1.319	0.406	0.541	0.407	1.432

Table 3.5 – Calibration Data for Copper (0 – 100 ppb).

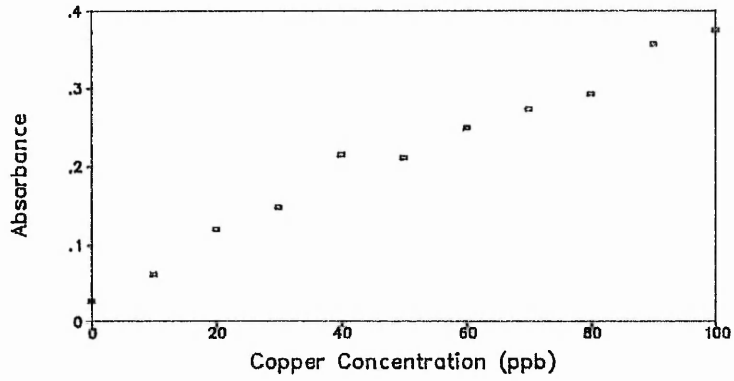

1% Hydrochloric Acid (a)

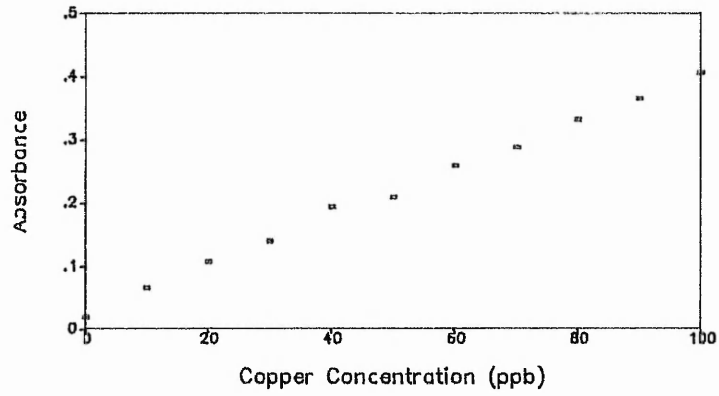

1% Nitric Acid (b)

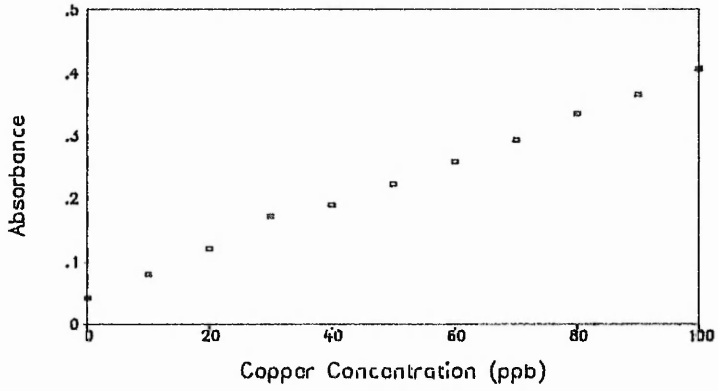

1% Phosphoric Acid (c)

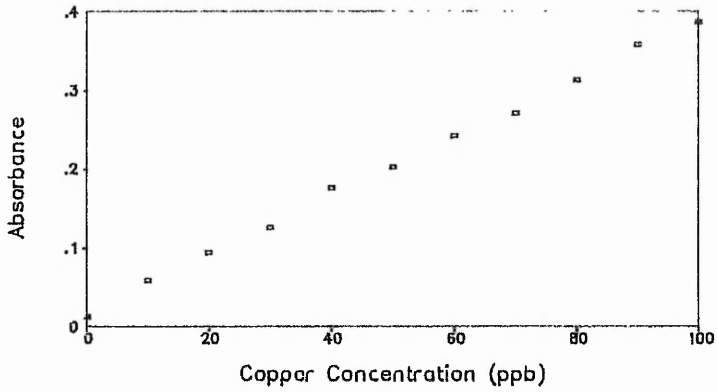

1% Sulphuric Acid (d)

Figure 3.5 – Calibration Curves for Copper

Hydrochloric Acid		Sulphuric Acid		Nitric Acid		Phosphoric Acid	
Absorbance	CV	Absorbance	CV	Absorbance	CV	Absorbance	CV
0.401	0.665	0.328	2.554	0.373	0.370	0.343	2.314
0.394	1.251	0.321	2.580	0.356	0.260	0.343	1.023
0.379	0.929	0.336	2.616	0.350	0.429	0.348	0.350
0.382	0.766	0.335	0.300	0.342	0.480	0.356	0.651
0.392	2.029	0.329	1.209	0.360	0.477	0.357	1.180
0.383	0.940	0.340	3.404	0.368	0.817	0.341	3.944
0.384	0.777	0.313	2.879	0.367	2.350	0.364	0.891
0.393	2.092	0.327	3.715	0.344	1.054	0.362	0.843
0.385	1.449	0.345	1.397	0.391	1.585	0.372	2.732
0.374	0.967	0.314	3.769	0.366	1.938	0.364	2.396
0.383	2.321	0.357	2.310	0.349	1.360	0.349	3.384
0.408	2.086	0.353	2.680	0.355	0.613	0.344	2.710
$\bar{x}$ = 0.388		$\bar{x}$ = 0.333		$\bar{x}$ = 0.360		$\bar{x}$ = 0.354	
s = 0.01		s = 0.007		s = 0.014		s = 0.01	

Table 3.6 – 80ppb Copper : repeatability of single solutions.

Hydrochloric Acid		Sulphuric Acid		Nitric Acid		Phosphoric Acid	
Absorbance	CV	Absorbance	CV	Absorbance	CV	Absorbance	CV
0.287	1.633	0.171	0.980	0.228	0.239	0.199	2.487
0.270	0.835	0.169	0.547	0.211	1.375	0.192	0.658
0.267	1.604	0.170	1.643	0.187	1.776	0.190	2.895
0.271	2.697	0.174	1.224	0.190	3.272	0.190	1.415
0.282	2.674	0.180	0.468	0.220	0.576	0.187	0.589
0.329	0.644	0.172	0.470	0.183	2.077	0.188	1.308
0.298	0.692	0.166	3.442	0.185	1.411	0.190	3.308
0.318	1.272	0.164	0.687	0.182	1.253	0.186	1.208
0.284	1.453	0.165	3.035	0.182	0.709	0.190	2.504
0.273	1.974	0.177	3.381	0.211	3.131	0.193	1.236
0.287	3.920	0.168	1.389	0.211	3.840	0.197	1.497
0.301	2.746	0.153	1.479	0.190	2.855	0.195	0.491
$\bar{x}$ = 0.289		$\bar{x}$ = 0.169		$\bar{x}$ = 0.198		$\bar{x}$ = 0.191	
s = 0.02		s = 0.007		s = 0.017		s = 0.004	

Table 3.7 – 40ppb Copper : repeatability of single solutions.

Hydrochloric Acid		Sulphuric Acid		Nitric Acid		Phosphoric Acid	
Absorbance	CV	Absorbance	CV	Absorbance	CV	Absorbance	CV
0.386	0.302	0.326	3.912	0.285	2.932	0.363	3.475
0.385	2.925	0.299	3.096	0.271	3.192	0.355	1.256
0.377	2.118	0.319	1.843	0.306	3.572	0.363	3.783
0.393	1.605	0.330	1.252	0.287	3.291	0.346	2.323
0.380	2.900	0.327	1.858	0.327	3.671	0.362	3.916
0.395	2.490	0.338	1.692	0.293	2.947	0.370	0.666
0.360	3.354	0.343	3.124	0.348	3.733	0.354	3.193
0.346	2.775	0.362	0.644	0.282	3.227	0.368	1.572
0.422	1.137	0.326	3.910	0.270	3.137	0.354	0.934
0.404	3.014	0.350	3.313	0.291	1.600	0.365	0.400
0.419	0.847	0.372	3.182	0.299	2.725	0.384	1.412
0.464	3.835	0.306	1.083	0.276	1.540	0.358	2.821
$\bar{x}$ = 0.394		$\bar{x}$ = 0.333		$\bar{x}$ = 0.295		$\bar{x}$ = 0.362	
s = 0.031		s = 0.021		s = 0.023		s = 0.01	

Table 3.8 – 80ppb Copper : repeatability of separate solutions.

Ash		Atomisation	
Temperature (°C)	Absorbance	Temperature (°C)	Absorbance
200	0.308	–	–
300	0.303	–	–
400	0.290	–	–
500	0.279	–	–
600	0.258	–	–
700	0.221	–	–
800	0.153	–	–
900	0.090	–	–
–	–	1100	0.305
–	–	1200	0.295
–	–	1300	0.299
–	–	1400	0.296
–	–	1500	0.293
–	–	1600	0.299
–	–	1700	0.288
–	–	1800	0.284

Table 3.9 – Ash/Atomisation Curve for Lead in 1% Hydrochloric Acid

Ash		Atomisation	
Temperature (°C)	Absorbance	Temperature (°C)	Absorbance
100	0.263	–	–
300	0.243	–	–
500	0.224	–	–
600	0.209	–	–
700	0.171	–	–
800	0.090	–	–
–	–	1100	0.255
–	–	1200	0.247
–	–	1300	0.253
–	–	1400	0.251
–	–	1500	0.246
–	–	1600	0.245

Table 3.10 – Ash/Atomisation Curve for Lead in 1% Nitric Acid

Ash		Atomisation	
Temperature (°C)	Absorbance	Temperature (°C)	Absorbance
100	0.310	–	–
200	0.323	–	–
300	0.315	–	–
400	0.315	–	–
500	0.300	–	–
600	0.282	–	–
700	0.261	–	–
800	0.211	–	–
900	0.104	–	–
–	–	1100	0.226
–	–	1200	0.270
–	–	1300	0.296
–	–	1400	0.294
–	–	1500	0.289
–	–	1600	0.287

Table 3.11 – Ash/Atomisation Curve for Lead in 1% Phosphoric Acid

Ash		Atomisation	
Temperature (°C)	Absorbance	Temperature (°C)	Absorbance
200	0.341	–	–
250	0.332	–	–
300	0.328	–	–
350	0.315	–	–
400	0.300	–	–
500	0.281	–	–
600	0.277	–	–
700	0.217	–	–
–	–	900	0.005
–	–	1000	0.005
.	–	1100	0.289
.	.	1200	0.290
	.	1300	0.293
	.	1400	0.294
.	.	1500	0.300
.	.	1600	0.297

Table 3.12 – Ash/Atomisation Curve for Lead in 1% Sulphuric Acid

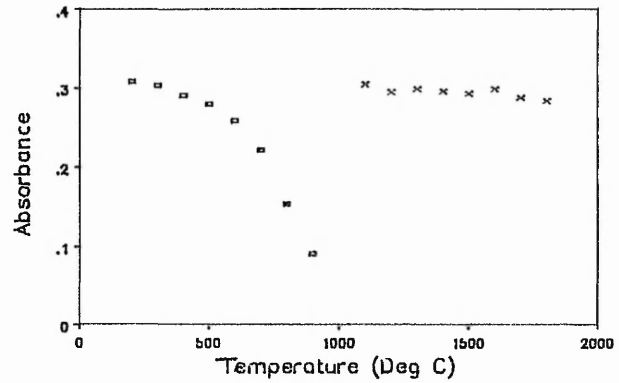

▫ Ash
× Atomisation

1% Hydrochloric Acid (a)

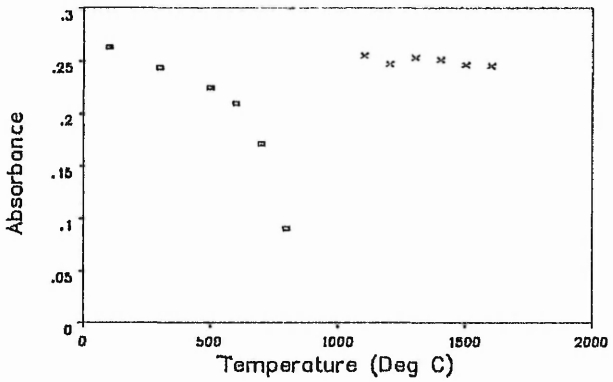

1% Nitric Acid (b)

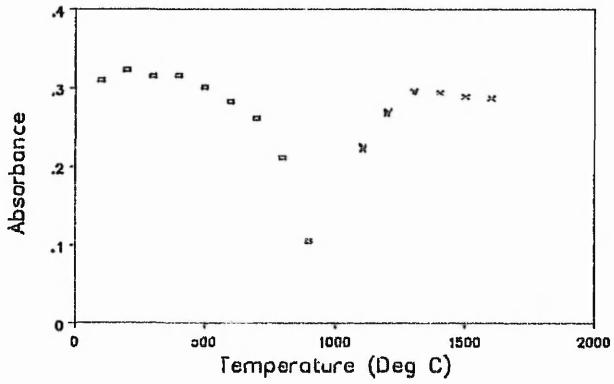

1% Phosphoric Acid (c)

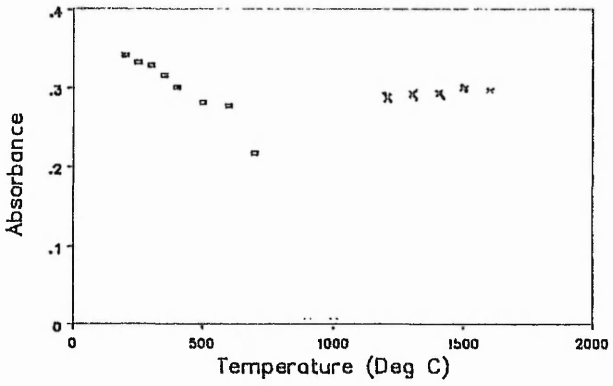

1% Sulphuric Acid (d)

Figure 3.6 – Ash/Atomisation Curves for Lead

Concentration (ppb)	Hydrochloric Acid		Sulphuric Acid		Nitric Acid		Phosphoric Acid	
	Absorbance	CV	Absorbance	CV	Absorbance	CV	Absorbance	CV
0	0.012	4.488	0.011	8.200	0.016	27.77	0.026	5.068
10	0.060	2.766	0.052	1.295	0.062	1.932	0.050	1.054
20	0.109	2.233	0.084	0.461	0.115	2.856	0.080	2.540
30	0.154	1.497	0.113	1.871	0.155	0.910	0.104	2.170
40	0.199	0.122	0.155	2.693	0.182	1.325	0.130	2.510
50	0.251	0.508	0.182	5.542	0.224	0.217	0.158	1.030
60	0.269	1.169	0.227	1.303	0.266	2.686	0.182	2.421
70	0.315	0.077	0.244	1.383	0.300	1.598	0.197	2.004
80	0.344	0.556	0.284	1.328	0.337	2.166	0.224	0.406
90	0.383	0.618	0.314	1.998	0.367	2.105	0.242	2.703
100	0.435	0.568	0.356	1.432	0.399	1.253	0.264	2.099

Table 3.13 – Calibration Data for Lead (0 – 100ppb).

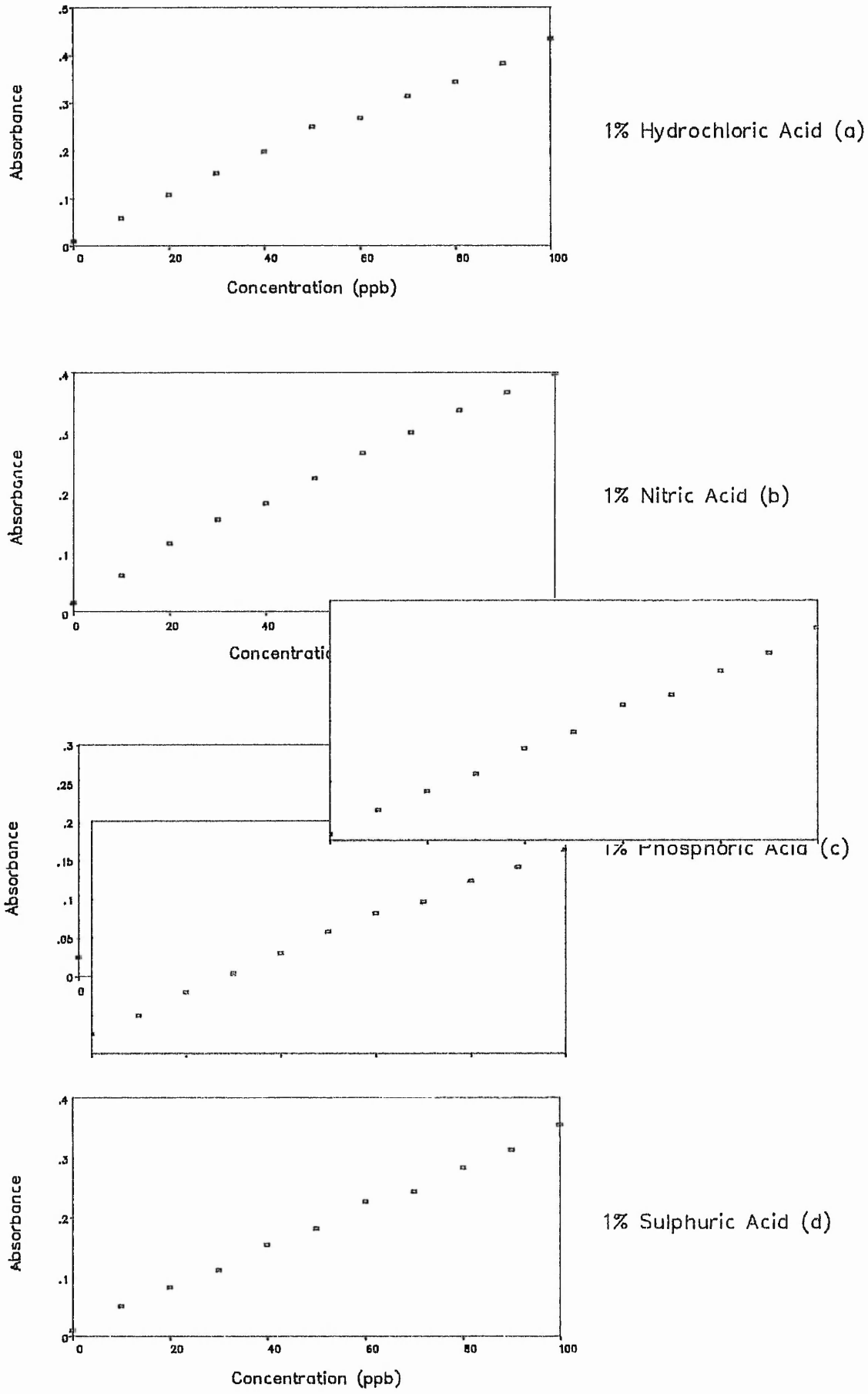

Figure 3.7 – Calibration Curve for Lead

Hydrochloric Acid		Sulphuric Acid		Nitric Acid		Phosphoric Acid	
Absorbance	CV	Absorbance	CV	Absorbance	CV	Absorbance	Cv
0.354	2.175	0.380	2.347	0.326	3.428	0.238	1.171
0.354	1.271	0.391	1.578	0.345	0.371	0.218	3.164
0.350	0.842	0.388	0.868	0.348	2.707	0.215	2.221
0.344	2.041	0.386	0.227	0.344	2.240	0.212	3.252
0.343	1.171	0.383	0.354	0.336	0.818	0.223	3.121
0.352	1.271	0.377	1.791	0.352	2.275	0.214	2.279
0.350	0.825	0.378	1.538	0.333	1.015	0.225	2.652
0.356	0.794	0.387	0.584	0.338	1.138	0.214	1.854
0.353	0.378	0.397	1.513	0.345	2.681	0.223	2.823
0.334	2.417	0.405	0.745	0.342	1.235	0.218	2.923
0.359	0.249	0.401	1.136	0.342	1.327	0.222	2.970
0.365	0.754	0.402	0.923	0.347	0.954	0.223	2.026
$\bar{x}$ = 0.351		$\bar{x}$ = 0.389		$\bar{x}$ = 0.341		$\bar{x}$ = 0.220	
s = 0.008		s = 0.01		s = 0.007		s = 0.007	

Table 3.14 — 80ppb Lead : repeatability of single solutions.

Hydrochloric Acid		Sulphuric Acid		Nitric Acid		Phosphoric Acid	
Absorbance	CV	Absorbance	CV	Absorbance	CV	Absorbance	CV
0.197	1.919	0.149	1.224	0.193	1.609	0.144	3.522
0.187	0.663	0.155	1.668	0.191	1.606	0.135	2.174
0.187	1.014	0.148	0.733	0.191	3.369	0.144	1.048
0.189	0.626	0.154	0.844	0.191	2.856	0.136	2.656
0.187	0.650	0.147	0.451	0.187	2.428	0.142	1.338
0.188	1.704	0.150	1.053	0.184	3.069	0.141	0.799
0.192	0.389	0.148	0.419	0.186	1.040	0.135	0.593
0.190	0.559	0.152	2.619	0.183	2.383	0.135	0.720
0.186	1.685	0.150	0.689	0.183	1.425	0.138	0.751
0.186	1.266	0.156	2.149	0.184	0.538	0.131	1.119
0.194	1.809	0.159	1.435	0.193	1.362	0.140	1.279
0.189	1.584	0.160	1.415	0.187	0.822	0.134	1.991
$\bar{x}$ = 0.189		$\bar{x}$ = 0.152		$\bar{x}$ = 0.188		$\bar{x}$ = 0.138	
s = 0.003		s = 0.004		s = 0.004		s = 0.004	

Table 3.15 – 40ppb Lead : repeatability of single solutions.

Hydrochloric Acid		Sulphuric Acid		Nitric Acid		Phosphoric Acid	
Absorbance	CV	Absorbance	CV	Absorbance	CV	Absorbance	CV
0.330	1.389	0.293	1.197	0.362	2.923	0.219	2.868
0.334	0.679	0.361	2.553	0.354	2.307	0.216	2.625
0.338	0.986	0.270	1.431	0.336	8.584	0.222	3.588
0.327	1.462	0.277	3.158	0.331	5.099	0.224	3.334
0.341	1.095	0.271	2.999	0.332	0.619	0.222	3.743
0.345	0.158	0.271	2.965	0.332	1.790	0.214	3.031
0.346	0.572	0.263	3.636	0.328	0.646	0.223	1.554
0.345	0.533	0.272	2.891	0.337	1.977	0.229	2.191
0.358	0.533	0.275	3.278	0.350	2.376	0.233	2.896
0.354	0.186	0.285	3.220	0.321	2.049	0.221	0.566
0.352	0.566	0.275	2.216	0.376	2.367	0.223	3.526
0.334	0.500	0.292	3.691	0.337	1.722	0.216	1.951
$\bar{x}$ = 0.342		$\bar{x}$ = 0.284		$\bar{x}$ = 0.341		$\bar{x}$ = 0.222	
s = 0.01		s = 0.026		s = 0.016		s = 0.005	

Table 3.16 – 80ppb Lead : repeatability of separate solutions.

Ash		Atomisation	
Temperature (°C)	Absorbance	Temperature (°C)	Absorbance
200	0.488	–	–
300	0.476	–	–
400	0.469	–	–
500	0.489	–	–
600	0.492	–	–
700	0.498	–	–
800	0.487	–	–
900	0.489	–	–
1000	0.487	–	–
1100	0.479	–	–
–	–	1600	0.140
–	–	1700	0.214
–	–	1800	0.285
–	–	1900	0.360
–	–	2000	0.449
–	–	2100	0.463
–	–	2200	0.479
–	–	2300	0.467

Table 3.17 – Ash/Atomisation Curve for Iron in 1% Hydrochloric Acid

Ash		Atomisation	
Temperature (°C)	Absorbance	Temperature (°C)	Absorbance
100	0.439	–	–
200	0.436	–	–
300	0.426	–	–
400	0.412	–	–
500	0.431	–	–
600	0.424	–	–
700	0.410	–	–
800	0.410	–	–
900	0.400	–	–
1000	0.394	–	–
–	–	1400	0.128
–	–	1600	0.135
–	–	1800	0.335
–	–	2000	0.440
–	–	2200	0.406
–	–	2300	0.412
–	–	2400	0.393

Table 3.18 – Ash/Atomisation Curve for Iron in 1% Nitric Acid

Ash		Atomisation	
Temperature (°C)	Absorbance	Temperature (°C)	Absorbance
200	0.586	–	–
400	0.628	–	–
600	0.655	–	–
800	0.653	–	–
1000	0.663	–	–
1200	0.593	–	–
1400	0.541	–	–
1500	0.358	–	–
1600	0.210	–	–
–	–	1600	0.178
–	–	1700	0.221
–	–	1800	0.324
–	–	1900	0.378
–	–	2000	0.492
–	–	2100	0.537
–	–	2200	0.565
–	–	2300	0.598
–	–	2400	0.592

Table 3.19 – Ash/Atomisation Curve for Iron in 1% Phosphoric Acid

Ash		Atomisation	
Temperature (°C)	Absorbance	Temperature (°C)	Absorbance
200	0.665	–	–
400	0.647	–	–
600	0.653	–	–
800	0.645	–	–
1000	0.619	–	–
1200	0.593	–	–
1400	0.529	–	–
1600	0.280	–	–
–	–	1600	0.171
–	–	1700	0.301
–	–	1800	0.412
–	–	1900	0.526
–	–	2000	0.616
–	–	2100	0.669
–	–	2200	0.650
–	–	2300	0.687

Table 3.20 – Ash/Atomisation Curve for Iron in 1% Sulphuric Acid

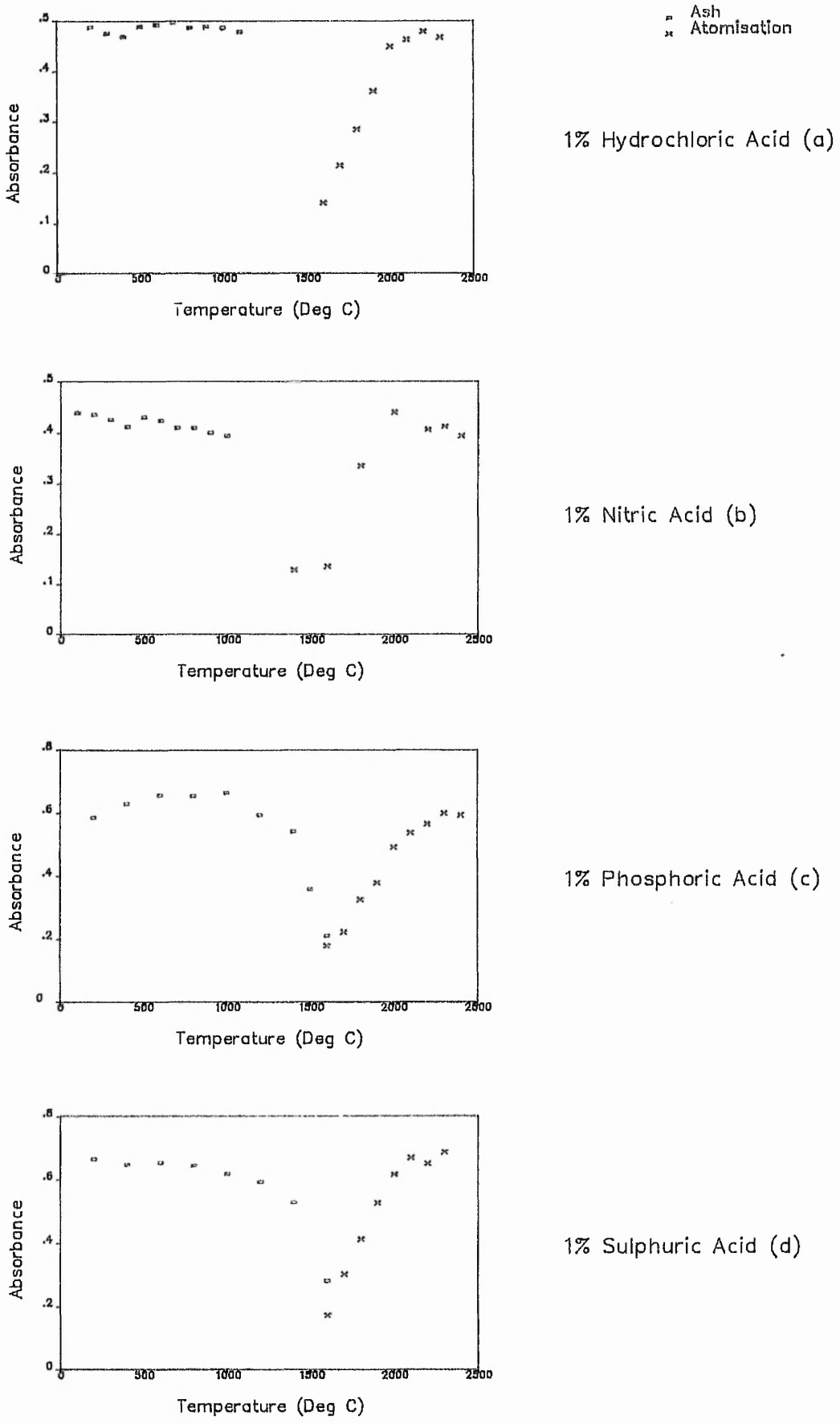

Figure 3.8 – Ash/Atomisation Curves for Iron

Concentration (ppb)	Hydrochloric Acid		Sulphuric Acid		Nitric Acid		Phosphoric Acid	
	Absorbance	CV	Absorbance	CV	Absorbance	CV	Absorbance	CV
0	0.095	2.438	0.073	12.38	0.108	3.269	–	–
10	0.140	2.734	0.172	1.096	0.180	0.904	–	–
20	0.205	0.978	0.255	0.684	0.228	1.129	–	–
30	0.253	1.367	0.282	0.251	0.226	1.758	–	–
40	0.299	1.412	0.369	2.602	0.310	2.181	–	–
50	0.325	1.412	0.406	0.968	0.363	1.882	–	–
60	0.390	1.198	0.456	1.794	0.406	2.607	–	–
70	0.442	1.476	0.506	3.738	0.458	3.017	–	–
80	0.457	0.844	0.540	0.747	0.511	1.940	–	–
90	0.514	0.388	0.583	2.508	0.568	2.526	–	–
100	0.546	1.159	0.608	0.734	0.721	1.446	–	–

Table 3.21 – Calibration Data for Iron (0 – 100 ppb).

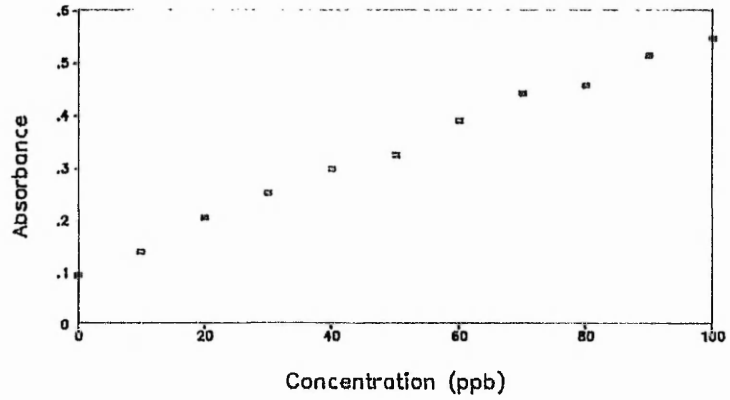

1% Hydrochloric Acid (a)

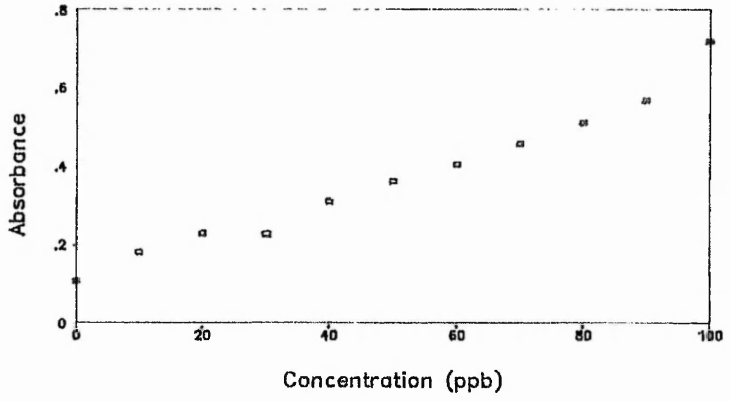

1% Nitric Acid (b)

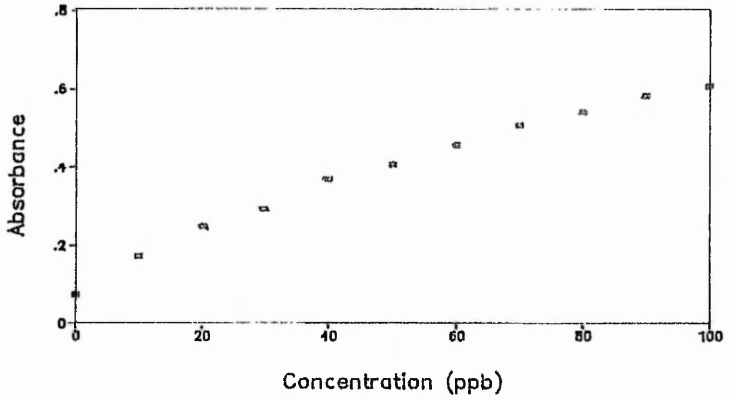

1% Sulphuric Acid (c)

Figure 3.9. – Calibration Curves for Iron

Hydrochloric Acid		Sulphuric Acid		Nitric Acid		Phosphoric Acid	
Absorbance	CV	Absorbance	CV	Absorbance	CV	Absorbance	CV
0.479	1.011	0.700	0.646	0.443	2.473	–	–
0.483	0.492	0.683	0.589	0.423	0.628	–	–
0.480	1.497	0.687	0.594	0.432	2.040	–	–
0.493	1.323	0.675	3.846	0.429	2.539	–	–
0.493	1.344	0.695	0.465	0.437	1.349	–	–
0.458	0.477	0.683	0.377	0.433	0.954	–	–
0.478	2.019	0.690	0.360	0.437	0.332	–	–
0.471	0.273	0.664	2.493	0.435	1.700	–	-
0.476	3.519	0.674	0.812	0.439	3.276	–	-
0.492	0.840	0.672	1.001	0.436	2.390	–	-
0.473	1.259	0.678	0.477	0.449	2.589	–	–
0.459	0.571	0.677	0.577	0.438	3.747	–	–
$\bar{x}$ = 0.476		$\bar{x}$ = 0.681		$\bar{x}$ = 0.436		-	
s = 0.013		s = 0.011		s = 0.007			

Table 3.22 – 80ppb Iron : repeatability of single solutions.

Hydrochloric Acid		Sulphuric Acid		Nitric Acid		Phosphoric Acid	
Absorbance	CV	Absorbance	CV	Absorbance	CV	Absorbance	CV
0.256	1.269	0.460	0.992	0.330	2.783	–	–
0.261	2.083	0.438	1.070	0.309	1.059	–	–
0.230	2.273	0.444	0.703	0.303	1.674	–	–
0.243	2.714	0.444	2.042	0.304	2.584	–	–
0.226	0.758	0.449	0.948	0.304	0.979	–	–
0.248	2.175	0.464	0.658	0.310	1.498	–	–
0.222	0.625	0.442	1.139	0.302	1.786	–	–
0.228	1.721	0.438	1.137	0.299	2.277	–	–
0.224	0.544	0.418	3.374	0.303	1.437	–	–
0.226	1.288	0.427	1.674	0.308	1.311	–	–
0.233	2.358	0.415	4.262	0.310	0.597	–	–
0.224	0.973	0.437	1.069	0.344	1.534	–	–
$\bar{x}$ = 0.235		$\bar{x}$ = 0.440		$\bar{x}$ = 0.310		-	
s = 0.013		s = 0.015		s = 0.014			

Table 3.23 – 40ppb Iron : repeatability of single solutions.

Hydrochloric Acid		Sulphuric Acid		Nitric Acid		Phosphoric Acid	
Absorbance	CV	Absorbance	CV	Absorbance	CV	Absorbance	CV
0.510	0.704	0.569	2.456	–	–	–	–
0.510	1.050	0.573	0.860	–	–	–	–
0.522	0.972	0.565	1.547	–	–	–	–
0.493	2.072	0.582	2.218	–	–	–	–
0.497	1.310	0.566	2.329	–	–	–	–
0.507	0.759	0.547	1.212	–	–	–	–
0.541	0.123	0.573	0.697	–	–	–	–
0.501	0.245	0.572	1.231	–	–	–	–
0.505	1.889	0.553	0.515	–	–	–	–
0.524	3.068	0.599	0.719	–	–	–	–
0.515	0.236	0.611	0.723	–	–	–	–
0.520	1.483	0.602	4.047	–	–	–	–
$\bar{x}$ = 0.514 s = 0.014		$\bar{x}$ = 0.576 s = 0.019		-		-	

Table 3.24 – 80ppb Iron : repeatability of separate solutions.

Ash		Atomisation	
Temperature (°C)	Absorbance	Temperature (°C)	Absorbance
50	0.145	–	–
100	0.167	–	–
150	0.172	–	–
200	0.177	–	–
300	0.180	–	–
400	0.182	–	–
600	0.191	–	–
800	0.201	–	–
1000	0.198	–	–
1200	0.203	–	–
1400	0.201	–	–
1600	0.184	–	–
1800	0.177	–	–
1950	0.141	–	–
2000	0.107	–	–
2050	0.065	–	–
–	–	2150	0.058
		2200	0.090
		2250	0.109
		2300	0.140
–		2400	0.155
–		2500	0.171
–	–	2600	0.170

Table 3.25 – Ash/Atomisation Curve for Aluminium in 1% Hydrochloric Acid

Ash		Atomisation	
Temperature (°C)	Absorbance	Temperature (°C)	Absorbance
200	0.233	–	–
400	0.247	–	–
600	0.222	–	–
800	0.242	–	–
1000	0.236	–	–
1200	0.222	–	–
1400	0.219	–	–
1600	0.212	–	–
1800	0.167	–	–
2000	0.067	–	–
–	–	2100	0.037
–	–	2200	0.092
-	–	2300	0.129
-	–	2350	0.171
–	–	2400	0.228
–	–	2500	0.228
–	–	2600	0.236

Table 3.26 – Ash/Atomisation Curve for Aluminium in 1% Nitric Acid

Ash		Atomisation	
Temperature (°C)	Absorbance	Temperature (°C)	Absorbance
200	0.275	–	–
400	0.303	–	–
600	0.300	–	–
800	0.309	–	–
1000	0.313	–	–
1200	0.317	–	–
1400	0.288	–	–
1600	0.289	–	–
1800	0.266	–	–
1900	0.231	–	–
2000	0.161	2100	0.032
–	–	2200	0.094
–	–	2300	0.134
–	–	2350	0.169
–	–	2400	0.225
–	–	2500	0.228
–	–	2600	0.234

Table 3.27 – Ash/Atomisation Curve for Aluminium in 1% Phosphoric Acid

Ash		Atomisation	
Temperature (°C)	Absorbance	Temperature (°C)	Absorbance
200	0.292	–	–
400	0.295	–	–
600	0.303	–	–
800	0.298	–	–
1000	0.293	–	–
1200	0.292	–	–
1400	0.296	–	–
1600	0.249	–	–
1700	0.270	–	–
1800	0.253	–	–
1900	0.227	–	–
2000	0.157	–	–
2100	0.083	–	–
–	–	2200	0.117
–	–	2250	0.144
–	–	2300	0.171
–	–	2350	0.192
–	–	2400	0.221
–	–	2450	0.246
–	–	2500	0.271
–	–	2600	0.264

Table 3.28 – Ash/Atomisation Curve for Aluminium in 1% Sulphuric Acid

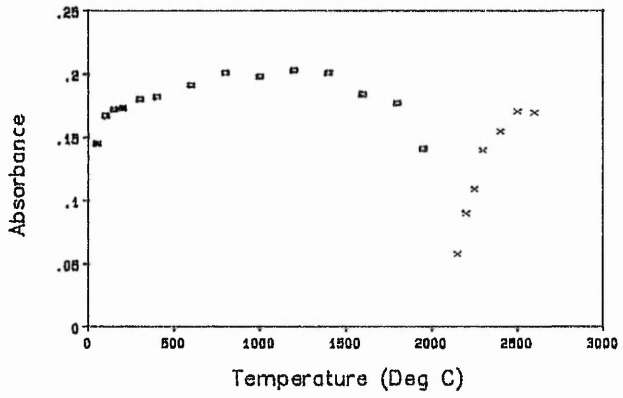

1% Hydrochloric Acid (a)

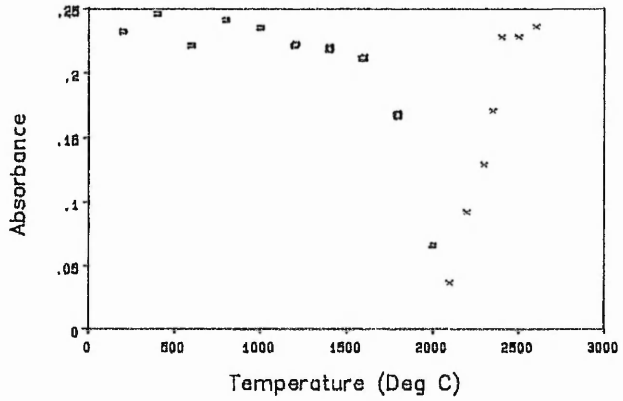

1% Nitric Acid (b)

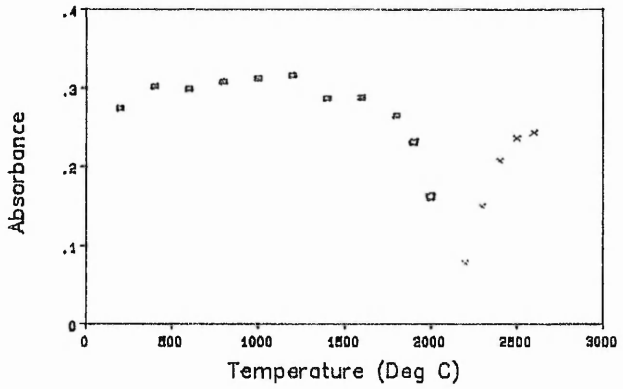

1% Phosphoric Acid (c)

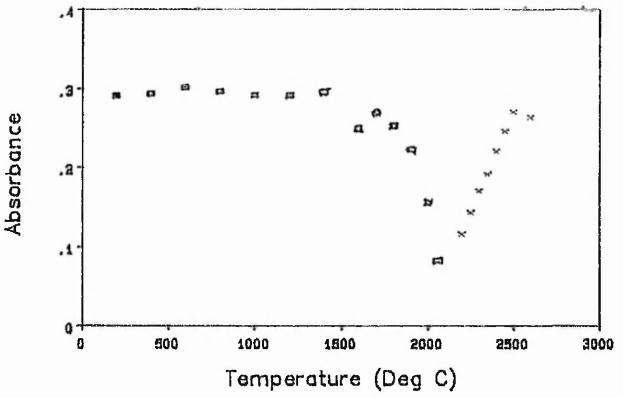

1% Sulphuric Acid (d)

Figure 3.10 – Ash/Atomisation Curves for Aluminium

Concentration (ppb)	Hydrochloric Acid		Sulphuric Acid		Nitric Acid		Phosphoric Acid	
	Absorbance	CV	Absorbance	CV	Absorbance	CV	Absorbance	CV
0	0.021	5.497	0.024	6.885	0.021	9.173	0.077	1.463
10	0.045	0.425	0.056	5.577	0.047	1.913	0.139	1.807
20	0.069	3.842	0.090	2.963	0.063	4.858	0.152	1.244
30	0.080	7.248	0.112	3.195	0.083	2.400	0.177	1.001
40	0.105	1.225	0.134	3.702	0.112	2.966	0.189	1.971
50	0.129	0.939	0.150	3.485	0.132	2.547	0.215	2.559
60	0.163	2.346	0.178	0.703	0.152	2.106	0.217	1.363
70	0.167	0.145	0.194	1.464	0.169	1.577	0.237	0.861
80	0.191	0.549	0.212	2.292	0.191	3.736	0.260	1.674
90	0.214	3.480	0.244	1.893	0.200	2.674	0.289	1.362
100	0.241	2.947	0.264	2.524	0.236	3.317	0.300	0.853

Table 3.29 – Calibration Data for Aluminium (0 – 100 ppb).

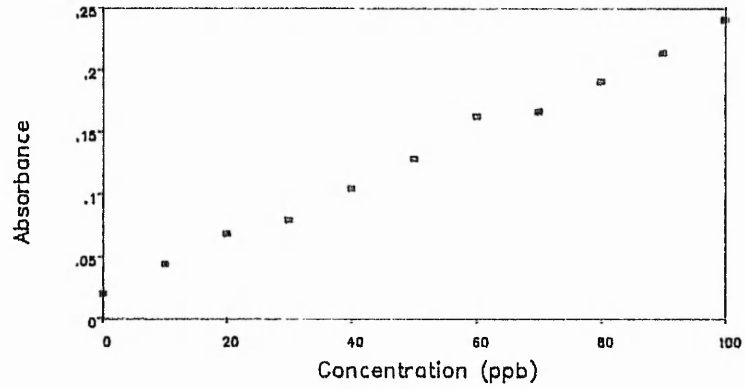

1% Hydrochloric Acid (a)

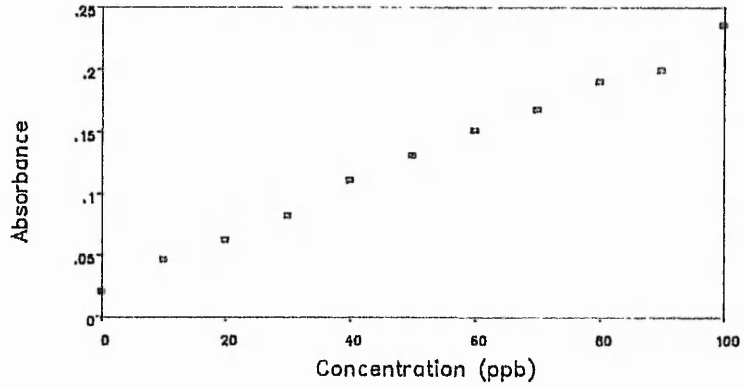

1% Nitric Acid (b)

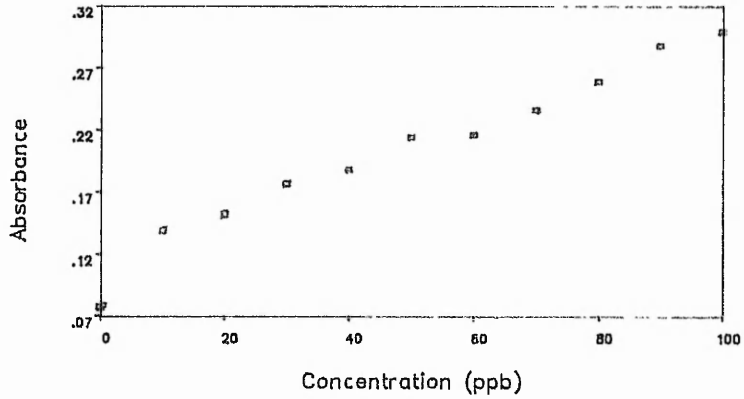

1% Phosphoric Acid (c)

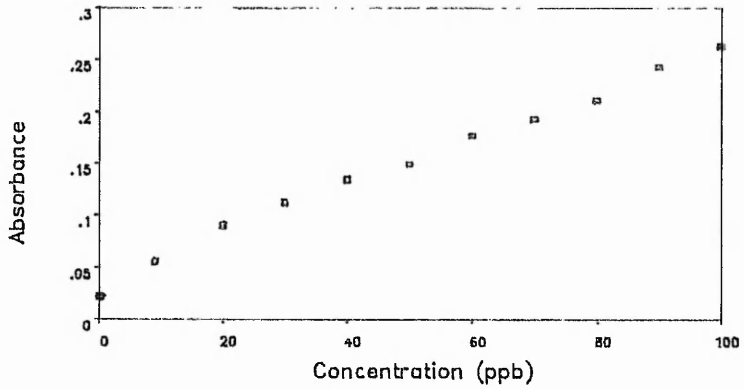

1% Sulphuric Acid (d)

Figure 3.11 – Calibration Curves for Aluminium

Hydrochloric Acid		Sulphuric Acid		Nitric Acid		Phosphoric Acid	
Absorbance	CV	Absorbance	CV	Absorbance	CV	Absorbance	CV
0.186	1.743	0.301	2.437	0.204	0.541	0.298	1.623
0.214	2.491	0.239	2.589	0.198	1.639	0.293	2.009
0.201	2.300	0.294	4.028	0.187	0.574	0.298	0.567
0.203	1.578	0.295	3.026	0.193	3.366	0.297	1.432
0.206	1.942	0.284	2.857	0.185	0.799	0.298	1.469
0.204	2.212	0.282	1.370	0.209	0.329	0.277	2.575
0.196	3.135	0.278	1.663	0.183	2.559	0.285	1.131
0.201	2.986	0.286	1.894	0.185	1.858	0.278	1.080
0.199	1.550	0.284	1.269	0.181	1.950	0.277	1.529
0.198	1.894	0.283	1.739	0.181	1.622	0.275	0.646
0.192	1.130	0.277	1.193	0.184	1.636	0.279	0.844
0.192	2.168	0.279	0.265	0.197	0.523	0.285	1.537
$\bar{x}$ = 0.199		$\bar{x}$ = 0.279		$\bar{x}$ = 0.197		$\bar{x}$ = 0.287	
s = 0.007		s = 0.015		s = 0.009		s = 0.01	

Table 3.30 – 80ppb Aluminium : repeatability of single solutions.

Hydrochloric Acid		Sulphuric Acid		Nitric Acid		Phosphoric Acid	
Absorbance	CV	Absorbance	CV	Absorbance	CV	Absorbance	CV
0.138	0.670	0.142	1.169	0.137	1.714	0.232	1.337
0.106	3.436	0.148	1.670	0.140	3.523	0.200	2.646
0.111	1.349	0.146	0.601	0.128	2.519	0.200	1.050
0.106	0.938	0.146	2.328	0.128	1.643	0.202	2.281
0.106	1.225	0.151	1.720	0.132	1.289	0.195	1.838
0.100	2.832	0.146	1.970	0.127	2.297	0.199	1.838
0.105	3.132	0.148	3.374	0.128	1.761	0.194	0.693
0.094	0.517	0.142	2.372	0.127	1.433	0.195	2.345
0.102	3.064	0.148	1.237	0.126	2.671	0.195	2.041
0.104	3.968	0.146	2.984	0.124	1.215	0.225	2.101
0.110	0.841	0.148	2.539	0.124	1.680	0.213	2.514
0.100	3.259	0.144	2.630	0.124	1.738	0.210	1.053
$\bar{x}$ = 0.107		$\bar{x}$ = 0.146		$\bar{x}$ = 0.129		$\bar{x}$ = 0.205	
s = 0.011		s = 0.003		s = 0.005		s = 0.012	

Table 3.31 – 40ppb Aluminium : repeatability of single solutions.

Hydrochloric Acid		Sulphuric Acid		Nitric Acid		Phosphoric Acid	
Absorbance	CV	Absorbance	CV	Absorbance	CV	Absorbance	CV
0.182	2.550	0.297	2.321	0.226	0.488	0.221	2.690
0.178	3.646	0.282	0.172	0.221	1.486	0.203	0.986
0.183	2.910	0.269	2.650	0.199	1.896	0.219	1.596
0.158	1.131	0.258	4.848	0.189	1.930	0.219	2.817
0.158	1.638	0.266	0.472	0.198	1.512	0.227	1.952
0.154	3.807	0.261	2.066	0.191	1.910	0.210	0.317
0.167	3.178	0.264	1.051	0.192	1.694	0.208	2.089
0.174	3.373	0.267	3.049	0.181	3.956	0.200	1.172
0.156	2.469	0.263	1.524	0.182	2.373	0.230	1.909
0.154	3.987	0.263	1.698	0.190	2.100	0.207	0.913
0.166	1.800	0.265	2.157	0.192	1.751	0.216	0.794
0.180	8.502	0.266	1.258	0.183	2.065	0.191	1.674
$\bar{x}$ = 0.167		$\bar{x}$ = 0.268		$\bar{x}$ = 0.195		$\bar{x}$ = 0.212	
s = 0.011		s = 0.011		s = 0.014		s = 0.011	

Table 3.32 – 80ppb Aluminium : repeatability of separate solutions.

3.6 Discussion

The establishment of electrothermal atomisation as a standard method in analytical laboratory technique has taken much longer than flame methods, even though they were suggested shortly after the introduction of atomic absorption itself.

There are two principal areas where electrothermal atomisation offers advantages over the flame,

(i) where detection limits are sought which are below those given by the flame,

(ii) when the amount of primary sample is strictly limited.

Such advantages can be of direct benefit to the type of analysis undertaken within the Engine Support and Services Laboratory (ESSL). However, the laboratory had little or no experience of the use of this technique and as such an understanding of the principles, both theoretically and on a practical basis, were essential.

Initial investigations illustrated that little reference material was available on the subject of this dissertation and as such the discussion is based almost entirely on personal observations.

The precision expected with replicate firings of the same sample or standard should be of the order of 1%, especially if an autosampler is used, as is the case with the equipment in the ESSL. However some of the basic differences between flame and electrothermal techniques can contribute a significant error to the analysis undertaken. Among these are the greater difficulty of weighing or measuring the microvolumes of sample employed, the very much greater effect, relatively speaking, of contamination, and the greater uncertainty in the measurement of the fast transient absorbance signals rather than integration of an almost

steady signal. In addition to these, instrumental or operator error and chemical effects in furnace atomisation are quite different to those in flame applications.

It was an appreciation of these difficulties and the development of a sound, basic understanding of the operation of an electrothermal system that was of benefit to the laboratory.

The work undertaken focussed on the analysis of copper, lead, iron and aluminium in a variety of acid matrices. The results were assessed in terms of precision, accuracy, ability to produce an acceptable standard curve in the range 0-100ppb and their overall potential to the development of a standard method of analysis.

In addition, a brief evalation of the use of organic solvents (section 4.0) in the analysis of elements by graphite furnace atomic absorption spectroscopy was undertaken. The results will be discussed initially on an individual basis with a review of the practical problems experienced being detailed at a later stage, as appropriate.

3.6.1 Copper

The heating cycle generated (see figure 3.1) from the observed sample drying sequence and the ash/atomisation curves was relatively consistant with only two exceptions. The first was the use of sulphuric acid which facilitated changes to the drying sequence (see figure 3.1). This change was incurred as a result of two observations,

(i) The sudden rise in temperature, denoting the first stage of drying, resulted in a plume of smoke being produced from the graphite tube inlet.

(ii) Upon completion of the first drying stage the sample was seen to boil and invoke a 'spluttering' of the solution.

It is essential that the drying sequence is accomplished in a controlled manner such that slow, even evaporation of the solvent from the matrix is obtained leaving behind the solid dried sample.

Several variations of the drying sequence were evaluated in an attempt to overcome these problems, resulting in the second stage of the drying sequence being changed from 25°C above ambient for 15 seconds to 25°C above ambient for 30 seconds. The use of a ramp or step change at the first stage did not eliminate the problem of the plume of smoke. This observation was consistant with the heating cycle containing no drying sequence. However the changing of the second sequence did reduce the ferocity of the observed boiling effect.

The second deviation was observed in the use of ortho phophoric acid, with a result that both the ash and atomisation temperatures were reduced from 600°C to 500°C and 2300°C to 2200°C respectively. The precision results, relating to the absorbance values recorded for concentrations of 40ppb and 80ppb copper, of 0.191 ± 0.008 and 0.354 ± 0.02 absorbance units (au) respectively, clearly indicate no detrimental effect on the analysis.

Similar results were obtained for the other acid radicals, table 3.33

Copper concentration (ppb)	Acid matrix	Mean ± 2s
80	HCL	0.388±0.020
80	HNO_3	0.360±0.028
80	H_2SO_4	0.333±0.026
80	H_3PO_4	0.354±0.020

Table 3.33 Analysis of copper - precision exercise.

The results for all four acid matrices have shown the technique to be both a precise and accurate method for determining trace levels of copper to a minimum concentration of 10ppb.

However, the use of these acid radicals in such a determination would be one of careful choice based on some of the observations made during this investigation.

Hydrochloric acid was a particularly difficult media as several attempts were required before an acceptable set of data could be generated. This was highlighted further with the individual analyses, such that the maximum number firings was required in the majority of cases before an acceptable result, in terms of the pre-set coefficient of variation of 4%, was obtained. As a result, the extended use of the graphite tube in this manner restricts its overall effective life.

3.6.2 Lead

The generation of the heating cycle required for the analysis of lead was limited by the method of temperature control used on the Shimadzu AA670. Attempts to obtain a satisfactory result using an atomisation temperature below 1100°C proved unsuccessful. The sharp, well defined peak obtained at 1100°C and above was impossible to recreate at 1099°C because of the different heating rates (see section 3.1.4) applied above and below this temperature and their subsequent effect on the recorder time window. A temperature in excess of 1099°C is obtained instantly in comparison to the delayed heating for temperatures below 1099°C.

A compromise atomisation temperature of 1300°C was eventually used and applied to all of the acid matrices evaluated. The heating programme was consistant throughout, with the exception of sulphuric acid, where

an ash temperature of 350°C was used. The results obtained in terms of precision were excellent, clearly demonstrating the ability of the technique to analyse trace levels of lead in the described solutions. However, the variation from solution to solution, be it from a single source or the twelve separately prepared solutions did not entirely satisfy the pre-set acceptance criteria that all data points will fall within two standard deviations of the sample mean. However such deviations were, on the whole, very marginal (0.001au outside the pre-set limits) and were considered acceptable.

The results relating to the analysis of twelve separate solutions, using sulphuric acid, indicate quite a wide band relating to the two standard deviations, e.g 0.052au. The results show an obvious 'flyer' within the data set, which when omitted alters the mean from 0.284au to 0.277au and reduces the two standard deviation value from 0.052 to 0.018au. It is clear that the use of sulphuric acid for the analysis of lead should be limited.

3.6.3 Iron

The heating cycle generated for the analysis of iron (see figure 3.1) was consistant for all of the acid matrices, with the exception of ortho phophoric acid. The general background level of iron in all grades of the acid, precluded any investigative work to be carried out, even to the extent of reducing the phosphoric acid concentration to 0.4% by volume, the relative high levels of iron persisted. The presence of background levels of iron was significantly higher than any other metal (see section 3.2) in all of the acids used. This was confirmed in practice with the following absorbance values being recorded for 1% acid solutions.

Phosphoric acid	0.435au
Nitric acid	0.108au
Hydrochloric acid	0.095au
Sulphuric acid	0.073au

The observed background levels obviously limit the range of acid matrices that can be used in the preparation of samples for iron analysis. However, not withstanding such limitations, the analysis of iron in 1% nitric, sulphuric and hydrochloric acid produced acceptable results in terms of the precision and accuracy of analysis. The graphical representation of the 0-100ppb calibrations (figure 3.21) clearly illustrates not only the ability to quantify to minimum levels of 10ppb, but also the variation of the solution blank.

3.6.4 Aluminium

The heating cycle generated for the analysis of aluminium (see figure 3.1) was consistant for all four acid matrices.

The results relating to each individual element-acid matrix combination indicate that acceptable measures of precision and accuracy are obtainable, any variations being of an acceptable nature as described previously for the other elements. In addition good calibration data, in the range of 0-100ppb, was obtained for each combination.

In general this study has shown the Shimadzu AA670 system to be perfectly capable of quantifying the likes of copper, lead, iron and aluminium to concentrations of 10ppb. The precision and accuracy of analysis has also been shown to be excellent with minor exceptions depending on the element and acid matrix being analysed.

The sample matrix is an important aspect to consider and cannot be overlooked when using graphite furnace atomic absorption. The chemistry involved can act as a modifier, in that the chemistry of the element is affected such that the heating programme can be optimised to best suit the analysis.

For instance the temperature programme generated for copper included an optimum ash temperature of 600°C. This was used throughout for each acid matrix, but consideration of the boiling points of the compounds involved can explain some of the problems that have been experienced.

Copper (I) chloride (M.pt 430°C, B.pt 1490°C) and copper (II) chloride (M.pt 620°C, B.pt 993°C decomposes to CuCl). The melting points are close to that of the ash temperature and could contribute to premature loss of copper. In addition the boiling point temperature of CuCl at 1490°C is below the atomisation temperature of 2300°C and subsequent losses due to vaporisation could occur before the atomisation temperature is obtained. Similar considerations have been given to the other elements investigated and as discussed earlier should form an integral part of the analysts approach to graphite furnace atomic absorption methodology.

SECTION 4.0

ORGANIC PHASE STUDIES

4.0 ORGANIC PHASE STUDIES

The combination of the analytical approaches to trace elemental analysis, discussed in section 2.0 and 3.0, forms the basis of the studies discussed in this section.

The ability of the extraction technique as an analytical tool has already been demonstrated. However, the extraction and subsequent flame atomic absorption analysis has identified limitations to the technique, not least the level of sensitivity obtained for the elements studied. The extraction studies discussed in section 2.0 concentrated on the aqueous phase being analysed with subsequent calculations following to determine the extraction efficiency of the system being studied. The inability to satisfactorily apply flame atomic absorption to the analysis of the organic phase, (i.e chloroform), limited investigations in terms of mass balance exercises with the extraction curves being produced.

To this end the advantages of electrothermal atomisation, in terms of increased sensitivity and the small sample size requirements, initiated a brief investigation into the potential of organic phase analysis using electrothermal atomisation. This investigation was limited to copper but provided useful information on the general applicability of the procedure.

4.1 Sample Preparation

4.1.1 The sample preparation technique for extracting copper from an aqueous system into chloroform using 8-hydroxyquinoline has been described in section 2.3.

4.1.2 The following samples were evaluated,

(i) Repeatability studies, using 80ppb copper solution. The best nine of ten firings were assessed in the manner described in section 3.4.

(ii) Mass balance, using a 80ppb copper solution. Each stage of the system was evaluated, e.g demineralised water, chloroform, 8-hydroxyquinoline in chloroform, 80ppb copper solution, and the aqueous and organic phase following extraction from systems containing no copper and 80ppb copper.

(iii) Analysis of demineralised water and 40, 80, 120, and 160ppb copper following extraction with 8-hydroxyquinoline with chloroform.

(iv) Repeat of (iii), but assess the percentage recovery by comparing the response to copper from the aqueous and organic phases.

4.1.2 The temperature programme used for these studies was the same as that outlined in figure 3.1.

4.2 Results

4.2.1 The results relating to the repeatability exercise were 0.421, 0.524, 0.553, 0.512, 0.480, 0.491, 0.500, 0.468, 0.473, and 0.468au. The arithmetic mean of the best nine was 0.496au with a coefficient of variation of 5.8%.

4.2.2 The results relating to the mass balance exercise are summarised below,

(i) Demineralised water, 0.058au

(ii) 80ppb copper in demineralised water, 0.504au

(iii) Chloroform, 0.018au

(iv) 1% 8-Hydroxyquinoline in chloroform, 0.198au

(v) Aqueous extract from system with no copper, 0.048au

(vi) Chloroform extract from system with no copper, 0.185au

(vii) Aqueous extract from system containing 80ppb copper, 0.054au.

(viii) Chloroform extract from system containing 80ppb copper, 0.521au.

4.2.3 The results relating to the extraction of 40, 80, 120, and 160ppb copper are shown in table 4.1.

4.2.4 The results relating to a repeat of exercise 4.2.3 are shown in table 4.2.

Copper Concentration	Copper Content of Aqueous Standard		Copper Content of Aqueous Phase after Extraction		Copper Content of Organic Phase after Extraction		Percentage Recovery
(ppb)	Absorbance	CV	Absorbance	CV	Absorbance	CV	(%)
40	0.175	1.394	0.030	9.493	0.173	2.362	98.8
80	0.371	1.005	0.029	9.802	0.238	9.542	64.1
120	0.593	0.435	0.022	1.130	0.422	3.651	71.2
160	0.728	2.141	0.015	4.087	0.490	17.570	67.3

Table 4.1 – Extraction of Copper by 8–Hydroxyquinoline

Copper Concentration	Copper Content of Aqueous Standard		Copper Content of Organic Phase after Extraction		Percentage Recovery
(ppb)	Absorbance	CV	Absorbance	CV	(%)
40	0.180	2.684	0.159	2.595	88.3
80	0.359	1.465	0.262	3.379	73.0
120	0.522	0.748	0.345	2.762	66.1
160	0.673	0.397	0.413	9.432	61.1

Table 4.2 – Repeat Extraction of Copper by 8–Hydroxyquinoline

4.3 Discussion

The results of this investigation have been encouraging in terms of the potential demonstrated by the electrothermal technique in coping with analyses involving organic solvents. However it should be stressed at this point, that significant variation in signal response, made it necessary for several attempts to be made at the various aspects of this investigation before totally satisfactory results were obtained.

The temperature programme used for this investigation was the same as that derived for the aqueous phase studies involving the analysis of copper. Attempts were made to re-optimise the system to accomodate the analysis of copper in chloroform, but with the signal variation experienced, no significant benefit was incurred by changing the temperature programme.

The repeatability study, which considered the best nine firings out of a maximum of ten (compared to the aqueous phase studies, section 3.0, which were the best three of four firings) still failed to comply with the pre-set acceptance criteria of a 4% coefficient of variation. However, considering the volatility of chloroform and the subsequent problems incurred by its use in electrothermal analysis, a coefficient of variation of 5.8% was an excellent result.

The mass balance evaluation attempted to identify the contribution made from each stage or phase of the extraction procedure. The results clearly show that each stage does have a contribution and directly affects the way in which the data should be interpreted. Demineralised water (0.058au) and chloroform in particular (0.018au) show negligible contribution and as such influence little in terms of background interference. However a 1% solution of 8-hydroxyquinoline (0.195au) has

a significant effect. Variation of the heating programme did little to eliminate the interference without influencing the atomisation characteristics of copper in a detrimental manner. It can only be concluded that 8-hydroxyquinoline was initially contaminated with approximately 30ppb copper. This was supported by the extraction procedure being carried out on demineralised water and subsequent analysis of the chloroform phase exhibiting a signal response of 0.185au.

The extraction of 80ppb copper in demineralised water (0.504au) and subsequent analysis of the chloroform layer (0.521au) appear to represent nearly a 100% recovery. However if the 8-hydroxyquinoline contribution is considered, the resultant response is 0.336au, which relates to a percentage recovery of 67%.

This compares well with the attempts to provide a calibration curve, produced from the analysis of the organic phase, whereby the percentage recoveries were similar, but inconsistant. These inconsistancies were highlighted by the values calculated for the coefficient of variance. Often in the region of 9% for the organic phase, but then on repeating the analysis could either improve or worsen the coefficient of variation without affecting the overall response.

Further analysis of such data indicates a limitation with respect to the concentration of copper in chloroform that can be analysed. Figure 4.1 illustrates the point more clearly, whereby significant losses occur at concentrations in excess of 40ppb copper. Indicating a limitation with respect to the loading capability of the furnace technique when analysing copper in organic matrices.

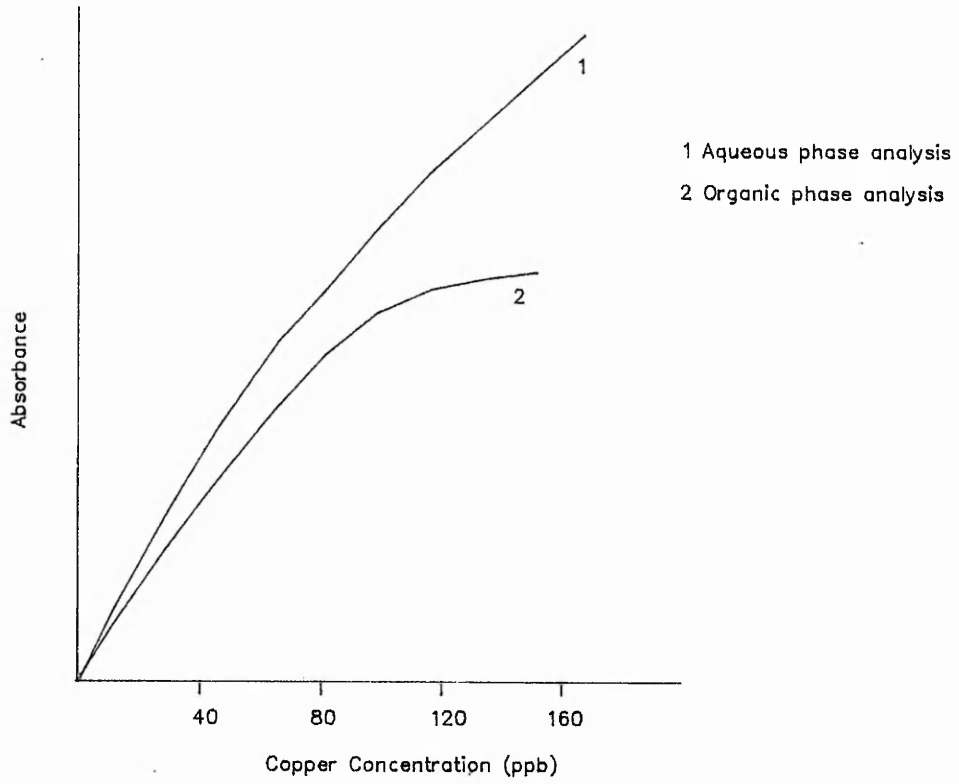

Figure 4.1 Loading Capability of Graphite Furnace Technique.

The problems of analysing organic matrices are further emphasised by assessing the coefficient of variation characteristics of the analyses. Table 4.1 shows the results from the different phases. It is clear that the analysis of copper in the aqueous phase is relatively easy with coefficient of variation values consistantly less than 2%. However analysis of the organic phase shows a considerable increase and results ranging from less than 4% coefficient of variation to in excess of 17% were obtained, highlighting the variability of the analysis.

These results were supported further by observations of the absorption of the chloroform solution into the surface of the graphite furnace,

rather than sitting proud and as a consequence introduced signal variation. The firing of an 80ppb copper in chloroform solution resulted in a given signal. However, subsequent firings, with no sample being injected resulted in a smaller, diminishing signal being produced (instead of a tube blank), proving that surface absorption had taken place.

The problems of working with organic solvents include its volatility, its affect on, and the effect of, the graphite furnace material, the effect on the temperature programme and the use of micropipettes for sample injection.

The correct alignment of the injector tip and depth to which it is inserted into the graphite tube are critical to the overall performance of the analysis. The horizontal, vertical and depth position of the injector tip were determined manually, but the injection cycle was carried out automatically. Experimental observations have shown that differences in the final analysis can be observed between automatic and manual injections of a sample, and also between a single and series of injections carried out automatically. In addition to the depth of the injector tip into the graphite tube, the angle of approach is equally important. The combination of the two ensure that the liquid sample is deposited onto the surface of the graphite tube, without the tip making contact with the graphite surface itself, such that the liquid retains its droplet form and rests on the surface of the graphite tube (figure 4.2a). This allows for slow, even drying of the sample to take place. However if the sample is incorrectly injected, then dispersion of the liquid may take place (figure 4.2b). This results in the sample being spread along the length of the tube, and if not lost by running out of the tube ends, results in uneven evaporation. Variability in atomisation

and hence erratic production of ground state atoms, incurs inconsistant results.

This scenario is certainly the case with regards to the use of organic solvents.

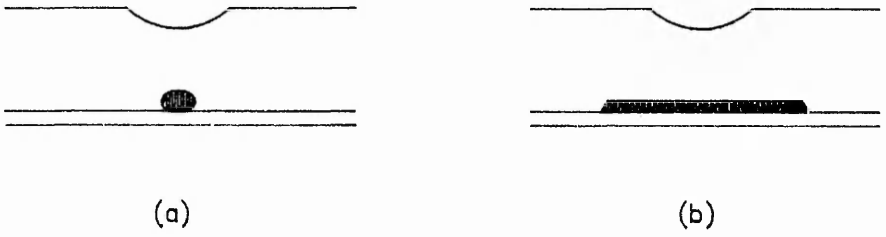

Figure 4.2 Profile of injected sample.

The design and composition of the micropipette tip is an important factor to consider. The dart like tip shown in figure 4.3 is ideal for injections of smaller volumes such as 50ul or less. This allows only a small 'dead' air space and assists the tip in almost reaching the surface of the graphite tube to deposit the sample.

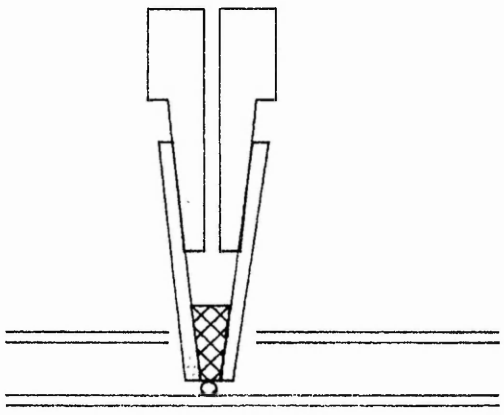

Figure 4.3 Dart-like micropipette tip

Standard tips are manufactured from polypropylene which has been treated to be non-wetting for aqueous solutions. However when non-aqueous solvents, such as ketones and chlorinated hydrocarbons are handled the precision or repeatability falls from a value of 1% to 10% and upwards. This is mainly due to the non-wetting finish being rapidly destroyed by the organic solvent, resulting in droplet formation in the tip after the solution has been dispensed. Such action will obviously incur subsequent errors in the analysis. An additional observation to note is that many instruments, including the Shimadzu AA670, offer the facility of rinsing the tip with both the blank and the sample solution under investigation, which under automation, at first sight would appear attractive. However experience has shown that even with aqueous samples this operation only encourages the breakdown of the non-wetting surface because of its extended use, with the subsequent analysis errors being introduced.

Further problems exist with the use of standard micropipette tips when dealing with organic solvents.

(1) The type of solvent used will, depending on its vapour pressure and subsequent volatility, suffer from the effects of premature sample ejection because of the build up of pressure from the dead volume void,

(2) Variation in sample concentration as a result of solvent evaporating,

(3) Dilution or concentrating effects can be incurred by the depth that the micropipette tip is immersed in the sample. Observations have shown that the deeper the tip immersion, the greater the capillary action in forcing extra solvent into the pipette before it collects the required volume. Again resulting in variations of the final result.

In an attempt to overcome such problems two designs of glass micropipette tip were assessed. The first, figure 4.4a, was similar to that of the dart like micropipette described earlier. The second incorporates a fine capillary tubing, cut across the tip 90° to the tube axis, figure 4.4b.

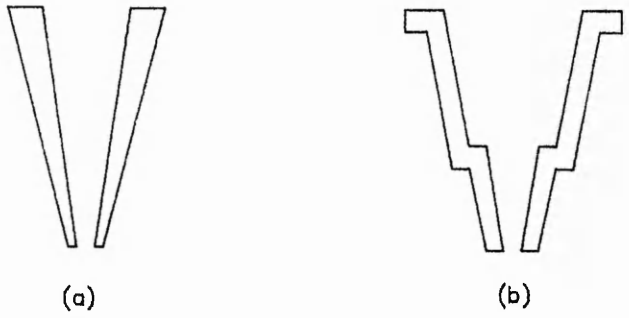

Figure 4.4 Glass Micropipette Designs

The use of such material reduced, but did not ultimately remove the droplet formation and the dart like design proved to be the more successful, although precision values were still of the order of 10%. The dart like design was used for the analysis of copper following extraction of the element into chloroform using 8-hydroxyquinoline. The results are represented in figure 4.5.

The analysis was set up such that a maximum of four firings of the sample would be taken and the best three assessed in terms of their repeatability. As can be seen from figure 4.5a all of the samples analysed in the aqueous matrix exhibited excellent repeatability and with the exception of the blank sample were all evaluated within three firings. A pre-set acceptance limit of 4% for the coefficient of variation was easily attained.

Extraction of copper with 8-hydroxyquinoline in chloroform, resulted in complete extraction of the element.

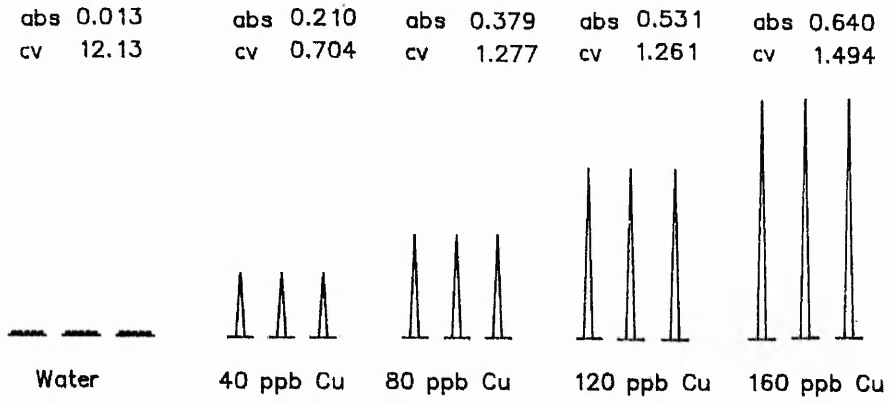

(a) Calibration range 0—160ppb in aqueous solution before extraction

(b) Analysis of aqueous layer after extraction

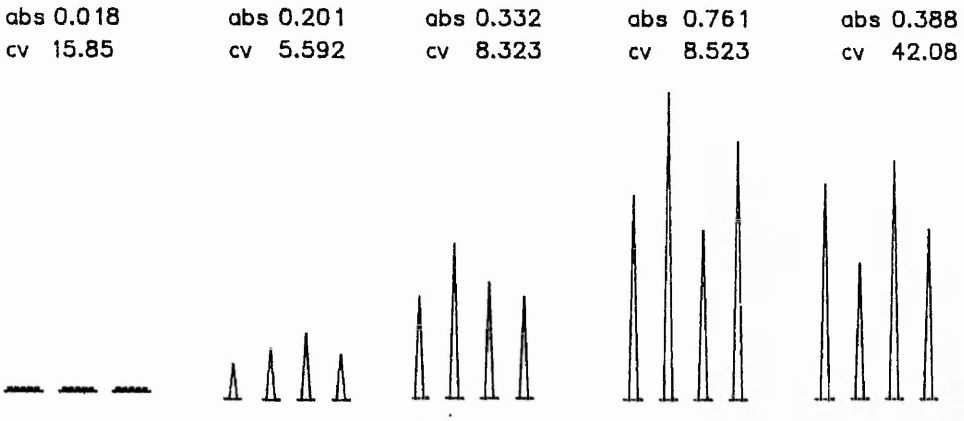

(c) Analysis of organic phase after extraction

Figure 4.5 Graphite Furnace Analysis of Extraction System

This was confirmed by figure 4.5b whereby analysis of the aqueous phase showed no discernable traces of copper to be present. However analysis of the organic phase, figure 4.5c, clearly shows the problems described earlier in analysing elements in organic solvents. In every case the maximum of four firings was required, but still the pre-set coefficient of variance value of 4% was consistantly exceeded. In addition the absorbance response indicates losses of the analyte and hence a completely quantitative approach could not be followed.

Additional observations with respect to the use of 8-hydroxyquinoline were noted. It was clear that subsequent dispensing of chloroform solutions containing 8-hydroxyquinoline were in fact depositing, due to rapid evaporation of the chelating agent on the walls of the micropipette tip. The ultimate result being to cause blockage of the tip and to incur losses in the analysis as the element could be retained with the chelate on the walls of the micropipette tip. To overcome this problem the use of the rinse facility, offered by the Shimadzu AA670 system, was incorporated into the analysis procedure. However the limitations with this system discussed earlier were apparent, but overall was considered the lesser in contributing errors into the analysis.

Clearly the results illustrated in figure 4.5c indicate significant variation in the recorded response and limit its real effective use. The reasons for such variation have been discussed already with respect to the problem associated with sample injection into the graphite furnace. However, upon closer examination of the results it is clear that the graphite tube itself contributes significantly to the problems experienced.

The problems of diffusion of the organic vapour through the walls of the graphite furnace are a major source of error in such analyses. The effect of "ghosting" is commonplace. That is, the removal of the diffused vapour may occur with a subsequent firing, resulting in a reduced signal in the first instance and an enhanced signal in the latter. Such an effect is enhanced further by the increase in porosity with sustained high temperature use (e.g during its life as an atomiser). Another disadvantage of graphite as an atomiser material is that some elements such as molybdenum and vanadium readily form stable carbides in contact with graphite at elevated temperatures. The ideal atomiser will be constructed from a material which is,

(1) chemically inert,

(2) has good thermal and electrical conductivity,

(3) can be obtained in a high state of purity,

(4) has low porosity,

(5) is easily machined,

(6) has a low expansion coefficient and

(7) a high melting point.

Graphite is the best compromise to such requirements, although some metals, particularly tungsten and tantalum have also been considered and used either as a tube material, or as a liner of a graphite tube (120-121).

The form of graphite known as pyrolytic graphite overcomes, to a large extent, both of these problems (122-123). Pyrolytic graphite can be formed as a coating on a graphite substrate by maintaining it in an inert atmosphere containing a small proportion of methane or other hydrocarbon, at a temperature up to 2500°C. A pyrolytic layer produced

in this way usually cannot exceed 1mm in thickness. In analytical use, the reduction in permeability of the pyrolytic graphite reduces the loss of atomic vapour by diffusion through the furnace walls and improves residence time. The pyrolytic form is also less inclined to form carbides with vanadium, molybdenum, titanium, tungsten and silicon and as such these elements may therefore be measured with greater sensitivity (124-127).

However a major practical problem in the use of pyrolytical coated graphite furnace tubes is the user will always be unsure as to the point where the coating begins to break down and introduce the porosity problems described earlier. No evaluation of such tubes was undertaken within this study.

The use of GFAA for trace metal analysis in organic phases clearly has its problems. However this should not detract from the overall potential of the technique. Careful choice of organic solvent, which is not as volatile as chloroform, could provide significant advantages over the likes of the cumbersome extraction techniques evaluated in section 2.0.

The Engine Support Services Laboratories analytical work is becoming increasingly involved in fuel analysis and trace metal contamination. The potential for direct analysis of fuel by GFAA, for trace elemental content, should be the subject of future study within the laboratory. Consideration will have to be given to limiting the significant contamination effects incurred due to carbon deposition. Such deposits tend to be produced all over the furnace and can cause problems in terms of electrical contact, resulting in poor atomisation and hence signal reproduceability.

SECTION 5.0

CONCLUSIONS

SECTION 5.0 CONCLUSIONS

5.1 The studies have shown that the classical approach of extracting a given element from an aqueous system, using a suitable chelating agent is still a viable technique.

5.2 The use of 8-hydroxyquinoline was relatively successful, clearly demonstrating the ability to chelate with the elements studied and to provide a means, depending upon the element, for preferential extraction from a given matrix.

5.3 The basic dissociation of 8-hydroxyquinoline below a pH of 4.0 was a significant limitation to the use of this chelating agent.

5.4 The choice of buffer system has to be based on experimental evaluation, as evidence clearly shows the extraction of the elements studied was significantly affected by the choice of buffer system.

5.5 The graphite furnace studies relating to aqueous samples clearly demonstrated the ability to quantify levels of copper, lead, iron and aluminium, in a range of acid matrices, to 10ppb.

5.6 The results of the precision and repeatability exercises were found to be excellent for the elements assessed.

5.7 Some difficulties were experienced mainly with the use of hydrochloric acid and phosphoric acid. Consequently careful

assessment of the sample matrix is essential before using such acids in the preparation sequence.

5.8 The use of chloroform as a solvent medium for elemental analysis by graphite furnace atomic absorption was a limited success.

5.9 The response of copper in chloroform solution, although good, was inconsistant.

5.10 The use of chloroform created significant problems with respect to the use of micropipettes and the type of injector tips being used.

SECTION 6.0

RECOMMENDATIONS

SECTION 6.0 RECOMMENDATIONS

6.1 Provided the procedure is fully evaluated the use of extraction techniques may be used, where appropriate, for a given application.

6.2 The use of graphite furnace atomic absorption spectroscopy for trace analysis of copper, lead, iron and aluminium should be implemented as a standard technique within the Engine Support Services Laboratory.

6.3 Phosphoric acid should not be used for the analysis of iron by graphite furnace atomic absorption spectroscopy.

6.4 The use of organic solvents in graphite furnace atomic absorption should be evaluated more fully. Particular attention should be applied to the less volatile solvents which would reduce the problems experienced whilst using chloroform.

6.5 An independant, or combination of extraction and graphite furnace atomic absorption techniques, should be evaluated further with respect to the analysis of fuels.

6.6 In an attempt to minimise matrix effects an investigation of the direct injection analysis of fuel and evaluation of solid samples via graphite furnace atomic absorption should be undertaken.

SECTION 7.0

REFERENCES

SECTION 7.0 REFERENCES

1. Berman, E. "Toxic and their Analysis"; Heyden, London. 1980

2. Pinta, M. "Modern Methods for Trace Element Analysis"; Ann Arbor Science, Ann Arbor, MI. 1978

3. Kuwana, T. Ed. Physical Methods in Modern Chemical Analysis"; Academic Press, New York. 1978, 1980; vols 1, 2.

4. Risby, T.H. Ed. "Ultratrace Metal Analysis in Biological Sciences and the Environment"; Advances in Chemistry Series No.172, American Chemical Society, Washington DC. 1979.

5. Pecsok, R.L. et al. "Modern Methods of Chemical Analysis"; Wiley, New York. 1976.

6. Willard, H.H.; Merritt, L.L. Jr.; Dean, J.A.; Settle, F.A. Jr.; "Instrumental Methods of Analysis", sixth edition, d. Van Nostrand Co, New York. 1981.

7. Skoog, D.A.; West, D.M. "Principles of Instrumental Analysis", second edition, Saunders, Philadelphia. 1980.

8. Lederer, M.; Nature 176, 462. 1955.

9. Bierman, W.J. and Gesser, H.; Anal Chem 32, 1525. 1960.

10. Brandt, W.W. and Heveran, J. E.; Division of Analytical Chemistry, 142nd meeting, Atlantic City, NJ. 1962.

11. Moshier, R.W. and Sievers, R. E.; "Gas Chromatography of Metal Chelates" Pergammon Press, Oxford. 1965.

12. Ross, W.D. and Sievers, R. E.; Anal Chem 41, 1109. 1969.

13. Savery, J. et al, Anal Chem 42, 294. 1970.

14. Guiochen, G and Pommier, C.; "Gas Chromatography in Inorganics and Organometallics"; Ann Arbor Science Publishers In, Ann Arbor. 1973.

15. Veening, H. et al; J. Gas Chromatography 5, 248. 1967.

16. Hansen, L.C. et al; Anal Chem 43, 349. 1971.

17. Wolf, W.R. et al; Anal Chem 44, 616. 1972.

18. Foreman, J.K. et al; The Analyst (London) 95, 797. 1970.

19. Eisentraut, K.J. et al; Anal Chem 43, 2003. 1971.

20. Uden, P.C. and Henderson, D.; The Analyst 102, 889-915. 1977.

21. Neeb, R. et al; Frensensius Z. Anal Chem 293, 211-219. 1978.

22. Neeb, R. et al; Frensensius Z. Anal Chem 293, 290-294. 1978.

23. Kupcik, J. et al; J.Chromat 171, 285-304. 1979.

24. Neeb, R. et al; Z. Anal Chem 282, 17-19. 1976.

25. Sucre, L. et al; HRC and CC 3, 452-459. 1980.

26. Masaryk, J. et al; J.Chromat 115, 256-258. 1975.

27. Stephen, W.I.; Summary of paper presented at meeting of Western region, Feb 17th. 1972 Proceedings, March issue, 52. 1972.

28. Samuelson, O. "Ion Exchange Separations in Analytical Chemistry"; J.Wiley and Sons, (NY). 1963.

29. Brinkman, U.A.Th. et al; J.Chrom 85, 187. 1973.

30. Scott, R.P.W. "Liquid Chromatography Detectors"; Elselvier, New York. 1977.

31. Jewitt, K.L. et al; Detectors in Liquid Chromatography"; Vickrey,T.M.Ed.; Dekker: New York. 1982.

32. Van Loon, J.C.; Anal Chem 51, 1139a-1150a. 1979.

33. Van Loon, J.C.; Amer Lab 5, 47-53. 1981.

34. Fernandez, F.J.; Perkin Elmer Atomic Absorption Newsletter 16(2), 33-36. 1977.

35. Vickers, T.J. In "Physical Methods in Modern Chemical Analysis", Kuwana, T.Ed.; Academic Press, New York. 1978.

36. Kahn, N. et al J Liquid Chrom 2(1), 23-26. 1979.

37. Koizumi, H. et al Anal Chem 51, 387-392. 1979.

38. Burns, D.T. et al The Analyst 106, 921. 1981.

39. Brinkman, F.E. et al J. Chrom Sci 15, 493-503. 1977.

40. Brinkman, F.E. et al J.Chrom 185, 583-572. 1979.

41. Kirchoff, G.R. "Pogg Ann" 109, 275. 1859.

42. Kirchoff, G.R. et al, "Pogg Ann", 110, 161. 1860.

43. Walsh, A. "Spectrochemistry since Kirchoff and Bunsen", Proceedings of the royal Australian Chemical Institute, 42, 297. 1975.

44. Slavin, M. "Emission Spectrochemical Analysis" Wiley-interscience, New York. 1971.

45. Koirtyomann, S.R. and Pickett, E.E. in "A History of Analytical Chemistry" (edited by H.A. Laitinen and G.W. Ewing) American Chemical Society 1977.

46. Hermann, R. and Alkemade, C.T.J.; Chemical Analysis of Flame Photometry (translated by P.T. Gilbert) Interscience, New York 1963.

47. Walsh, A. Spectrochim Acta, 7, 108. 1955.

48. Alkemade, C.T.J. and Milatz, J.M.W. J Opt Soc Am; 45, 583. 1955.

49. Lundegardh, H. Ark Kemi, Mineral Geol, No.1, 10a. 1928.

50. Lundegardh, H. "The Qualatative Emission Spectral Analysis of Inorganic Elements in Solution" Lantbruks-Hogskol. Ann; 3, 49-97. 1936.

51. Lundegardh, H. "Qualatative Spectrum Analysis of Metals by Means of Flame and Spark"; Metalwirtschaft, 17, 1222-1226. 1938.

52. Lundegardh, H. and Philpson, T. The Spark-in-Flame Method for Spectral Analysis. Lantbruks-Hogskol. Ann; 5, 249-260. 1938.

53. Jansen, W.H.; Heyes, J. and Richter, C. III "The Microanalysis of Sodium in Human Blood Serum" Z.Physik Chem, A, 168, 267-273. 1934.

54. Jansen, W.H. et al, IV "The Microanalysis of Potassium and Calcium"; Z.Physik Chem, A, 171, 268-280. 1934.

55. Schuhknecht, W. Spectroanalytical Determination of Potassium; Angew Chem; 50, 299-301. 1937.

56. Dean, J.A. "Use of Organic Solvents in Flame Photometry"; Am.Soc Testing Materials Spec Tech Publ. 238, 43-54. 1958.

57. Dean, J.A. et al; Application of Organic Solvent Extraction to Flame Photometry. Determination of Iron in Nonferrous Alloys. Anal Chem 28, 1887-1889. 1956.

58. Margoshes, M. and Valee, B.L. "Flame Photometry and Spectrometry Principles and Applications in D. Glick (ed) "Methods of Biochemical Analysis" Vol 3, intersci NY 1956.

59. Aldous, K.M. et al Anal Chem 45, 1990. 1973.

60. Sturgeon, R.E. et al Anal Chem 47, 1240,1250. 1975.

61. Burrows, J.A. et al Anal Chem 37, 579. 1965.

62. Dean, J.A. Analyst 85, 621. 1960.

63. D'Silva et al Anal Chem 36, 1287. 1964.

64. Fassel et al Spectrochim Acta, 19, 1187. 1963.

65. Knisely et al Anal Chem 35, 911. 1963.

66. Medlun et al At Absorp Newsletter 8, 25. 1969.

67. Slavin, W. et al Anal Chem 35, 253. 1963.

68. Allan, J.E. Spectrochim Acta 17, 467. 1961.

69. Robinson, J.W. Anal Chem 33, 1067. 1961.

70. David, P.J. Spectrochim Acta 20, 1185. 1964.

71. Willis, J.B. Nature 207, 715. 1965.

72. Amers, M.D. and Willis, J.B. Spectrochim Acta 22, 1325. 1966.

73. Burman, J.A. and Willis, J.B. Anal Chem 39, 1210. 1967.

74. Koirtyohann, S.R. et al Spectrochim Acta 23B, 235. 1968.

75. Manning, D.C At Absorp Newsletter 5, 127. 1966.

76. Manning, D.C. At Absorp Newsletter 6, 35. 1967.

77. Pickett, E.E. and Koirtyohann, S.R. Spectrochim Acta 23B, 235. 1968.

78. Pickett, E.E. and Koirtyohann, S.R. Spectrochim Acta 24B, 325. 1969.

79. Slavin, W. et al At Absorp Newsletter 5, 84. 1966.

80. Husler, J.W. At Absorp Newsletter 10, 60. 1971.

81. Luecke, W. N Jb Miner. Mh. 263. 1971.

82. Smith, R. Spectry Letters 1, 157. 1968.

83. Marks and Welcher, Anal Chem 42, 1033. 1970.

84. Kahn, M.L. et al At Absorp Newsletter 9, 33. 1970.

85. Kahn, M.L. et al AT Absorp Newsletter 7, 35. 1968.

86. Burrell, D.C. et al Anal Chim Acta 48, 45. 1969.

87. Lamm, S. et al New England J. Med 289, 574. 1973.

88. Molak, W. At Absorp Newsletter 12, 63. 1973.

89. Delves, M.T. Analyst 95, 431. 1970.

90. Price, W.J. "Spectrochemical Analysis by Atomic Absorption" Heyden and Son Ltd 57-59. 1979.

91. King, A.S. J. Astrophysics 27, 253. 1908.

92. Mandelohtam, S.L. et al Zhur Analit Khim, 11, 9. 1956.

93. L'vov, B. J.Eng. Phys (USSR) 2, 44. 1959.

94. L'vov, B. Spectrochim Acta 24B, 53. 1969.

95. Woodriff, R. Spectrochim Acta 23B, 665. 1968.

96. Massmann, H. Spectrochim Acta 23B, 215. 1968.

97. Sandell, E. B, "Colorimetric Determination of Trace Metals," Third Edition, Interscience, New York, 1959.

98. Stary, J. "Solvent Extraction of Metal Chelates" Ch.3, 21-33. 1964.

99. Morrison, G.H. and Freiser, H. "Solvent Extraction in Analytical Chemistry" J.Wiley and Sons NY 162-166. 1957.

100. Hambali, C.S. and Haddad, P.R. Chromatographia 13(10), 63. 1980.

101. Wenclawiak, B. Frensenius Z.Anal Chem 120, 308. 1981.

102. Wenclawiak, B. Frensenius Z Anal Chem 144, 310. 1982.

103. Hoffman, B. Schewdt, G. J High Resol Chrom. Chrom comm, 5, 439. 1982.

104. Lajunen, L.H. et al Analyst 109, 609. 1984.

105. Haddad, P.R. et al "Reverse Phase HPLC of 8-Hydroxyquinoline of Mo(VI), Al(III), Co(III) and Cu(II), J High resol Chrom Chrom comm, 127-128. 1986.

106. Maeda, M. and Tsufi, A. Chem Pharm Bull, 27, 797. 1979.

107. Miura, K. et al Jour Chrom 210, 536-539. 1981.

108. Kendall, D.R. et al "The Thermal Degradation of Aviation Fuels in Jet Engine Injector Feed Arms Part II - Results from Full Scale Rig." B7-Tokyo-IGTC-49.

109. Freiser, H. Anal Chem 31, 1440. 1959.

110. Juvet, R.S. and Wachi, F.M. Anal Chem 32, 290. 1960.

111. Sandell, E.B. "Colorimetric Determination of Trace Metals", 3rd edition, Interscience, New York 1959.

112. Irving, H.M.N.H. "Dithizone", Analytical Sciences Monograph no.5. The Chemical Society, London 1977.

113. Dryssen, D. et al Acta Chem, Scand, 7, 1186. 1953.

114. Schweitzer, G.K. et al Anal Chim Acta 23, 419. 1960

115. Schweitzer, G.K. et al Anal Chim Acta 24, 311. 1961.

116. Panova, M.G. et al Radiokhimiya, 197, 2. 1960.

117. Motojima, K. et al Bunseki kaguku, 9, 151. 1960.

118. Oosting, M.; Anal Chim Acta 21, 301,397,505. 1959.

119. Stary, J. Anal Chim Acta 28, 132-149. 1963.

120. Baird R.B. et al, Appl. Spectrosc 28, 273 (1974).

121. Fuller, C.W. Analyst, 99, 739 (1974).

122. L'vov, B.V. Atomic Absorption Spectrochemical Analysis, Adam Hilger, London, 1970.

123. L'vov, B.L. Spectrochim Acta 24B, 53 (1970).

124. Monte, V.L.A. et al, Journal Anal Atom Spec, 21-24, 5 Feb 1990.

125. Lechotycki, A. Journal Anal Atom Spec, 25-28, 5, 1990.

126. Chakrabarti, Wu, S. et al, Spectrochim Acta, Part B, 651,41, 1986.

127. Nakahara, T. et al, Anal Chim Acta, 99, 104, 1979.